AN ABSTRACT OF THE THESIS OF

Younghoon Whang for the degree of Doctor of Philosophy in Electrical and Computer Engineering presented on May 17, 2016 .

Title: Transmission and Combining for Hybrid Automatic Repeat Request in Multiple-Input Multiple-Output Systems

Abstract approved: _____

Huaping Liu

Hybrid automatic repeat request (HARQ) schemes combine packet retransmission with forward error correction to ensure a reliable communications. In multiple-input multiple-output (MIMO) systems, interference cancellation (IC) detection is widely used where the detection and cancellation steps of the simultaneously transmitted data streams occur. In principle, the signal stream estimated at one IC stage is utilized to cancel the interference of other signal streams at the next IC stage. Thus, the detection probabilities of the transmitted data streams are mutually dependent. With HARQ, the detection performance of a packet also depends on how many times the packet has been retransmitted. The dissertation consists of three main contributions.

Firstly, we develop a HARQ transmission state control algorithm for MIMO systems with IC detection to improve throughput. The HARQ transmission state is defined as the distribution of the initial packets and retransmission packets transmitted during a packet transmission time interval (PTTI). The proposed algorithm generates the transmission state in which initial packets and retransmission packets are sent together. The

outcome is that it achieves a lower error probability for initial packets by exploiting the IC process and a significantly higher throughput than the conventional HARQ system, which is verified by simulation results. However, the maximum allowable number of retransmission is limited to one in this algorithm.

Secondly, in order to extend the analysis for a more general case, we define the concept of the effective interference level (EIL) as the performance parameter to choose the set of packets during one PTTI and establish a relationship between EIL and the effective signal-to-interference-plus-noise ratio (SINR). We then show that choosing the set of packets that minimize the EIL successively from the lowest to the highest HARQ round leads to a lower packet error and higher throughput than conventional HARQ, which is verified by simulation. Also, the proposed EIL-based scheme uses only the acknowledgement feedback messages like a conventional HARQ, because the number of HARQ rounds of each packet is the only required information to calculate the EIL. Simulation results highlight the superiority of the proposed scheme over the conventional scheme in terms of throughput with the signal-to-noise ratio gain of about 4.2 dB at maximum for MIMO systems with four transmit and four receive antennas.

Thirdly, a low-complexity symbol-level combining (SLC) scheme is developed for Chase combining-based HARQ (CC-HARQ) in MIMO systems, when the linear detection is considered at the receiver. In the proposed scheme, instead of using the entire channel matrix as in the existing SLC schemes, a subset of row vectors in the channel matrix is selected in the proposed scheme, and the selected row vectors are sequentially used during the estimation procedures of the retransmitted symbols, where the sequential utilization is enabled by using the Sherman-Morrison-Woodbury (SMW) lemma. Therefore, according to the number of the selected row vectors, this approach enables the proposed SLC scheme to have an advantage in complexity compared to the existing

SLC schemes. In addition, we develop a row vector selection criterion for the proposed scheme to compute the amount of the SINR improvement by using a squared norm of each row vector with a significantly lower computational complexity. Simulation results show that compared to the existing SLC schemes, the proposed SLC scheme achieves similar or better error performance, while its computational complexity is lower or in the worst case similar.

Transmission and Combining for Hybrid Automatic Repeat Request in Multiple-Input Multiple-Output Systems

by

Younghoon Whang

A THESIS

submitted to

Oregon State University

in partial fulfillment of
the requirements for the
degree of

Doctor of Philosophy

Presented May 17, 2016
Commencement June 2016

Doctor of Philosophy thesis of Younghoon Whang presented on May 17, 2016 .

APPROVED:

Major Professor, representing Electrical and Computer Engineering

---

Director of the School of Electrical Engineering and Computer Science

---

Dean of the Graduate School

I understand that my thesis will become part of the permanent collection of Oregon State University libraries. My signature below authorizes release of my thesis to any reader upon request.

Younghoon Whang, Author

ACKNOWLEDGEMENTS

In conducting the research and preparing this dissertation, I have been blessed with the help, inspiration and motivation of many people although I may not remember all of them.

I would like to thank my advisor, Prof. Huaping Liu, for his invaluable advice throughout my study and research. This thesis has significantly benefited from his incessant guidance and continuous encouragement.

I would also like to express my sincere gratitude to my Ph.D. thesis committee members. Their remarks and comments have made significant contributions to improving the quality of my thesis.

I am thankful to the former and current members in my research group at Oregon State University for their help, encouragement, and numerous discussions in my long journey to this thesis.

I am grateful to friends of mine for their constant support and friendship. They have helped me overcome setbacks and stay focused on my study and research.

Finally, I owe a great deal to my parents and brother. It would have been impossible to maintain my spirit without their endless love and affection. This thesis is dedicated to them.

TABLE OF CONTENTS

Page

1 Introduction 1

1.1 Backgrounds . . . 1

1.2 Motivations . . . 8

1.3 Dissertation Outline . . . 10

1.4 List of Mathematical Notations . . . 11

1.5 List of Abbreviations . . . 12

2 HARQ Transmission State Control Algorithm for MIMO Systems with IC Detection 14

2.1 Introduction . . . 14

2.2 System Model . . . 15

2.3 Proposed HARQ Transmission State Control Algorithm . . . 17

2.4 Simulation Results . . . 22

2.5 Conclusion . . . 27

3 EIL-based Packet Transmission for MIMO Systems with HARQ and IC Detection 28

3.1 Introduction . . . 28

3.2 System Model . . . 29

3.3 Proposed EIL-based Packet Transmission Strategy . . . 33

3.3.1 Analysis of System Characteristics . . . 33

3.3.2 EIL-based Transmission Strategy . . . 39

3.4 Simulation Results . . . 43

3.5 Conclusion . . . 52

4 Low-Complexity SLC for CC-HARQ in MIMO Systems with Linear Detection 54

4.1 Introduction . . . 54

4.2 System Model . . . 55

4.3 Existing SLC Schemes . . . 57

4.3.1 Brute-Force Combining Scheme . . . 57

4.3.2 Post-Combining Scheme . . . 58

4.3.3 Pre-Combining Scheme . . . 59

TABLE OF CONTENTS (Continued)

Page

4.3.4 QRD-SLC Scheme 60
4.4 Proposed Low-Complexity SLC Scheme 62
4.4.1 SMW Lemma-based Combining and Detection Procedures 62
4.4.2 Squared Norm-based Row Vector Selection Criterion 66
4.4.3 The Complexity of Existing and Proposed SLC Schemes 68
4.5 Simulation Results 71
4.6 Conclusion 78

5 Conclusions and Future Work 79
5.1 Conclusions 79
5.2 Future Work 80

Bibliography 82

LIST OF FIGURES

Figure Page

1.1 Two types of HARQ processes in MIMO systems. 7

2.1 Packet generation process at the transmitter. 16

2.2 An example of the transmission states at the tth PTTI ($N_{\mathrm{T}} = 2$, $S(t-1) = S_2$, and $a_{t-1,i} = 0\ \forall p_i \in \mathbf{P}_{t-1}$). 21

2.3 Average PERs of the initial packets in each of HARQ transmission states. 22

2.4 Distributions of the transmission states. 23

2.5 Average PERs of the initial packets in the proposed and the conventional systems. 25

2.6 Average throughputs of the proposed and the conventional systems. . . . 26

2.7 Average queuing delays of the retransmission packets in the proposed and the conventional systems. 26

3.1 Transmission process with three independent CC. 29

3.2 BLC-based reception process of the system. 32

3.3 Average PERs according to $\mathbf{P}_t$ when $N_{\mathrm{T}} = N_{\mathrm{R}} = 2$, $R = 2$ and $|\mathbf{P}_{t,r}|$ is the number of the packets at the rth round in the tth PTTI. 45

3.4 Probability of each $\mathbf{P}_t$ with the conventional strategy when $N_{\mathrm{T}} = N_{\mathrm{R}} = 2$, $R = 2$, $B = N_{\mathrm{T}}$ and $|\mathbf{P}_{t,r}|$ is the number of the packets at the rth round in the tth PTTI. 46

3.5 Probability of each $\mathbf{P}_t$ with the proposed strategy when $N_{\mathrm{T}} = N_{\mathrm{R}} = 2$, $R = 2$, $B = 2N_{\mathrm{T}}$ and $|\mathbf{P}_{t,r}|$ is the number of the packets at the rth round in the tth PTTI. 47

3.6 Average PERs with different transmission strategies when $N_{\mathrm{T}} = N_{\mathrm{R}} = 2$, $R = 2$, $B = N_{\mathrm{T}}$ and $2N_{\mathrm{T}}$ for the conventional and proposed transmission strategies, respectively. 49

3.7 Average throughputs of the transmission strategies by the number of successfully decoded packets per PTTIs when $B = N_{\mathrm{T}}$ and $2N_{\mathrm{T}}$ for the conventional and proposed transmission strategies, respectively. 50

LIST OF FIGURES (Continued)

Figure		Page
3.8	Average number of required PTTIs per terminated packet with the transmission strategies when $B = N_{\mathrm{T}}$ and $2N_{\mathrm{T}}$ for the conventional and proposed transmission strategies, respectively.	51
4.1	Transmitter block diagram.	55
4.2	Average uncoded BER performances of the SLC schemes based on the ZF detection when $N_{\mathrm{T}} = N_{\mathrm{R}} = 3$.	73
4.3	Average uncoded BER performances of the SLC schemes based on the MMSE detection when $N_{\mathrm{T}} = N_{\mathrm{R}} = 3$.	75
4.4	Average FER performances of the SLC schemes when $N_{\mathrm{T}} = N_{\mathrm{R}} = 3$ and $R = 3$.	76

LIST OF TABLES

Table		Page
2.1	Proposed transmission state control algorithm	20
3.1	Summary of the proposed transmission strategy	42
3.2	Parameters of simulation environments	43
4.1	Computational complexity of the SLC schemes with linear detection for retransmissions	68

To my parents,
for their endless sacrifice and support

Chapter 1: Introduction

1.1 Backgrounds

Multiple-input multiple-output (MIMO) systems have been adopted in various wireless communication standards, such as Institute of Electrical and Electronics Engineers (IEEE) 802.11 (for wireless local area networks), IEEE 802.16 (for wireless metropolitan area networks), IEEE 802.20 (for mobile broadband wireless access) and 3rd Generation Partnership Project (3GPP) long-term evolution (LTE) [1] to improve system reliability and spectral efficiency significantly by exploiting a rich multipath fading environment with multiple transmit and receive antennas [2–4, 6, 13, 15–22].

Two typical approaches in the MIMO systems are to provide diversity gain as in space-time coding (STC) or to allow spatial multiplexing (SM). While STC is capable of improving system reliability through coding across space domain and/or time domain, SM transmission is capable of increasing data transmission rate.

The basic concept of SM is to transmit independent and separately encoded bit streams, from each of the multiple transmit antennas. It increases the transmission rate for the same bandwidth without additional power expenditure and generally allows a capacity increase proportionally with the number of transmit-receive antenna pairs. Bell Laboratories layered space-time (BLAST) is a transceiver architecture for offering SM gain over MIMO systems [3].

In BLAST-type SM MIMO systems, interference cancellation (IC) detection is widely used to enhance the performance by eliminating the interference from each transmitted

data stream instead of maximum likelihood (ML) detection with higher computational complexity [2–4,6]. For MIMO systems with IC detection, the detection and cancellation steps of the simultaneously transmitted data streams occur [3, 4]. Generally, the signal-to-noise ratio (SNR) gain due to IC is higher for the data stream with a lower detection probability.

There are error control schemes such as automatic repeat request (ARQ), and forward error correction (FEC). For an ARQ scheme, erroneously received packets are retransmitted until they are detected as error-free or until they reached the maximum allowable number of transmissions. The cylic redundancy check (CRC) is used for simple error detection and receiver send transmitter the feedback information such as acknowledgment or negative acknowledgment based on the CRC detection result. This scheme can achieve a higher throughput in high SNR regions than a FEC scheme but a lower throughput in intermediate SNR region and is sensitive to channel error ratio under severe fading conditions.

On the other hand, the sender adds redundancy to its messages for a FEC scheme, that is also known as an error correction code. This allows the receiver to detect and correct errors within some bound without asking the sender for additional data. The representative examples are convolutional code, turbo code, low-density parity-check (LDPC) code and so on. The retransmission of data can be avoided at the cost of higher bandwidth requirements on average. So it provides one-way connection between the transmitter and the receiver without feedback information unlike ARQ scheme and it is insensitive to channel error ratio. However, it shows lower throughput in high SNR for a fixed coding rate than ARQ. Furthermore, throughput can degrade with redundancy, decoder complexity.

In order to mitigate each error control scheme's drawbacks, hybrid automatic repeat

request (HARQ) [11–23] schemes combine packet retransmission with FEC to ensure a reliable communications without the knowledge of channel state information. Thereby, HARQ is an integral part of modern communication standards such as 3GPP LTE and LTE advanced (LTE-A) [1] as well and so on.

Based on whether soft combining is available or not, HARQ processes can be divided in three categories: type-I, type-II and type-III processes. In type-I HARQ process, for every transmission attempt, the receiver discards the received packet if decoding fails without soft combining. Then, it asks for another retransmission until the packet is correctly received or it reaches the maximum allowable number of retransmissions. So there are overheads associated with transmissions. By way of contrast, in both type-II and type-III HARQ processes, a receiver combines the erroneous packet received previous transmission with that of the later retransmissions to decode the overall packet. According to whether each retransmission is self-decodable or not, type-III or type-II HARQ process can be defined respectively.

According to which part of a mother codeword will be utilized for retransmissions with soft combining, the HARQ schemes can be mainly classified into the following three types: Chase combining-based HARQ (CC-HARQ) [11], partial incremental redundancy-based HARQ (PIR-HARQ) [28], and full incremental redundancy-based HARQ (FIR-HARQ) [29].

FIR-HARQ can be regarded as type-II HARQ process without self-decodability as follows:

In FIR-HARQ, new parity bits which have not been sent up to the previous transmission are sent without systematic part utilization for each retransmission. Therefore, it can obtain coding gain provided by parity bits. However, if the systematic part is severely distorted or corrupted because of deep fading condition, it is impossible to recover it via

retransmissions. Furthermore, it is difficult to implement it.

In particular, we can further distinguish two kinds of type-III HARQ processes with with self-decodability as follows:

In CC-HARQ (i.e., type-III HARQ process with one redundancy version), all the coded bits for the initial transmission are reused for retransmissions. Therefore, it is also called as repetition time diversity scheme. This scheme can get SNR gain with easy hardware implementation. Moreover, it generally requires smaller buffer size in a receiver than PIR-HARQ and FIR-HARQ.

In PIR-HARQ (i.e., type-III HARQ process), a part of the coded bits for the initial transmission, mainly the systematic part, is utilized for retransmissions, while some additional parity bits are newly sent for each retransmission. It is able to obtain both SNR and coding gains.

Sometimes CC-HARQ is regarded as a special case of PIR-HARQ. Because both schemes send same information bits with same and different parity bits every retransmission for CC-HARQ and PIR-HARQ, respectively.

Since coding gain is more dominant than SNR gain in terms of performance, FIR-HARQ shows the best performance, and PIR-HARQ outperforms CC-HARQ as well.

Three common diversity combining schemes, namely, selection combining (SC), equal gain combining (EGC), and maximal ratio combining (MRC), entail various trade-offs between performance and complexity [2]. SC selects the branch with the highest SNR among the received signals, then used for detection. On the other hands, EGC co-phases and adds signal from the different antennas by fixing the weight. Thereby, it requires the perfect knowledge at the combiner of the signal phase.

MRC is comparatively deemed to be superior to the others because it maximizes output SNR by combining after optimal weighting proportional to individual SNRs. It

is mathematically similar to the principle of matched filter. It is also widely known that MRC shows the optimal performance for addictive white Gaussian noise (AWGN) channel in single-input single-output systems. However, the performance of MRC in AWGN channel is much degraded if it is employed in Rayleigh channel. Moreover, the most challenging one in MIMO systems is that symbols transmitted from each antenna interference with each other. Thereby, even if overall SNR is good, overall SINR can be unacceptable, and it makes MRC show worse performance even in AWGN channel for MIMO systems.

To overcome the drawback of MRC in MIMO systems, there are two types of combining schemes, symbol-level combining (SLC) or bit-level combining (BLC) based on whether combining is done before or after demodulation, respectively.

The examples of SLC schemes can be used for CC-HARQ and PIR-HARQ because of operation only when more than one transmit symbols are repeatedly transmitted. However, it is hard to combine with symbols every transmission because of different symbol every transmission for FIR-HARQ. Moreover, the required buffer in SLC scheme occupies larger memory in the receiver compared to BLC scheme.

Zheng *et al.* proposed a vertical BLAST-type SM MIMO systems with multiple HARQ processes instead of single HARQ process [18]. A single HARQ process jointly encodes the bit streams at the transmitter with a single CRC. Then, the resulting data streams are channel encoded and modulated into a packet. Finally, a packet is spatially multiplexed across the transmit antennas. If an error occurs, the entire packet has to be retransmitted because it depends on the single CRC over the whole packet. Retransmission of already correctly received subpackets waste throughput. On the other hand, in multiple HARQ processes, the bit streams are multiplexed at first. Each resulting bit stream is encoded with its own independent CRC. Then, each CRC encoded

bit is individually channel encoded and modulated into a packet. In the end, packets are independently transmitted into each transmit antenna. In other words, the multiple HARQ processes prevent wasteful retransmissions because each HARQ process retransmits packets independently [18–22] to enhance the throughput. Two sorts of HARQ processes for MIMO systems are illustrated in Fig. 1.1.

Onggosanusi *et al.* compared performance of two SLC schemes for single HARQ process, pre-combining and post-combining in MIMO systems with linear detection [35]. Pre-combining is operated before filtering but post-combining is performed after filtering in symbol-level. Through numerical results, pre-combining has better performance than post-combining.

However, since SLC is designed based solely on single HARQ condition, throughput is much worse with SLC scheme in multiple HARQ processes. Thereby, the log-likelihood ratio-based BLC (LLR-BLC) scheme is more profitable than SLC scheme in MIMO systems with multiple HARQ processes. Basically, the LLR-BLC scheme is operated after demodulation which consists of bit-level and LLR estimations. Due to this operation, it can be applicable no matter what type of HARQ process is used for MIMO systems.

Wang *et al.* proposed the BLC for LLR calculation to minimize the error propagation in MIMO systems with single HARQ process and IC detection [19]. Then, Jang *et al.* proposed a new LLR calculation method for both optimal SLC and BLC schemes for MIMO systems with single HARQ process. However, the complexity imposed in increases exponentially with both the number of bits per symbol and the number of transmit antennas [36].

To solve this probelm, Xia *et al.* proposed a novel BLC scheme based on Dempster-Shafer (DS) evidence theory, termed DS combining, for MIMO systems with multiple HARQ processes. The DS combining is assisted by the proposed DS detection for per-

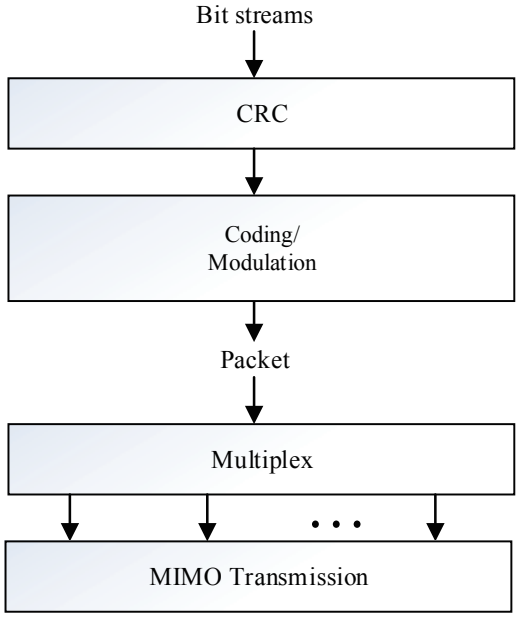

(a) Single HARQ.

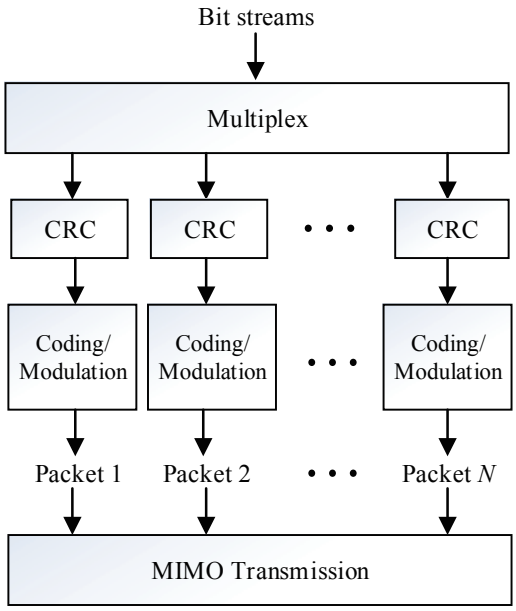

(b) Multiple HARQ.

Figure 1.1: Two types of HARQ processes in MIMO systems.

formance improvement. Therefore, more reliable decisions are achieved. It significantly outperforms its LLR combining with only moderate complexity increases [38]. Afterward, a DS-SLC is proposed in [39].

1.2 Motivations

The motivations of dissertation stems from the following three-fold observations.

Firstly, in HARQ with soft combining (i.e., type-II and type III-HARQ processes), the decoding probability of a packet depends on how many times it has been retransmitted; that is, instead of discarding the previously received packet detected to contain errors, a receiver buffers and refreshes erroneous packet by combining the soft information of the buffered packet of the previous transmission with that of the following retransmissions until it successfully decodes the original bit streams from received packet or until it reaches the maximum number of retransmission. Therefore, the probability of successful decoding of a retransmitted packet is higher than that of an initial packet. Especially, for a MIMO system with IC detection, the detection performances of the simultaneously transmitted data streams are mutually dependent [3, 4]. Therefore, in a MIMO system that employs IC detection with HARQ, the set of packets chosen from the transmission buffer during a packet transmission time interval (PTTI) will affect the system throughput, considering the fact that successful decoding of an initial packet is more rewarding whereas a retransmission packet is more likely to be decoded successfully than an initial packet [23]. Thereby, we need to take into consideration of the above characteristics of initial and retransmission packets in a MIMO system with IC detection and HARQ to find the transmission state for throughput improvement.

Secondly, if the maximum number of retransmission is more than one, the choice of

the set of packets from the packet queue that contains packets with various numbers of retransmission (i.e., initially transmitted packets, retransmitted packet, second retransmission, and so on) for simultaneous transmission during one PTTI will greatly affect the overall error performance and throughput. However, there are no existing strategies to optimize such choice of packets. Hence, transmission strategies based on specific criterion are necessary to extend the analysis for a more general case.

Thirdly, the basic approach to the combining scheme for CC-HARQ in MIMO systems is to interpret the entire MIMO channel matrices up to the current transmission as a single aggregated MIMO channel matrix, i.e. interpreting all system models up to the current transmission as single transmission model with a larger number of receive antennas [36], [37]. However, such a brute-force combining scheme requires a significantly higher computational complexity for detection than the conventional detection in MIMO systems without HARQ. To address the complexity issues, the post-combining and the pre-combining schemes were proposed for retransmissions in MIMO systems [35]. The post-combining scheme has a simpler detection structure than the pre-combining, but the latter outperforms the former for CC-HARQ in MIMO systems by achieving a lot more space diversity at the price of the complicated structure. Then, the work in [36] has shown that the pre-combining scheme achieves the identical performance to the brute-force combining scheme with a reduced computational complexity. To further reduce the computational complexity, the QR decomposition-based SLC (QRD-SLC) scheme was proposed, which has the same performance as the pre-combining scheme with a reduced computational complexity in case of the ML detection [37]. However, if linear detection such as the minimum mean square-error (MMSE), or zero-forcing (ZF) is considered instead of ML detection at the receiver, the QRD-SLC scheme can still require the additional computational complexity than the pre-combining scheme by performing the

QRD on the aggregated channel matrix in every retransmission. Moreover, to the best of our knowledge, there is little research work in the literature dealing with SLC schemes based solely on linear detection for CC-HARQ in MIMO systems [35].

1.3 Dissertation Outline

In this dissertation, we mainly focus on developing efficient HARQ transmission and combining schemes with IC and linear detections in MIMO systems in the aspect of performance and complexity, respectively. We develop a simple HARQ transmission state control algorithm for MIMO systems with IC detection in Chapter 2. However, it is assumed that only one HARQ retransmission for any packets is allowed. Therefore, to extend the analysis for a more general maximum allowable number of retransmission for a packet, a HARQ packet transmission strategy based on the concept of the effective interference level (EIL) is proposed in Chapter 3. The reduced complexity SLC scheme is proposed for CC-HARQ in MIMO systems with linear detection in Chapter 4. Finally, we draw conclusions and future work in Chapter 5.

1.4 List of Mathematical Notations

$(\cdot)^{-1}$	the inverse of a matrix
$(\cdot)^{T}$	the transpose of a matrix
$(\cdot)^{H}$	the conjugate-transpose or Hermitian of a matrix
$\|\cdot\|^2$	the squared norm of a matrix
$\mathrm{rank}(\cdot)$	the rank of a matrix
$\mathbb{E}[\cdot]$	the mathematical expectation
$(\mathbf{I})_N$	the identity matrix of dimension $N \times N$
$\binom{n}{k}$	the binomial coefficient, $\binom{n}{k} = \frac{n!}{k!(n-k)!}$ for $0 \leq k \leq n$

1.5 List of Abbreviations

ARQ	automatic repeat request
BER	bit error ratio
BLAST	Bell Laboratories layered space-time
BLC	bit-level combining
BP	belief propagation
CC	Chase combining
CRC	cyclic redundancy check
EIL	effective interference level
FEC	forward error correction
FER	frame error ratio
FIR	full incremental redundancy
HARQ	hybrid automatic repeat request
IC	interference cancellation
LDPC	low-density parity-check
LLR	log-likelihood ratio
MIMO	multiple-input multiple-output
ML	maximum-likelihood
MMSE	minimum mean square-error
PER	packet error ratio
PIR	partial incremental redundancy
PTTI	packet transmission time interval
QPSK	quadrature phase-shift keying
QRD	QR decomposition
SINR	signal-to-interference-plus-noise ratio

SLC	symbol-level combining
SM	spatial multiplexing
SMW	Sherman-Morrison-Woodbury
SNR	signal-to-noise ratio
ZF	zero-forcing

Chapter 2: HARQ Transmission State Control Algorithm for MIMO Systems with IC Detection

2.1 Introduction

In MIMO systems [2–4, 6, 13, 15–18, 20–22], IC detection is widely used to enhance the performance by eliminating the interference from each transmitted data stream. For MIMO systems with IC detection, it consists of multiple detection stages and the data stream estimated at the previous stage is utilized to cancel the interference of the other data streams at the next stage. Generally, the SNR gain due to IC is higher for the data stream with a lower detection probability.

HARQ [11–18, 20–23] schemes combine packet retransmission with FEC to ensure reliable communications. In such schemes, the decoding probability of a packet depends on how many times it has been retransmitted because of soft combining; that is, a receiver buffers and refreshes erroneous packet by combining the soft information of buffered packet of the previous transmission with that of the following retransmissions until either it successfully decodes the original bit streams from received packet or it reaches the maximum allowable number of retransmissions. Therefore, the probability of successful decoding of a retransmitted packet is higher than that of an initial packet. In terms of system throughput, successful decoding of an initial packet is more critical than successful decoding of a retransmission packet since retransmission requires additional time resources [23].

In a SM MIMO system with multiple HARQ processes, the simultaneously transmitted packets could have independent HARQ processes [18, 20–22] to enhance the throughput. In other words, the packet at each antenna can be independently coded and modulated, such that it can be independently retransmitted.

For a BLAST-type SM MIMO system with IC detection, the detection performances of the simultaneously transmitted data streams are mutually dependent [3, 4]. Therefore, in a MIMO system that employs IC detection and HARQ, the set of packets chosen from the transmission buffer during a PTTI will affect the system throughput, considering the fact that successful decoding of an initial packet is more rewarding whereas a retransmitted packet is more likely to be decoded successfully than an initial packet.

The goal of this thesis is to develop a HARQ transmission state control algorithm to improve the throughput of such a system [50]. The HARQ transmission state is defined as the distribution of the initial packets and the retransmission packets transmitted during a transmission time slot. The proposed algorithm generates the transmission state, where initial packets and retransmission packets are transmitted together to minimize the average error probability of the initial packets in a MIMO system with IC detection and HARQ.

2.2 System Model

Consider a vertical BLAST-type SM MIMO system with N_{T} transmit and N_{R} receive antennas for multiple HARQ communications. The number of packets transmitted simultaneously during any transmission time slot equals the number of transmit antennas. Each of the simultaneously transmitted packets has an independent HARQ retransmission process. For simplicity, we assume that only one retransmission is allowed for any

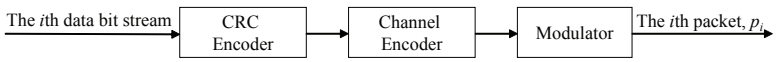

Figure 2.1: Packet generation process at the transmitter.

packets; thus, the packets at a given transmission time slot can be either an initial packet or a retransmission packet. Also, we assume that all the packets to be transmitted during the entire transmission time slots are stored in the transmission buffer and N_{T} packets from the buffer are selected for the transmission during each transmission time slot. Let p_i be the ith packet to be transmitted. Each p_i is generated from the packet generation process that includes the CRC encoder, the channel encoder, and the modulator. The system is illustrated in Fig. 2.1.

Let $\mathbf{P}_t$ with $|\mathbf{P}_t| = N_{\mathrm{T}}$ denote the set of the packets selected for transmission during the tth transmission time slot. Also, let $n_{t,i}^{\mathrm{rtx}}$ be the number of retransmissions of p_i at the tth transmission time slot, where $n_{t,i}^{\mathrm{rtx}} = 0$ or $n_{t,i}^{\mathrm{rtx}} = 1$ represents, respectively, that p_i is an initial packet or a retransmission packet. The HARQ transmission state at the tth transmission time slot, $S(t)$, is defined as the number of initial packets in $\mathbf{P}_t$, and is expressed as

$$S(t) = S_k \text{ with } k = \sum_{p_i \in \mathbf{P}_t} 1 - n_{t,i}^{\mathrm{rtx}}, \tag{2.1}$$

where S_k represents the HARQ transmission state with k initial packets.

The reception process will be applied to the entire $p_i \in \mathbf{P}_t$. After the reception process, an acknowledgement feedback index for each $p_i \in \mathbf{P}_t$ is generated and transmitted from the receiver to the transmitter. Let $a_{t,i}$ be the acknowledgement feedback index for $p_i \in \mathbf{P}_t$, where $a_{t,i} = 0$ and $a_{t,i} = 1$ represents that the decoded bit stream for $p_i \in \mathbf{P}_t$ has errors or is error-free, respectively. If $a_{t,i} = 1$, p_i will be eliminated from the transmis-

sion buffer; otherwise, p_i is eliminated from the transmission buffer only if it reaches the maximum number of retransmissions allowed. If $a_{t,i} = 0$ and $n_{t,i}^{\mathrm{rtx}} = 0$, then p_i becomes a retransmission packet from the next transmission time slot, and $n_{t',i}^{\mathrm{rtx}} = 1$ $(t' > t)$ for the t'th transmission time slot.

An iterative IC detection with BLC is used at the receiver. After combining with the LLR values stored in the LLR buffer after LLRs calculation is performed. After one turbo iteration (i.e., the given number of decoding iterations per turbo iteration), the IC operation is performed for all packets regardless of the decoding result of packets Thereby, CRC operation for IC detection is not necessary. It is very similar to turbo BLAST receiver operation with addition of deinterleaver except the BLC.

2.3 Proposed HARQ Transmission State Control Algorithm

The HARQ transmission state at the tth PTTI, $S(t)$, is defined as the number of initial packets in $\mathbf{P}_t$, and is expressed as

$$S(t) = S_k \text{ with } k = \sum_{p_i \in \mathbf{P}_t} 1 - n_{t,i}^{\mathrm{rtx}}, \tag{2.2}$$

where S_k represents the HARQ transmission state with k initial packets.

Before presenting the proposed transmission state control algorithm, we derive the relationship between the throughput and the average PER of HARQ employed MIMO systems. Let $\mathrm{TP_p}$ denote the throughput of the MIMO system that employs HARQ, defined as the average number of successfully decoded packets per PTTI. Then, $\mathrm{TP_p}$ can be calculated using the average decoding probability of packets divided by the average required number of PTTIs per packet. The average decoding probability can be cal-

culated by multiplying the average PERs of initial packets and retransmission packets. Note that in the system we are considering only one retransmission is allowed; that is, no additional transmissions are allowed for retransmission packets regardless of their decoding results. Therefore, the average required number of PTTIs per packet is determined by the average PER of the initial packets [23]. Since the system can transmit N_{T} packets simultaneously in one PTTI, $\mathrm{TP_p}$ is written as

$$\mathrm{TP_p} = \frac{N_{\mathrm{T}}(1 - \mathrm{PER_0PER_1})}{1 + \mathrm{PER_0}}, \tag{2.3}$$

where $\mathrm{PER_0}$ and $\mathrm{PER_1}$ denote the average PERs of initial packets and retransmission packets, respectively. It is clear from Eq. (2.2) that the effects of $\mathrm{PER_0}$ on $\mathrm{TP_p}$ is more significant than that of $\mathrm{PER_1}$. That is, the decoding success of an initial packet affects the throughput more than does the decoding success of a retransmission packet, since the average required transmission time per packet is determined by $\mathrm{PER_0}$ while the average decoding probability of a packet is determined by both $\mathrm{PER_0}$ and $\mathrm{PER_1}$.

In general, the successful decoding probability of a packet increases as the number of retransmissions increases [11,13–18,20–23], owing to the HARQ process, which allows the system to benefit from processes such as exploiting time diversity and packet combining for improved SNR. In other words, a retransmission packet is more likely to be decoded correctly than an initial packet. Therefore, if an IC detection scheme is utilized at the receiver, a retransmission packet is more likely to be cancelled correctly from the received signals in the IC process than an initial packet. That is, a packet is more likely to benefit from the IC process when the packet is transmitted together with a retransmission packet than with an initial packet. Therefore, as the opportunity of the simultaneous transmissions of initial packets and retransmission packets increases, $\mathrm{TP_p}$

can be improved by obtaining a lower PER_0 in the MIMO system with HARQ and IC.

We now verify the above observation about the system throughput improvement with the number of the simultaneous transmissions of initial packets and retransmission packets by using the relationship between PER_0 and the transmission states for MIMO systems that employ HARQ and IC detection. Let P_{S_k} for $0 \leq k \leq N_\mathrm{T}$ with $\sum_{k=0}^{N_\mathrm{T}} P_{S_k} = 1$ denote the probability of the transmission state S_k among all transmission states for each PTTI, that is, P_{S_k} is the number of S_k over the entire PTTIs divided by the number of the entire PTTIs. PER_0 can be written as a function of P_{S_k} as

$$\mathrm{PER}_0 = \frac{\sum\limits_{k=1}^{N_\mathrm{T}} kP_{S_k} \cdot \mathrm{PER}_0(S_k)}{\sum\limits_{k=1}^{N_\mathrm{T}} kP_{S_k}}, \tag{2.4}$$

where $\mathrm{PER}_0(S_k)$ is the average PER of the initial packets transmitted when the transmission state is S_k and kP_{S_k} is the average number of the initial packets per PTTI, when the transmission state is S_k. Since a retransmission packet in general has a higher reliability than an initial packet, it can be assumed that $\mathrm{PER}_0(S_k)$ increases with k, i.e.,

$$\mathrm{PER}_0(S_1) \leq \mathrm{PER}_0(S_2) \leq \cdots \leq \mathrm{PER}_0(S_{N_\mathrm{T}}). \tag{2.5}$$

Eqs. (2.4) and (2.5) imply that it is feasible to have a higher P_{S_k} as k is getting smaller in order to obtain a better PER_0 and TP_p; that is, $P_{S_{N_\mathrm{T}}}$, which sends only the initial packets and therefore has the largest number of the initial packets among all the possible transmission states, should be considered as the last option to select if other P_{S_k} with $1 \leq k \leq (N_\mathrm{T} - 1)$ is possible for selection. This shows that the above observation about the system throughput improvement with the number of the simultaneous transmissions

Table 2.1: Proposed transmission state control algorithm

Step 1)	Initialization: Form an empty set $\mathbf{P}_t$.
Step 2)	Find S_k: If there are no initial packets in the transmission buffer, then set $k = 0$. Otherwise, find the minimum positive integer k that satisfies $(k + N^{\mathrm{rtx}}) \geq N_{\mathrm{T}}$, where N^{rtx} is the number of retransmission packets in the transmission buffer prior to the tth transmission time slot.
Step 3)	Set S_k as $S(t)$: With k from Step 2), set $S(t) = S_k$.
Step 4)	Assign initial packets to $\mathbf{P}_t$: Find p_i with $n_{t,i}^{\mathrm{rtx}} = 0$ that has the minimum i among the entire initial packets in the transmission buffer, and assign p_i as the member of $\mathbf{P}_t$. Repeat this step until $\lvert\mathbf{P}_t\rvert$ reaches k.
Step 5)	Assign retransmission packets to $\mathbf{P}_t$: Find p_i with $n_{t,i}^{\mathrm{rtx}} = 1$ packets that has the minimum i among the entire retransmission in the transmission buffer, and assign p_i as the member of $\mathbf{P}_t$. Repeat this step until $\lvert\mathbf{P}_t\rvert$ reaches N_{T}.

of initial packets and retransmission packets is valid for MIMO systems that employ HARQ and IC detection.

Now, we develop a transmission state control algorithm, aiming to increase the opportunities of simultaneous transmissions of initial packets and retransmission packets on entire PTTIs. The proposed algorithm is summarized in Table 2.1. For simplicity of notation, it is assumed in Table 2.1 that there are always at least N_{T} packets in the transmission buffer regardless of t. First, before the transmission in the tth PTTI, among all of the transmission states $S_k, 0 \leq k \leq N_{\mathrm{T}}$, search for possible candidates as $S(t)$ based on the number of retransmission packets in the transmission buffer. Then, among all of the possible candidates, selects S_k with the smallest positive integer k as $S(t)$, since $\mathrm{PER}_0(S_k)$ decreases with k as shown previously; that is, among all the possible

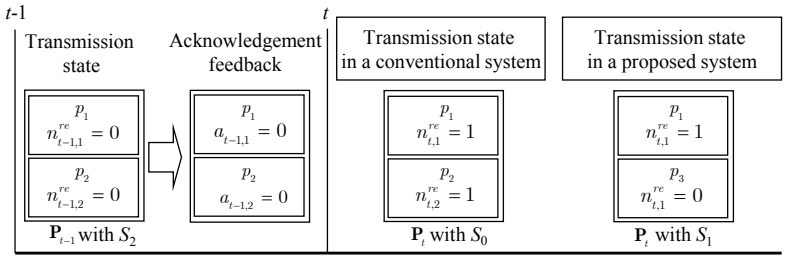

Figure 2.2: An example of the transmission states at the tth PTTI ($N_{\mathrm{T}} = 2$, $S(t-1) = S_2$, and $a_{t-1,i} = 0\ \forall p_i \in \mathbf{P}_{t-1}$).

transmission states that transmit simultaneous initial packets and retransmission packets, the proposed algorithm selects the transmission state that will result in minimum error probability for the initial packets. If no such S_k is possible with a positive integer k, then the proposed algorithm selects S_0, which consists of only retransmission packets only, as $S(t)$. Note that in the proposed algorithm, S_0 will be selected as $S(t)$ only when there are no remaining initial packets in the transmission buffer. If there is at least one retransmission packet in the buffer, then $S_{N_{\mathrm{T}}}$ will not be selected as $S(t)$. Finally, with a given $S(t)$, $\mathbf{P}_t$ is determined by using the packets in the transmission buffer. Since the index i indicates the order of p_i among all the packets to be transmitted, the packets with the lowest orders in the transmission buffer are selected for $\mathbf{P}_t$.

Fig. 2.3 shows an example of the transmission state at the tth PTTI, where $N_{\mathrm{T}} = 2$, $S(t-1) = S_2$, and the initial packets transmitted during the $(t-1)$th PTTI encounter a decoding failure, i.e., $a_{t-1,i} = 0$ for any $p_i \in \mathbf{P}_{t-1}$. In this case, the conventional system will generally retransmit the previously failed packets [18, 20]; $S(t) = S_0$ in a conventional system. With the proposed algorithm, $S(t) = S_1$ according to the procedure described in Table I. Therefore, the proposed algorithm tends to transmit simultaneously initial packets and retransmission packets, resulting in an increased throughout than the conventional system.

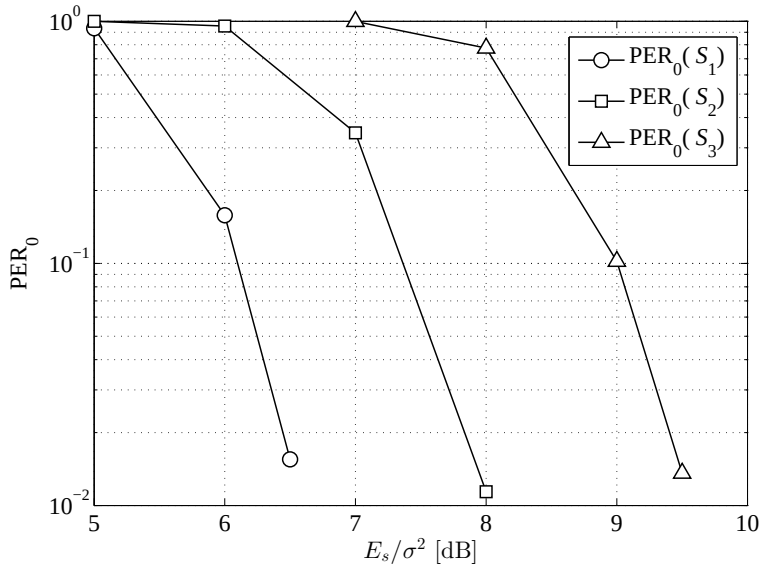

Figure 2.3: Average PERs of the initial packets in each of HARQ transmission states.

As shown in Table 2.1 and Fig. 2.3, the proposed algorithm selects the transmission state that can decrease PER_0 to improve TP_p. To implement this transmission state control, as shown in Fig. 2.3, some of the retransmission packets might have a longer queuing delay in the transmission buffer than the conventional system. In the next section, we will show via simulation that the increased queuing delay with the proposed algorithm is negligible.

2.4 Simulation Results

Parameters chosen for the simulation: $N_\mathrm{T} = N_\mathrm{R} = 3$, CRC-24 with the generator polynomial $g(x) = x^{24} + x^{23} + x^6 + x^5 + x + 1$ is considered in the CRC encoder, and the LDPC code in [10] with a code rate of 3/4 and a codeword length of 768 bits is adopted as the channel encoder. LDPC encoded bit streams are QPSK modulated and transmitted

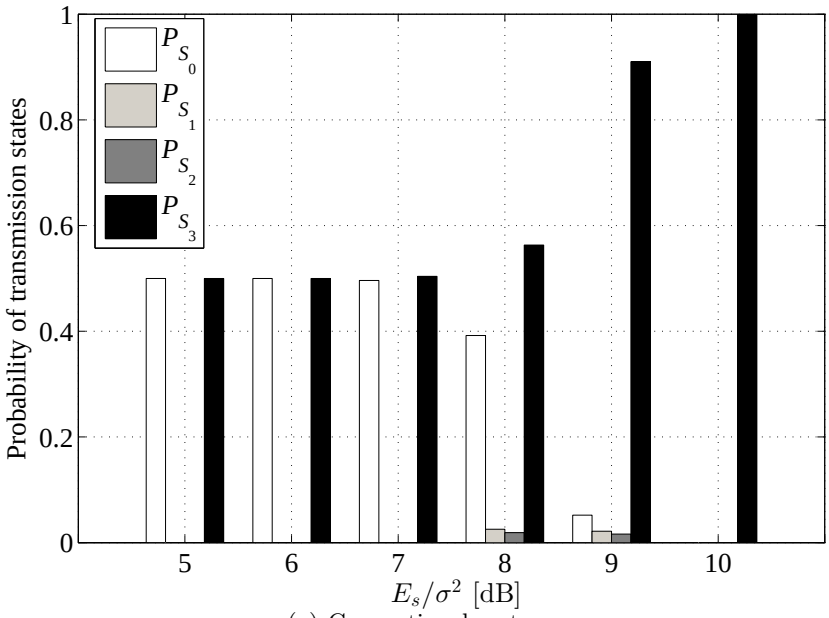

(a) Conventional system.

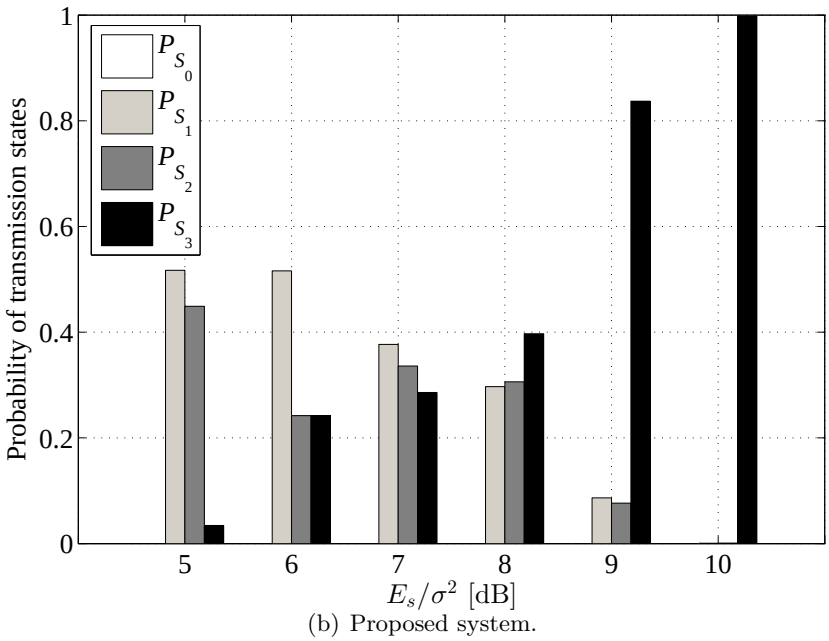

(b) Proposed system.

Figure 2.4: Distributions of the transmission states.

over independent Rayleigh fast fading channels. For every transmit signal vector, the MIMO channel varies independently. CC [11] is adopted to process the retransmitted packets. The iterative IC detection scheme [4] is implemented at the receiver, where the number of turbo iterations is set to 4. In each turbo iteration, the LLR calculation is performed after interference cancellation and the linear MMSE filtering. The calculated LLRs of a retransmission packet are combined with the LLRs calculated for its initial transmission that were stored in the receiver buffer. The combined LLRs are then utilized in the channel decoder that implements the BP decoding algorithm [25], where the number of the BP decoding iterations for each packet per turbo iteration is set to 20. At the end of the reception process, the acknowledgement feedback indices are transmitted through an error-free feedback channel.

Fig. 2.3 shows the average PERs of the initial packets in each of possible HARQ transmission states. Note that for state S_k, there are k initial packets and $(N_{\mathrm{T}} - k)$ retransmission packets. Since there are no initial packets transmitted in S_0, the results for S_0 are not shown. It is observed that if k initial packets decrease, $\mathrm{PER}_0(S_k)$ decreases as $(N_{\mathrm{T}} - k)$ retransmission packets increase. This shows that the average PER of initial packets can improve, as the opportunity of simultaneous transmission of initial and retransmission packets increases.

The distributions of the transmission states in the conventional and the proposed systems are shown in Figs. 2.4(a) and 2.4(b), respectively. As shown in Fig. 2.4(a), most of the initial packets in the conventional system are transmitted during state S_3, regardless of the SNR values. Note that S_3 has the highest average PERs for the initial packets among all the states (refer to $\mathrm{PER}_0(S_k)$ in Fig. 2.3). However, as shown in Fig. 2.4(b), P_{S_0}, which is the probability of the state that only transmits retransmission packets, greatly decreases and P_{S_1} and P_{S_2}, which are the probabilities of the states that

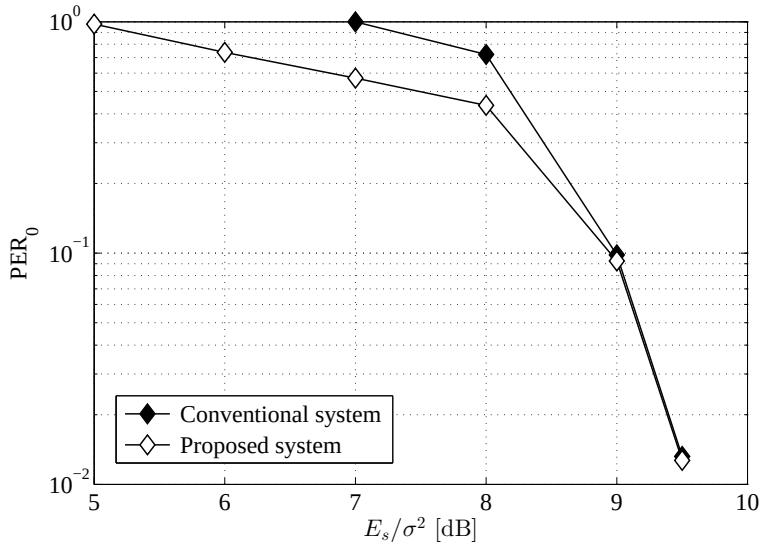

Figure 2.5: Average PERs of the initial packets in the proposed and the conventional systems.

transmit both initial and retransmission packets, significantly increase by the proposed algorithm compared with the case in Fig. 2.4(a). It is worthwhile to mention that the probabilities of the simultaneous transmissions of initial packets and retransmission packets, i.e., P_{S_1} and P_{S_2}, by the proposed algorithm are reduced as the operating SNR increases, since a retransmission of a packet is less likely to occur as SNR increases.

Fig. 2.5 illustrates the average PERs of the initial packets in the conventional and the proposed systems. As expected from the results in Fig. 2.3 and Fig. 2.4, the proposed system has an improved PER_0 compared with the conventional system. Due to the same reason for the cases in Figs. 2.4(a) and 2.4(b), both systems have similar PER_0 in the high operating SNR region, but the proposed system outperforms the conventional system in terms of PER_0 in the low and the middle SNR regions.

The results in Figs. 2.3–2.5 show that the system throughput will improve by implementing the proposed algorithm. This is demonstrated in Fig. 2.6, which compares the

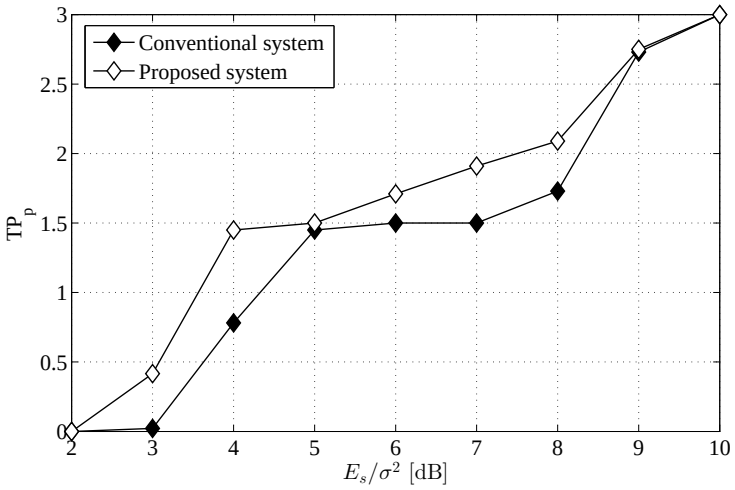

Figure 2.6: Average throughputs of the proposed and the conventional systems.

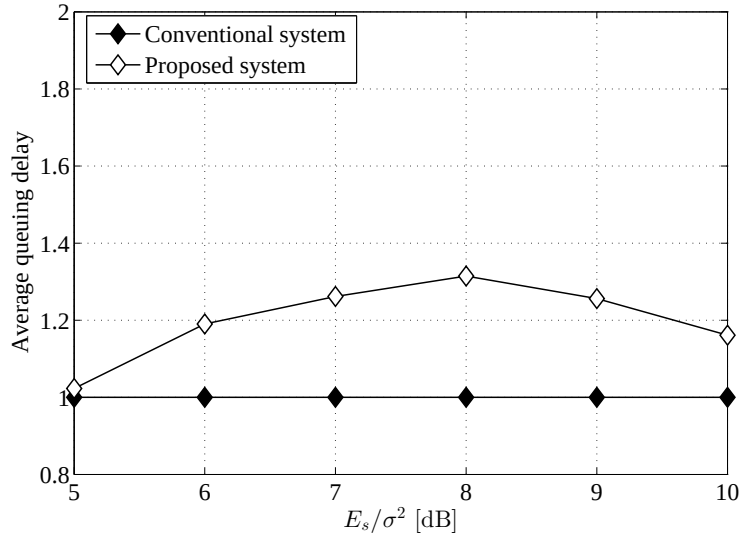

Figure 2.7: Average queuing delays of the retransmission packets in the proposed and the conventional systems.

average throughput of the proposed system and the conventional system. Specifically, the maximum improvement of $\mathrm{TP_p}$ (in percentage) through the proposed algorithm is about 28% at the SNR of 7 dB. Therefore, it is verified that increasing the probabilities of the simultaneous transmissions of initial packets and retransmission packets, i.e., increasing P_{S_1} and P_{S_2} in our simulation environments, can improve the throughput of HARQ employed MIMO systems with an IC detection.

Finally, in Fig. 2.7, the average queuing delays of the retransmission packets in the proposed and the conventional systems are compared. The average queuing delay is defined as the average number of elapsed PTTIs between the initial transmission and the retransmission of a packet. As shown in Fig. 2.7, the proposed system has a slightly longer average queuing delays than the conventional system, but the average queuing delay gap between them is quite small (about 0.3 maximum PTTI per retransmission packet). Note that the average queuing delay of the retransmission packets in the conventional system equals 1 regardless of the SNR values, because an initial packet, if decoding has errors, is always retransmitted during the next PTTI.

2.5 Conclusion

A simple HARQ transmission state control algorithm has been developed for MIMO systems with IC detection. By increasing the opportunity of simultaneous transmissions of initial packets and retransmission packets, the proposed algorithm improves the average PER of the initial packets, and thus enhances the throughput. Simulation results highlight the superiority of our proposed scheme. Since the only information required to implement the proposed algorithm is the number of retransmissions of the packets in the transmission buffer, it is very simple to implement.

Chapter 3: EIL-based Packet Transmission for MIMO Systems with HARQ and IC Detection

3.1 Introduction

In Chapter 2, we have proposed a simple HARQ transmission state control algorithm for MIMO systems with IC detection in order to improve the performance [50].

By the way of contrast, this proposed algorithm is not sufficiently profitable for general wireless communication standards. Because the maximum allowable number of retransmissions is limited to one. If the maximum number of allowable retransmission is more than one, the choice of the set of packets from the packet queue that contains packets with various number of retransmission for simultaneous transmission during one PTTI will affect the overall error performance and throughput. In this thesis, in order to extend the analysis for a more general case, a specific criterion based packet transmission strategy is proposed for BLAST-type SM MIMO systems with IC detection and multiple HARQ processes [51]. We first introduce a concept of the EIL, and establish a relationship between EIL and the effective SINR. We then show that maximizing the throughput can be transformed into successively minimizing the average EIL from the lowest to the highest ARQ round. Therefore, in order to improve the system throughput, the proposed packet transmission strategy selects a set of packets that successively minimize the EIL. This provides an effective and simple way to optimize the transmission for better performance than the conventional HARQ.

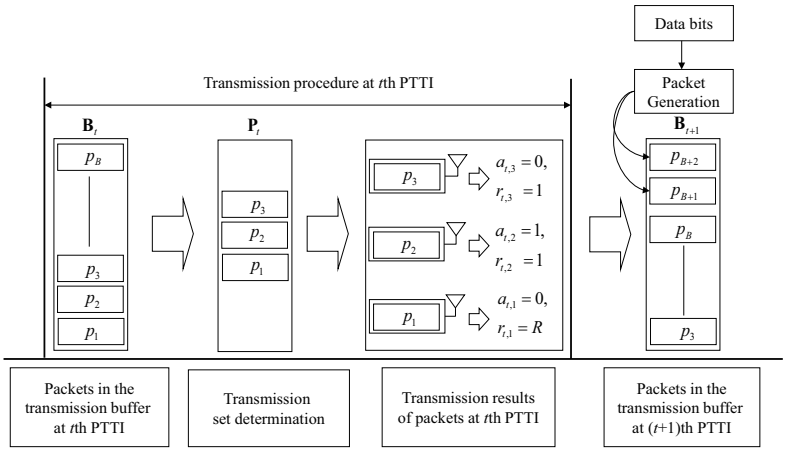

Figure 3.1: Transmission process with three independent CC.

3.2 System Model

A SM MIMO system with multiple HARQ processes and vertical BLAST architecture [3] is considered in this thesis, where the numbers of transmit and receive antennas are N_{T} and N_{R} ($\geq N_{\mathrm{T}}$), respectively. During one PTTI, N_{T} packets are simultaneously transmitted through the N_{T} transmit antennas and the symbol stream for each packet is sent from one of the transmit antennas.

We define some notations that will be used throughout the rest of this thesis as follows:

- T: the last PTTI for the entire transmission process, i.e., no more transmissions are required after the Tth PTTI ($1 \leq t \leq T$).
- p_i: a packet from the ith data bit stream generated through the packet generation process ($1 \leq i \leq TN_{\mathrm{T}}$).
- $r_{t,i}$ ($= n_{t,i}^{\mathrm{rtx}} + 1$): the number of times p_i has been transmitted up to the tth PTTI ($1 \leq i \leq TN_{\mathrm{T}}$).

- R: the maximum allowable number of transmissions (the highest HARQ round) per a packet ($1 \leq r_{t,i} \leq R$).
- $\mathbf{B}_t$: the set of packets in the transmission buffer before the tth PTTI in Fig. 3.1.
- $\mathbf{P}_t$: the set of packets generated from $\mathbf{B}_t$ with $|\mathbf{P}_t| = N_{\mathrm{T}}$ for the transmission in the tth PTTI ($\mathbf{P}_t \subseteq \mathbf{B}_t$).
- $\mathbf{P}_{t,r}$: the subset of $\mathbf{P}_t$ that includes all $p_i \in \mathbf{P}_t$ with $r_{t,i} = r$.

Through the packet generation process, K bits for the ith packet are CRC coded at first; then the resulting data stream is channel encoded, for example, by using a LDPC code, into a sequence of C bits; finally, the channel coded bit stream is modulated into a sequence of L symbols for p_i, where $Q = C/L$ is the number of coded bits per symbol.

The transmission buffer size B is fixed to $|\mathbf{B}_t|$, and it is assumed that the buffer is always filled up. Among the entire B ($\geq N_{\mathrm{T}}$) packets in the transmission buffer, the transmitter chooses N_{T} packets for the transmission in the tth PTTI. If $B = N_{\mathrm{T}}$, then the transmitter should choose the entire packets in the transmission buffer for the transmission in the tth PTTI. This corresponds to the conventional HARQ retransmission strategy which immediately retransmits the packets failed at the previous transmissions. Then, upon completing the reception process for the tth PTTI, for each $p_i \in \mathbf{P}_t$ the receiver sends an acknowledgement message $a_{t,i}$ to the transmitter, where $a_{t,i} = 0$ or 1 represents that p_i has errors or no errors, respectively. If p_i is transmitted during the tth PTTI, then this transmission becomes the $r_{t,i}$th HARQ round of p_i. If $a_{t,i} = 1$, or $a_{t,i} = 0$ but $r_{t,i}$ reaches R, then $p_{i'}$, a next packet instead of p_i, is included in $\mathbf{B}_{t+1}$ with $r_{t+1,i'} = 1$. Otherwise, if $a_{t,i} = 0$ and $r_{t,i} < R$, then p_i is included in $\mathbf{B}_{t+1}$ with $r_{t+1,i} = r_{t,i} + 1$. If $p_i \in \mathbf{B}_t$ but $p_i \notin \mathbf{P}_t$, p_i is included in $\mathbf{B}_{t+1}$ and $r_{t+1,i} = r_{t,i}$, since

p_i was not transmitted during the tth PTTI. An example of the HARQ transmission process with CC [10, 11] for the above system model is illustrated in Fig. 3.1.

Now, we develop the MIMO symbol transmission model and the reception process. Let $s_{i,r,l}$ for $1 \leq l \leq L$ denote the lth transmit symbol for p_i at its rth HARQ round. The retransmission of a packet is performed by CC, i.e., the transmitted symbols of $p_i \in \mathbf{P}_t$ with $r_{t,i} > 1$ are identical to the transmitted symbols of $p_i \in \mathbf{P}_{t'}$ with $t' < t$ and $r_{t',i} = 1$, thereby the index r can be omitted. Also, without loss of generality, the index l is omitted throughout the remainder. Consequently, s_i denotes the transmit symbol for p_i. Let $\mathbf{s}_t$ denote the $N_{\mathrm{T}} \times 1$ transmit signal vector during the tth PTTI which includes all the transmit symbols for the entire N_{T} packets in $\mathbf{P}_t$, i.e., all s_i with $p_i \in \mathbf{P}_t$. Then, the relationship between the transmit signal vector and the receive signal vector during the tth PTTI can be written as

$$\mathbf{y}_t = \mathbf{H}_t \mathbf{s}_t + \mathbf{n}_t, \tag{3.1}$$

where $\mathbf{y}_t$ is the $N_{\mathrm{R}} \times 1$ receive signal vector and $\mathbf{H}_t$ is the $N_{\mathrm{R}} \times N_{\mathrm{T}}$ channel matrix for $\mathbf{s}_t$. $\mathbf{n}_t$ is the $N_{\mathrm{R}} \times 1$ noise vector whose elements are complex Gaussian random variables with zero mean and variance σ^2.

In Fig. 3.2, the BLC [18, 20] based reception process with IC at the tth PTTI is illustrated. First, $\mathbf{y}_t$ is passed through the linear filter such as the MMSE filter or the ZF filter, and the LLR values for the coded bits of each $p_i \in \mathbf{P}_t$ are calculated from the filtered outputs. Then, for any $p_i \in \mathbf{P}_t$ transmitted more than one rounds, the LLRs calculated from $\mathbf{y}_t$ are combined with the LLRs stored in the LLR buffer. Then, based on its combined LLRs, each $p_i \in \mathbf{P}_t$ is decoded using the iterative decoder for the adopted channel code and the decoded bit streams for $p_i \in \mathbf{P}_t$ are sequentially generated

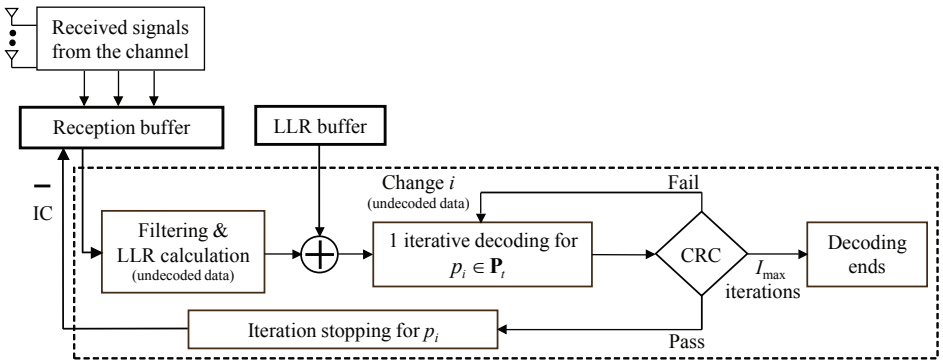

Figure 3.2: BLC-based reception process of the system.

at each decoding iteration. Then, the CRC is performed for the decoded bit stream at each decoding iteration and IC is performed when the CRC decoder finds a decoded bit stream detected as error-free [5]. For example, let p_f denote the first packet among the N_{t} packets in $\mathbf{P}_t$ detected as error-free during the reception process for the tth PTTI and $\hat{s}_f$ denote the regenerated transmit symbol for p_f using its decoded bit stream. Then, the IC operation is performed as

$$\mathbf{y}_{t,1} = \mathbf{y}_t - \mathbf{h}_{t,z(t,s_f)}\hat{s}_f, \tag{3.2}$$

where $\mathbf{y}_{t,1}$ is the receive signal vector for the tth PTTI after the first IC operation and $\mathbf{h}_{t,z(t,s_f)}$ is the $N_{\mathrm{R}} \times 1$ vector corresponding to the channel that p_f was transmitted over during the tth PTTI, i.e., s_f was sent from the $z(t, s_f)$th transmit antenna during the tth PTTI. Then, after the IC operation, the LLRs of the remaining packets, i.e., all $p_i \in \mathbf{P}_t$ except p_f, are recalculated using $\mathbf{y}_{t,1}$, and the combining and iterative decoding processes are performed again for the remaining packets using the recalculated LLRs. These whole procedures are repeated until a stopping criterion is satisfied, e.g., the number of executed decoding iterations reaches the number of maximum decoding iterations, $I_{\max}$. Finally,

the LLRs of the unsuccessfully decoded $p_i \in \mathbf{P}_t$ with $r_{t,i} < R$ are stored in the LLR buffer.

3.3 Proposed EIL-based Packet Transmission Strategy

3.3.1 Analysis of System Characteristics

In this section, we analyze the characteristics of the MIMO system with IC detection and HARQ described in Sec. 3.2. First, using the pre-detection average interference level and the average received SINR of the transmitted symbols, it will be shown that the choices of $\mathbf{P}_t$ at the transmitter do not affect the performance of the MIMO system without IC. Then, it will be shown that the instantaneous EIL and the effective SINR can be represented by $\mathbf{P}_t$, which indicates that the performance of the MIMO system with IC detection can be affected by the choices of $\mathbf{P}_t$ at the transmitter. Finally, based on the previously obtained results, we will show that the problem of maximizing the system throughput can be transformed into a successive optimization of the instantaneous EILs from the lowest to the highest HARQ round, which implies the possibilities of throughput improvements for the MIMO system with IC detection and HARQ by the choices of $\mathbf{P}_t$.

Let SINR_r denote the average received SINR of the transmitted symbols per receive antenna before the linear filtering, where the transmitted symbols are included in p_i with $r_{t,i} = r$. Also, let E_s be the average symbol energy, i.e., $\mathbb{E}[|s_i|^2] = E_s$ for any s_i. Finally, we assume that all elements of $\mathbf{H}_t$ are complex Gaussian random variables with zero mean and unit variance and $\mathbf{H}_t$ varies independently every transmission. Then, the mth

$(1 \leq m \leq N_{\mathrm{R}})$ element of $\mathbf{y}_t$, $y_{t,m}$, can be written as

$$y_{t,m} = \sum\nolimits_{s_i \in \mathbf{s}_t} h_{t,m,z(t,s_i)} s_i + n_{t,m}, \tag{3.3}$$

where $h_{t,m,z(t,s_i)}$ is the element at the mth row and the $z(t,s_i)$th column of $\mathbf{H}_t$ and $n_{t,m}$ is the mth element of $\mathbf{n}_t$. Therefore, $\mathbb{E}[|n_{t,m}|^2] = \sigma^2$, $\mathbb{E}[|s_i|^2] = E_s$, and $\mathbb{E}[|h_{t,m,z(t,s_i)}|^2] = 1$, also $h_{t,m,z(t,s_i)}$ and s_i are independent of each other regardless of t, m, $z(t,s_i)$, and i. Therefore, for a given m, the average symbol energy of all p_i with $r_{t,i} = r$ in $y_{t,m}$ for $1 \leq t \leq T$ is equal to $\sum_{t=1}^{T} \sum_{\{i|p_i \in \mathbf{P}_{t,r}\}} \mathbb{E}[|h_{t,m,z(t,s_i)} s_i|^2] / \sum_{t=1}^{T} |\mathbf{P}_{t,r}| = \sum_{t=1}^{T} |\mathbf{P}_{t,r}| E_s / \sum_{t=1}^{T} |\mathbf{P}_{t,r}| = E_s$, and the average noise power for $1 \leq t \leq T$ is $\sum_{t=1}^{T} \mathbb{E}[|n_{t,m}|^2]/T = \sigma^2$. Since the above results are valid regardless of m, SINR_r can be written as

$$\mathrm{SINR}_r = \frac{E_s}{I_r E_s + \sigma^2}, \tag{3.4}$$

where I_r is the pre-detection average interference level of the transmitted symbols per receive antenna. The interference of each symbol comes from other simultaneously transmitted symbols; that is, for any $p_i \in \mathbf{P}_t$ with $r_{t,i} = r$, the interference of p_i comes from the other packets in $\mathbf{P}_t$. Then, I_r is defined as the ratio of the total amount of interference of any $p_i \in \mathbf{P}_t$ with $r_{t,i} = r$ and the number of $p_i \in \mathbf{P}_t$ with $r_{t,i} = r$. Let T be the last PTTI for the entire transmission process, i.e., no more transmissions are required after the Tth PTTI. Then, I_r can be written as

$$I_r = \frac{\sum_{t=1}^{T} \sum_{k=1}^{|\mathbf{P}_{t,r}|} \hat{I}_{t,r,k}}{\sum_{t=1}^{T} |\mathbf{P}_{t,r}|}, \tag{3.5}$$

where $\mathbf{P}_{t,r}$ is a subset of $\mathbf{P}_t$ that includes all $p_i \in \mathbf{P}_t$ with $r_{t,i} = r$ and $\hat{I}_{t,r,k}$ is the pre-detection instantaneous interference level of the kth element of $\mathbf{P}_{t,r}$. Since $I_r E_s$ is the

total amount of interference power and E_s is the average energy per interfering symbol, I_r and $\hat{I}_{t,r,k}$ are determined by the number of interfering symbols per transmitted symbol for $p_i \in \mathbf{P}_{t,r}$. Therefore, no matter what the values of t and k are, $\hat{I}_{t,r,k}$ is written as

$$\hat{I}_{t,r,k} = N_{\mathrm{T}} - 1. \tag{3.6}$$

Eq. (3.6) implies that the choices of $\mathbf{P}_t$ at the transmitter affect neither the pre-detection average interference level nor the average received SINR of the transmitted symbols. However, if IC is employed at the receiver, then there is a mutual dependence among the error performance of the simultaneously transmitted symbols. In this case, the impact of the choices of $\mathbf{P}_t$ on the system performance is not observed from the pre-detection average interference level or the average received SINR of each transmitted symbol. Therefore, instead of using SINR_r, I_r, and $\hat{I}_{t,r,k}$, we need to define another measure to assess the impact of the choices of $\mathbf{P}_t$ on the system performance.

Let $\hat{I}_{\mathrm{ef}_{t,r,k}}$ denote the instantaneous EIL of the kth packet of $\mathbf{P}_{t,r}$ before IC for the kth packet begins, which is defined as the expected number of the interfering packets before IC for the kth packet of $\mathbf{P}_{t,r}$ begins. Also, here we assume that IC of a packet begins only if this packet is error-free. Therefore, the order of the IC process is determined by the error probability of each packet; a packet with a higher SINR is detected before one with a lower SINR. Then $\hat{I}_{\mathrm{ef}_{t,r,k}}$ is determined by packets with a lower SINR than the kth element of $\mathbf{P}_{t,r}$. Let $\mathbf{P}^*_{t,r,k}$ represent a subset of $\mathbf{P}_t$ that contains the packets whose instantaneous error probabilities, i.e., PER, are lower than the error probability of the kth element of $\mathbf{P}_{t,r}$. We have

$$\hat{I}_{\mathrm{ef}_{t,r,k}} = \left(\sum\nolimits_{l=1}^{|\mathbf{P}^*_{t,r,k}|} \hat{P}_{\mathrm{er}_{\mathbf{P}^*_{t,r,k}(l)}} \right) + |\mathbf{P}_t - \mathbf{P}^*_{t,r,k}| - 1, \tag{3.7}$$

where $\hat{P}_{\mathrm{er}_{\mathbf{P}^*_{t,r,k}{}^{(l)}}}(0 \leq \hat{P}_{\mathrm{er}_{\mathbf{P}^*_{t,r,k}{}^{(l)}}} \leq 1)$ is the instantaneous error probability of the lth packet of $\mathbf{P}^*_{t,r,k}$. The normalized average EIL of the transmitted symbols in p_i with $r_{t,i} = r$ per receive antenna is defined as

$$I_{\mathrm{ef}_r} = \frac{\sum_{t=1}^{T}\left(\sum_{k=1}^{|\mathbf{P}_{t,r}|}\left(\sum_{l=1}^{|\mathbf{P}^*_{t,r,k}|}\hat{P}_{\mathrm{er}_{\mathbf{P}^*_{t,r,k}{}^{(l)}}}\right)+|\mathbf{P}_t-\mathbf{P}^*_{t,r,k}|-1\right)}{\sum_{t=1}^{T}|\mathbf{P}_{t,r}|}. \tag{3.8}$$

By replacing I_r in Eq. (3.4) by I_{ef_r} in Eq. (3.8), the average received effective SINR of the transmitted symbols in p_i with $r_{t,i} = r$ per receive antenna is written as

$$\mathrm{SINR}_{\mathrm{ef}_r} = \frac{E_s}{I_{\mathrm{ef}_r}E_s + \sigma^2}. \tag{3.9}$$

Note that if no IC is employed at the receiver, then $\hat{I}_{\mathrm{ef}_{t,r,k}} = \hat{I}_{t,r,k}$, $I_{\mathrm{ef}_r} = I_r$, and $\mathrm{SINR}_{\mathrm{ef}_r} = \mathrm{SINR}_r$; that is, the choice of $\mathbf{P}_t$ does not affect the system performance.

Next, we analyze the relationship between the system throughput and I_{ef_r}. Let $\mathrm{TP_b}$ denote the throughput, defined as the number of successfully decoded data bits per PTTI, expressed as

$$\mathrm{TP_b} = K \cdot \mathrm{TP_p}(\mathrm{bits/s/Hz}), \tag{3.10}$$

where K is the number of data bits per packets. Note that $\mathrm{TP_p}$ is also the average

number of successfully decoded packets per PTTI, which can be written as

$$\begin{aligned}
\mathrm{TP_p} &= \frac{\text{The number of successfully decoded packets}}{\text{The number of PTTIs}} \\
&= \frac{N_\mathrm{T} \cdot (\text{Average decoding success probability of packets})}{\text{Average required PTTIs per packet}} \\
&= \frac{N_\mathrm{T}(1 - P_{\mathrm{er}_1} P_{\mathrm{er}_2} \cdots P_{\mathrm{er}_R})}{1 + P_{\mathrm{er}_1} + P_{\mathrm{er}_1} P_{\mathrm{er}_2} + \cdots + P_{\mathrm{er}_1} P_{\mathrm{er}_2} \cdots P_{\mathrm{er}_{R-1}}} \\
&= \frac{N_\mathrm{T} - N_\mathrm{T} \prod_{r=1}^{R} P_{\mathrm{er}_r}}{1 + \sum_{k=1}^{R-1} \prod_{r=1}^{k} P_{\mathrm{er}_r}},
\end{aligned} \tag{3.11}$$

where $P_{\mathrm{er}_r} (0 \leq P_{\mathrm{er}_r} \leq 1)$ is the average PER of the packets at their rth HARQ round. Note that a maximum of R transmissions is allowed per packet. Therefore, P_{er_R} does not affect the average number of required PTTIs per packet, since all packets will be terminated after their Rth HARQ round.

If the received SINR is sufficiently high so that the average decoding success probability considering HARQ effects approaches 1, i.e., $\prod_{r=1}^{R} P_{\mathrm{er}_r} = 0$, then, the numerator of Eq. (3.11) equals N_T and the maximization problem of $\mathrm{TP_p}$ can be written as

$$\max(\mathrm{TP_p}) = \min \left(\sum\nolimits_{k=1}^{R-1} \prod\nolimits_{r=1}^{k} P_{\mathrm{er}_r} \right). \tag{3.12}$$

Since the probability of successfully decoding a packet increases with the packet's SINR [24], P_{er_r} is a decreasing function of the average SINR of the packets at the rth HARQ round. Also, as shown by Eqs. (3.7)–(3.9), $\mathrm{SINR}_{\mathrm{ef}_r}$, instead of SINR_r, can be considered as the performance metric for the system with IC detection. Let P_{er_r} be the decreasing function of $\mathrm{SINR}_{\mathrm{ef}_r}$, i.e., $P_{\mathrm{er}_r} = f_r(\mathrm{SINR}_{\mathrm{ef}_r})$ with $f_r^{'}(\mathrm{SINR}_{\mathrm{ef}_r}) \leq 0$.

Then, Eq. (3.12) can be rewritten as

$$\max(\mathrm{TP_p}) = \min\left(\sum_{k=1}^{R-1}\prod_{r=1}^{k} f_r(\mathrm{SINR}_{\mathrm{ef}_r})\right). \tag{3.13}$$

It is clear from Eqs. (3.11)–(3.13) that the impact of P_{er_r} and $\mathrm{SINR}_{\mathrm{ef}_r}$ on $\mathrm{TP_p}$ rapidly grows as r decreases. Therefore, we can transform the problem of maximizing $\mathrm{TP_p}$ into an optimization problem that successively finds $\mathrm{SINR}^*_{\mathrm{ef}_r}$, for $1 \le r \le R$, where each of $\mathrm{SINR}^*_{\mathrm{ef}_r}$ is determined as

$$\begin{aligned}
\mathrm{SINR}^*_{\mathrm{ef}_1} &= \min(f_1(\mathrm{SINR}_{\mathrm{ef}_1})),\\
\mathrm{SINR}^*_{\mathrm{ef}_2} &= \min(f_2(\mathrm{SINR}_{\mathrm{ef}_2}|\mathrm{SINR}^*_{\mathrm{ef}_1})),\\
&\vdots\\
\mathrm{SINR}^*_{\mathrm{ef}_R} &= \min(f_R(\mathrm{SINR}_{\mathrm{ef}_R}|\mathrm{SINR}^*_{\mathrm{ef}_1},\cdots,\mathrm{SINR}^*_{\mathrm{ef}_{R-1}})).
\end{aligned} \tag{3.14}$$

Since each $f_r(\cdot)$ is a decreasing function of $\mathrm{SINR}_{\mathrm{ef}_r}$ for $1 \le r \le R$, finding $\mathrm{SINR}^*_{\mathrm{ef}_r}$ for $1 \le r \le R$ in Eq. (3.14) is equivalent to the following problem:

$$\begin{aligned}
\mathrm{SINR}^*_{\mathrm{ef}_1} &= \max(\mathrm{SINR}_{\mathrm{ef}_1}),\\
\mathrm{SINR}^*_{\mathrm{ef}_2} &= \max(\mathrm{SINR}_{\mathrm{ef}_2}|\mathrm{SINR}^*_{\mathrm{ef}_1}),\\
&\vdots\\
\mathrm{SINR}^*_{\mathrm{ef}_R} &= \max(\mathrm{SINR}_{\mathrm{ef}_R}|\mathrm{SINR}^*_{\mathrm{ef}_1},\cdots,\mathrm{SINR}^*_{\mathrm{ef}_{R-1}}).
\end{aligned} \tag{3.15}$$

Also, from Eq. (3.9), for a given E_s/σ^2, maximization of $\mathrm{SINR}_{\mathrm{ef}_r}$ can be rewritten as

$$\begin{aligned} \max(\mathrm{SINR}_{\mathrm{ef}_r}) &= \min((\mathrm{SINR}_{\mathrm{ef}_r})^{-1}) = \min\left(\frac{I_{\mathrm{ef}_r}E_s+\sigma^2}{E_s}\right) \\ &= \min\left(I_{\mathrm{ef}_r}+\frac{\sigma^2}{E_s}\right) = \min(I_{\mathrm{ef}_r}). \end{aligned} \tag{3.16}$$

Therefore, the problem of maximizing $\mathrm{TP_p}$ can be transformed into the successive optimization problems to find $I^*_{\mathrm{ef}_r}$ for $1 \le r \le R$, where each of $I^*_{\mathrm{ef}_r}$ can be obtained as

$$\begin{aligned} I^*_{\mathrm{ef}_1} &= \min(I_{\mathrm{ef}_1}), \\ I^*_{\mathrm{ef}_2} &= \min(I_{\mathrm{ef}_2}|I^*_{\mathrm{ef}_1}), \\ &\vdots \\ I^*_{\mathrm{ef}_R} &= \min(I_{\mathrm{ef}_R}|I^*_{\mathrm{ef}_1},\cdots,I^*_{\mathrm{ef}_{R-1}}). \end{aligned} \tag{3.17}$$

3.3.2 EIL-based Transmission Strategy

Based on the analysis results in Sec. 3.3.1, we propose a packet transmission strategy to improve the throughput of MIMO systems where all data packets go through independent HARQ processes. The ideal transmission strategy is to find the solution of Eq. (3.17), i.e., to find $\mathbf{P}^*_t$ for $1 \le t \le T$, that can achieve $I^*_{\mathrm{ef}_r}$ for $1 \le r \le R$. However, finding the optimal solution $\mathbf{P}^*_t$ for $1 \le t \le T$ requires the instantaneous error probabilities from the first PTTI to the last PTTI, as shown in Eqs. (3.7) and (3.8). While obtaining the expected error probability of a packet is possible, it is impossible to obtain the instantaneous error probability because of the randomness of noise at the receiver. Although the average PERs may be used as an alternative to the instantaneous error

probabilities, estimating the average PERs can be done only when all the related system parameters are fixed. In practice, however, many parameters are time varying, such as transmit power allocation, transmitter-receiver distance, modulation level and coding rate, reception algorithm, and so on. Another requirement to find $\mathbf{P}_t^*$ for $1 \leq t \leq T$, which can achieve $I_{\mathrm{ef}_r}^*$ for $1 \leq r \leq R$, is that the entire $\mathbf{P}_t^*$ for $1 \leq t \leq T$ should be determined before the first PTTI. This requires a very large transmission buffer size B, which is impractical.

Considering the above difficulties of the ideal transmission strategy, a more practical approach will be desirable. The average decoding success probability of a packet in the HARQ process increases with r [11, 13, 15–18, 20–22], i.e., $0 \leq P_{\mathrm{er}_R} \leq P_{\mathrm{er}_{R-1}} \leq \cdots \leq P_{\mathrm{er}_1} \leq 1$. Therefore, it is reasonable to assume that if $r_{t,l} > r_{t,i}$ then any $p_l \in \mathbf{P}_t$ will have a lower instantaneous error probability than $p_i \in \mathbf{P}_t$. Consequently, $\mathbf{P}_{t,r,k}^*$ becomes the set of $p_l \in \mathbf{P}_t$ with $r_{t,l} > r$, where $\hat{P}_{\mathrm{er}_{\mathbf{P}_{t,r,k}^*(l)}} \cong 0$ for any $l \in \mathbf{P}_{t,r,k}^*$. Also $\hat{I}_{\mathrm{ef}_{t,r,k}}$ does not change as a function of k. Let $\widetilde{I}_{\mathrm{ef}_{t,r}}$ be $\hat{I}_{\mathrm{ef}_{t,r,k}}$ for any packet in $\mathbf{P}_{t,r}$ with the above assumption, which can be written as

$$\widetilde{I}_{\mathrm{ef}_{t,r}} = \begin{cases} |\mathbb{P}_{t,r}|-1=|\mathbf{P}_{t,r}|+|\mathbb{P}_{t,r-1}|-1, & \text{if } |\mathbf{P}_{t,r}| \geq 1 \\ 0, & \text{if } |\mathbf{P}_{t,r}|=0 \end{cases}, \tag{3.18}$$

where $\mathbb{P}_{t,r}$ is the union of $\mathbf{P}_{t,r'}$ from $r'=1$ to $r'=r$, i.e., $\mathbb{P}_{t,r} = \bigcup_{r'=1}^{r} \mathbf{P}_{t,r'}$.

In other words, it can be defined as the number of the other packets which have the number of transmission equal to or smaller than the rth round in the tth PTTI.

It is also possible to find $\mathbf{P}_t$ with the average EILs or the average effective SINR based on $\widetilde{I}_{\mathrm{ef}_{t,r}}$, but this approach also requires estimating the average PERs for a given set of system parameters.

The proposed transmission strategy for the tth PTTI finds $\mathbf{P}_t^*$ with the approximated minimum EILs at the tth PTTI, $\widetilde{I}_{\mathrm{ef}_{t,r}}^*$ for $1 \le r \le R$. Since $\mathbf{P}_t = \bigcup_{r=1}^{R} \mathbf{P}_{t,r}$, the goal of the proposed transmission strategy is to find $\mathbf{P}_t^* = \bigcup_{r=1}^{R} \mathbf{P}_{t,r}^*$, where $\mathbf{P}_{t,r}^*$ can be successively determined from $r = 1$ to $r = R$ as

$$\begin{aligned} \mathbf{P}_{t,r}^* &= \arg\min_{\mathbf{P}_{t,r}} \mathrm{g}(|\mathbf{P}_{t,r}|, |\mathbb{P}_{t,r-1}^*|) \\ \text{s.t.} \quad & 1) \quad \left\{\mathbf{P}_{t,r} \cup \mathbb{P}_{t,r-1}^*\right\} \subset \mathbf{G} \text{ for any arbitrary } \mathbf{G} \subset \mathbf{B}_t \\ & \qquad \text{with } |\mathbf{G}| = N_{\mathrm{T}} \\ & 2) \quad r_{t,i} = r \text{ for all } p_i \in \mathbf{P}_{t,r} \end{aligned} \tag{3.19}$$

with $\mathbb{P}_{t,r-1}^* = \bigcup_{r'=1}^{r-1} \mathbf{P}_{t,r'}^*$ and

$$\mathrm{g}(a,b) = \begin{cases} a+b-1, & \text{if } a \ge 1 \\ 0, & \text{if } a = 0 \end{cases}. \tag{3.20}$$

Based on Eqs. (3.19) and (3.20), the proposed transmission strategy to find $\mathbf{P}_t^*$ is summarized in Table 3.1. Note that $\mathbf{B}_{t,r}$ in Table 3.1 denotes the subset of $\mathbf{B}_t$, where all $p_i \in \mathbf{B}_{t,r}$ satisfy $p_i \in \mathbf{B}_t$ and $r_{t,i} = r$. The first constraint in Eq. (3.19) comes from the fact that each $\mathbf{P}_{t,r}$ should be a subset of $\mathbf{P}_t$, which has N_{T} packets to be transmitted during the tth PTTI; the second constraint is because $\mathbf{P}_{t,r}$ should be a set of the packets with $r_{t,i} = r$. Therefore, the proposed transmission strategy only needs the number of transmissions of each p_i, $r_{t,i}$. Also in Table 3.1 $\mathbf{n}_{\mathrm{P}_t}^*$ is determined prior to the selection of $\mathbf{P}_t^*$, where $\mathbf{n}_{\mathrm{P}_t}^*(r)$ is the number of the packets with the rth HARQ round that will be included in $\mathbf{P}_t^*$, i.e., $\mathbf{n}_{\mathrm{P}_t}^*(r) = |\mathbf{P}_{t,r}^*|$.

It is worthwhile to mention that the selection of the largest $\mathbf{n}_{\mathrm{P}_t}(r)$ in Step 2) is because

Table 3.1: Summary of the proposed transmission strategy

Step 1)	[Initialization] Compose the set $\mathbf{N}_{\mathrm{P}_t}$ including any $R \times 1$ vector $\mathbf{n}_{\mathrm{P}_t}$ that satisfies $\sum_{r=1}^{R} \mathbf{n}_{\mathrm{P}_t}(r) = N_{\mathrm{T}}$, $0 \leq \mathbf{n}_{\mathrm{P}_t}(r) \leq \lvert\mathbf{B}_{t,r}\rvert$, and $\mathbf{n}_{\mathrm{P}_t}(r) \in \mathbb{Z}$ with the set of integers $\mathbb{Z}$. Make the $R \times 1$ all-zero vector $\mathbf{n}^*_{\mathrm{P}_t}$. Make an empty set $\mathbf{P}_t$. Set $r := 1$.
Step 2)	[Find the number of the packets with the rth HARQ round] Find $\mathbf{n}_{\mathrm{P}_t}(r)$ of any $\mathbf{n}_{\mathrm{P}_t} \in \mathbf{N}_{\mathrm{P}_t}$ that satisfies $\mathrm{g}(\mathbf{n}_{\mathrm{P}_t}(r), \sum_{r'=1}^{r-1} \mathbf{n}_{\mathrm{P}_t}(r'))$ $\leq \mathrm{g}(\mathbf{a}(r), \sum_{r'=1}^{r-1} \mathbf{a}(r'))$ for any other $\mathbf{a} \in \mathbf{N}_{\mathrm{P}_t}$, and set $\mathbf{n}^*_{\mathrm{P}_t}(r) = \mathbf{n}_{\mathrm{P}_t}(r)$. If more than one values are found, choose the largest one as $\mathbf{n}^*_{\mathrm{P}_t}(r)$.
Step 3)	[Update $\mathbf{N}_{\mathrm{P}_t}$] Exclude the entire $\mathbf{n}_{\mathrm{P}_t}$ with $\mathbf{n}_{\mathrm{P}_t}(r) \neq \mathbf{n}^*_{\mathrm{P}_t}(r)$ from $\mathbf{N}_{\mathrm{P}_t}$. If $r = R$, go to Step 4). Otherwise, go back to Step 2).
Step 4)	[Determine $\mathbf{P}_t$ using $\mathbf{n}^*_{\mathrm{P}_t}$] From $r = 1$ to $r = R$, select $\mathbf{n}^*_{\mathrm{P}_t}(r)$ packets from $\mathbf{B}_{t,r}$ that satisfy $r_{t,i} = r$ as the members of $\mathbf{P}_t$. If $\lvert\mathbf{B}_{t,r}\rvert > \mathbf{n}^*_{\mathrm{P}_t}(r)$, sort the entire $p_i \in \mathbf{B}_{t,r}$ in the ascending order of the packet index i and select the first $\mathbf{n}^*_{\mathrm{P}_t}(r)$ packets.

the normalized average EIL defined in Eq. (3.8) decreases as $|\mathbf{P}_{t,r}|$ increases for a fixed amount of the effective instantaneous interference. Therefore, it is feasible to select the largest $\mathbf{n}_{\mathrm{P}_t}(r)(= |\mathbf{P}_{t,r}|)$ for the equal EIL, i.e., select the largest $\mathbf{n}_{\mathrm{P}_t}(r)$ as $\mathbf{n}^*_{\mathrm{P}_t}(r)$ if there are more than one $\mathbf{n}_{\mathrm{P}_t}(r)$ that satisfy $\mathrm{g}(\mathbf{r}(r), \sum_{r'=1}^{r-1} \mathbf{n}_{\mathrm{P}_t} r(r')) \leq \mathrm{g}(\mathbf{a}(r), \sum_{r'=1}^{r-1} \mathbf{a}(r'))$ for any other $\mathbf{a} \in \mathbf{N}_{\mathrm{P}_t}$. Also, the packet selection in Step 4) based on the packet index is to minimize the latency of the proposed transmission strategy for a given $\mathbf{n}^*_{\mathrm{P}_t}$, since the packet index represents the original transmission order of the packet, i.e., p_i is the ith transmitted packet.

Table 3.2: Parameters of simulation environments

Channel code	802.16e LDPC code in [10]
Code rate	3/4
Error detection code	CRC-24
Number of data bits per packet	552
Number of coded bits per packet	768
Modulation	QPSK
Number of symbols per packet	384
Transmission buffer size	$2N_{\mathrm{T}}$ (Proposed scheme) N_{T} (Conventional scheme)
Channel	Independent Rayleigh fading
Decoding algorithm	BP algorithm in [25]
Number of decoding iterations	50

3.4 Simulation Results

The parameters of simulation environments to verify the performance of the proposed strategy are summarized in Table 3.2. In the simulation, we consider the LDPC code in [10] as a mother code with a rate 3/4, a data bit stream of $K = 552$, and a coded bit stream of $C = 768$. CRC-24 is considered in the packet generation process, and QPSK modulation with $Q = 2$ is used to generate $L = 384$ transmitted symbols. The transmission buffer size is $B = 2N_{\mathrm{T}}$ for the proposed scheme. For comparison, we also consider the conventional HARQ packet transmission strategy with $B = N_{\mathrm{T}}$, where $\mathbf{B}_t = \mathbf{P}_t$, so that all non-terminated packets until the latest PTTI are retransmitted at the current PTTI based solely on the acknowledgement feedback message. Since the number of packets to be transmitted in the current PTTI is smaller than the size of the transmission buffer ($N_{\mathrm{T}} < B$) in the proposed transmission strategy, the time interval between two consecutive HARQ rounds of a packet could be greater than that of the conventional strategy. Because of this large time interval, independent Rayleigh fast

fading channel coefficients are generated for different PTTIs.

The Iterative IC operation for the simulation is designed to satisfy the assumption of system analysis in Sec. 3.3.1, i.e. IC operation is performed only when CRC decoder finds a decoded bit stream is detected as error-free after a given number of decoding iteration. The BP algorithm [25] is utilized during the decoding process, while the number of BP iterations for each packet per PTTI is set to 50.

First, the system error characteristics according to $\mathbf{P}_t$ in terms of $|\mathbf{P}_{t,r}|$ for the simple case with $N_{\mathrm{T}} = N_{\mathrm{R}} = 2$ and $R = 2$ are assessed. There are three cases of $\mathbf{P}_t$ in terms of $|\mathbf{P}_{t,r}|$: $\{|\mathbf{P}_{t,1} = 2|, |\mathbf{P}_{t,2} = 0|\}$, $\{|\mathbf{P}_{t,1} = 1|, |\mathbf{P}_{t,2} = 1|\}$, and $\{|\mathbf{P}_{t,1} = 0|, |\mathbf{P}_{t,2} = 2|\}$. Figs. 3.3(a) and 3.3(b) show P_{er_r} for the three cases assuming the MMSE filter and the ZF filter, respectively. It is observed that with an MMSE filter and a ZF filter at a PER of 0.1, the SNR gains of $\{|\mathbf{P}_{t,1} = 1|, |\mathbf{P}_{t,2} = 1|\}$ over $\{|\mathbf{P}_{t,1} = 2|, |\mathbf{P}_{t,2} = 0|\}$ are about 3.0 dB and 4.6 dB, respectively. Since $\widetilde{I}_{\mathrm{ef}_{t,1}} = 0$ for $\{|\mathbf{P}_{t,1} = 1|, |\mathbf{P}_{t,2} = 1|\}$ and $\widetilde{I}_{\mathrm{ef}_{t,1}} = 1$ for $\{|\mathbf{P}_{t,1} = 2|, |\mathbf{P}_{t,2} = 0|\}$, it verifies our assumption that the EIL is a valid measure of the error performance. The SNR gain due to the decreased EIL is more clear with the ZF filter than with the MMSE filter. Unlike P_{er_1}, P_{er_2} for both $\{|\mathbf{P}_{t,1} = 1|, |\mathbf{P}_{t,2} = 1|\}$ and $\{|\mathbf{P}_{t,1} = 0|, |\mathbf{P}_{t,2} = 2|\}$ are similar, since both $\{|\mathbf{P}_{t,1} = 1|, |\mathbf{P}_{t,2} = 1|\}$ and $\{|\mathbf{P}_{t,1} = 0|, |\mathbf{P}_{t,2} = 2|\}$ have the same EIL, $\widetilde{I}_{\mathrm{ef}_{t,2}} = 1$.

Figs. 3.4 and 3.5 show the probabilities of occurrence of $\mathbf{P}_t$ in terms of $|\mathbf{P}_{t,r}|$ for the proposed and the conventional transmission strategies for the system with $N_{\mathrm{T}} = N_{\mathrm{R}} = 2$ and $R = 2$. It is shown that the probability of $\{|\mathbf{P}_{t,1} = 1|, |\mathbf{P}_{t,2} = 1|\}$ with the conventional strategy is very small for the entire E_s/σ^2 range regardless of the filter used; $\{|\mathbf{P}_{t,1} = 2|, |\mathbf{P}_{t,2} = 0|\}$ and $\{|\mathbf{P}_{t,1} = 0|, |\mathbf{P}_{t,2} = 2|\}$ occur a lot more frequently than $\{|\mathbf{P}_{t,1} = 1|, |\mathbf{P}_{t,2} = 1|\}$. On the other hand, the probability of $\{|\mathbf{P}_{t,1} = 1|, |\mathbf{P}_{t,2} = 1|\}$ under the proposed strategy is significantly higher than the case of the conventional

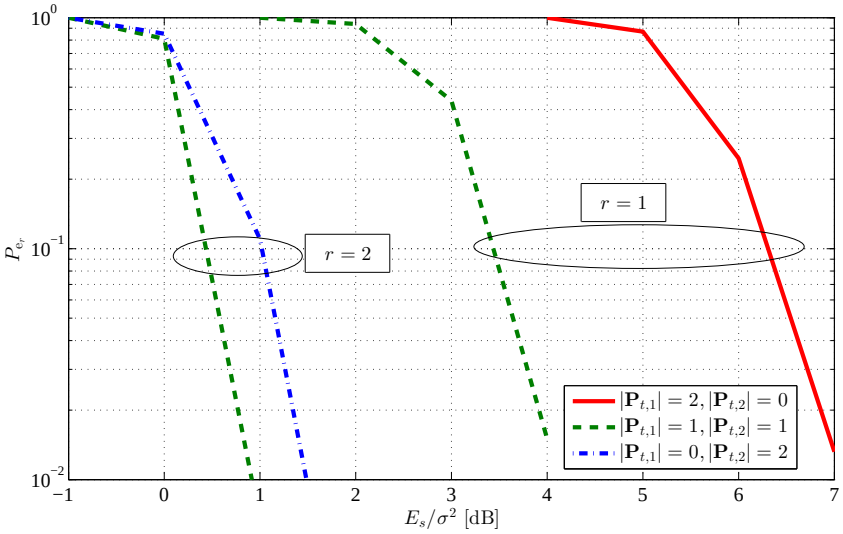

(a) MMSE filter.

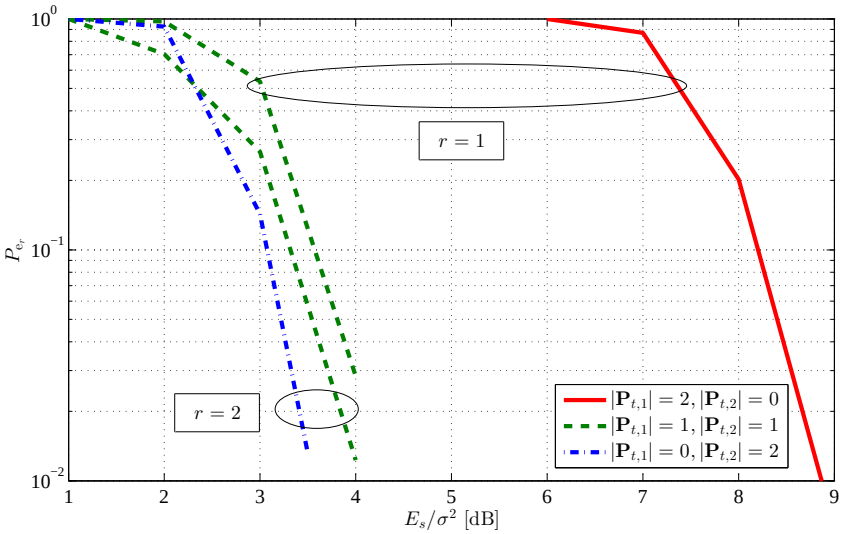

(b) ZF filter.

Figure 3.3: Average PERs according to $\mathbf{P}_t$ when $N_{\mathrm{T}} = N_{\mathrm{R}} = 2$, $R = 2$ and $|\mathbf{P}_{t,r}|$ is the number of the packets at the rth round in the tth PTTI.

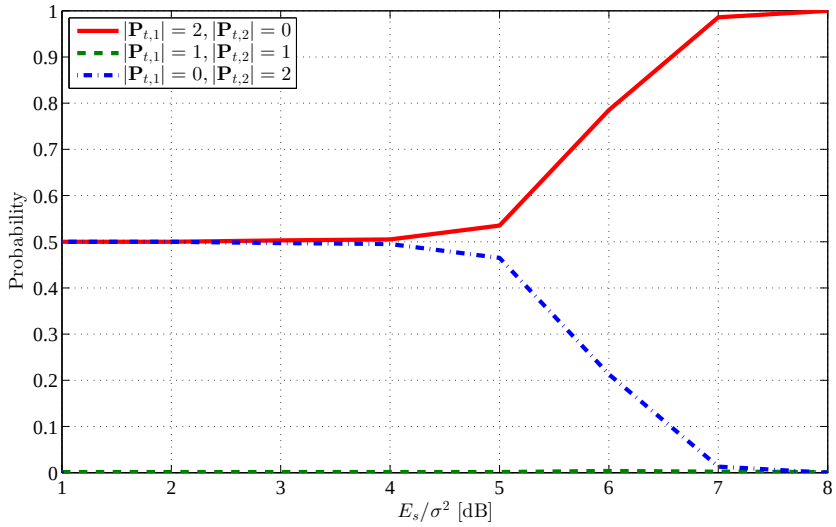

(a) MMSE filter.

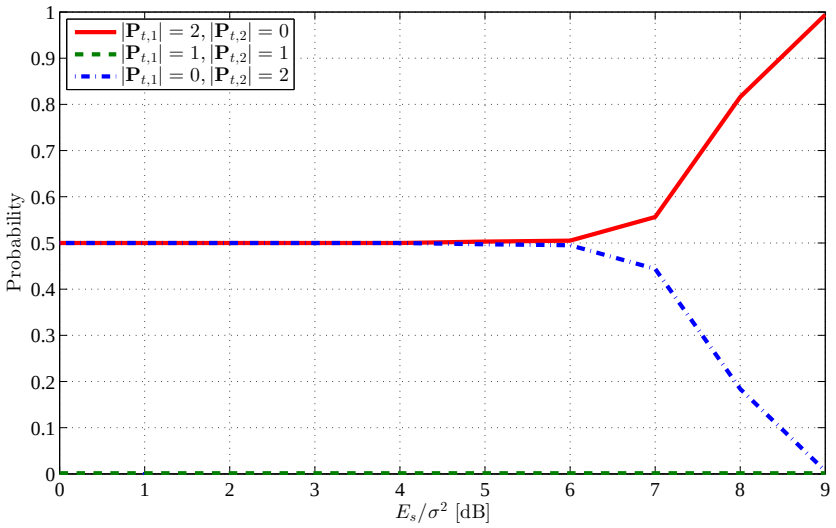

(b) ZF filter.

Figure 3.4: Probability of each $\mathbf{P}_t$ with the conventional strategy when $N_{\mathrm{T}} = N_{\mathrm{R}} = 2$, $R = 2$, $B = N_{\mathrm{T}}$ and $|\mathbf{P}_{t,r}|$ is the number of the packets at the rth round in the tth PTTI.

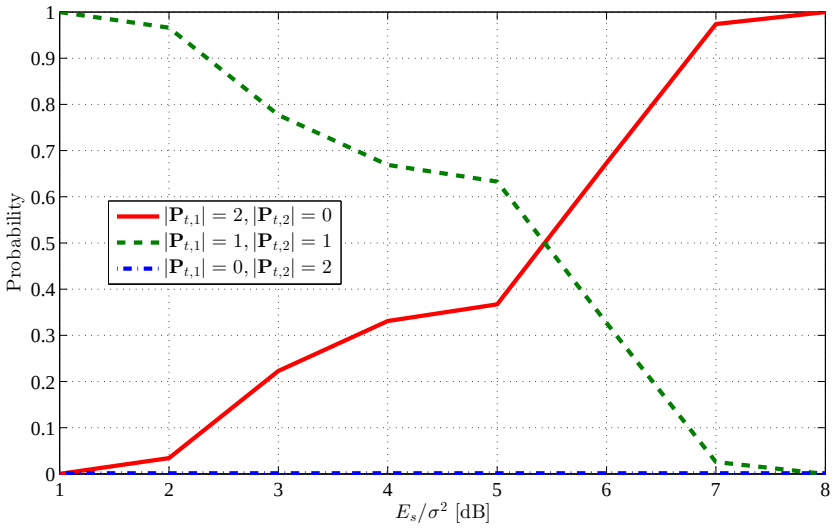

(a) MMSE filter.

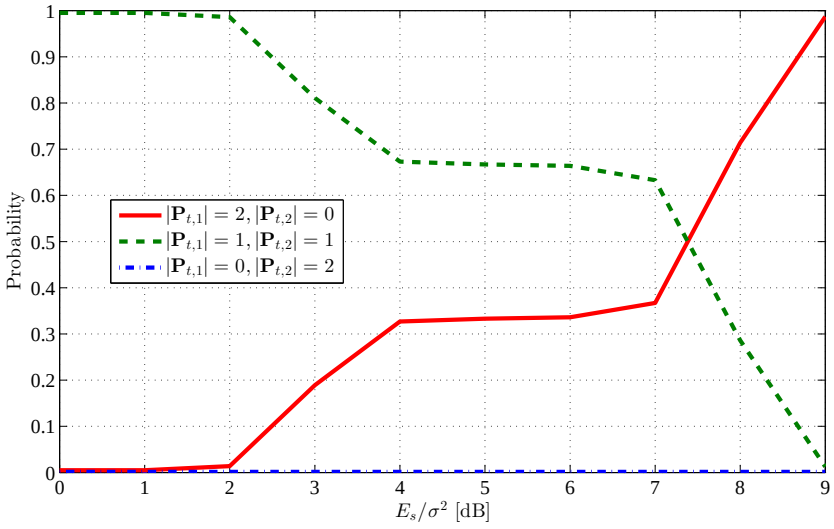

(b) ZF filter.

Figure 3.5: Probability of each $\mathbf{P}_t$ with the proposed strategy when $N_{\mathrm{T}} = N_{\mathrm{R}} = 2$, $R = 2$, $B = 2N_{\mathrm{T}}$ and $|\mathbf{P}_{t,r}|$ is the number of the packets at the rth round in the tth PTTI.

strategy regardless of the utilized filter. Since P_{er_1} for the case of $\{|\mathbf{P}_{t,1}=2|,|\mathbf{P}_{t,2}=0|\}$ is much higher than for the case of $\{|\mathbf{P}_{t,1}=1|,|\mathbf{P}_{t,2}=1|\}$ due to the difference of $\widetilde{I}_{\mathrm{ef}_{t,1}}$, it is expected that the system with the conventional strategy will have a much higher P_{er_1} than the system with the proposed strategy because of the increased EIL. Meanwhile, as E_s/σ^2 increases, P_{er_1} decreases, so $|\mathbf{B}_{t,2}|$ becomes smaller. This implies that the selection of $\mathbf{P}_t$ with a non-zero $|\mathbf{P}_{t,2}|$ becomes more difficult as E_s/σ^2 increases. Therefore, instead of $\{|\mathbf{P}_{t,1}=0|,|\mathbf{P}_{t,2}=2|\}$ and $\{|\mathbf{P}_{t,1}=1|,|\mathbf{P}_{t,2}=1|\}$, $\{|\mathbf{P}_{t,1}=2|,|\mathbf{P}_{t,2}=0|\}$ is more likely to occur in the high E_s/σ^2 region regardless of the transmission strategy adopted.

Figs. 3.6(a) and 3.6(b) show the simulated P_{er_r} of the transmission strategies assuming $N_{\mathrm{T}}=N_{\mathrm{R}}=2$ and $R=2$, with the MMSE filter and the ZF filter, respectively. As expected, the proposed strategy outperforms the conventional strategy in terms of P_{er_1} especially in the low E_s/σ^2 region, since the performance improvement of the proposed strategy over the conventional strategy comes from the probability of the occurrence of $\{|\mathbf{P}_{t,1}=1|,|\mathbf{P}_{t,2}=1|\}$, which decreases as E_s/σ^2 increases (see Figs. 3.3–3.5). Meanwhile, the proposed strategy and the conventional strategy have a similar P_{er_2}. Since the impact of P_{er_r} on the system throughput increases as r decreases as shown previously, the proposed strategy will result in a higher throughput than the conventional strategy because of the improved P_{er_1}.

The comparison of $\mathrm{TP_P}$ of the proposed strategy and the convention strategy is presented in Figs. 3.7(a) and 3.7(b), where $N_{\mathrm{T}}=N_{\mathrm{R}}=2$ and $R=3$ in Fig. 3.7(a) and $N_{\mathrm{T}}=N_{\mathrm{R}}=4$ and $R=3$ in Fig. 3.7(b). When $N_{\mathrm{T}}=N_{\mathrm{R}}=2$, the proposed strategy obtains an SNR gain of about 2.6 dB over the conventional strategy at the $\mathrm{TP_P}$ of 1.2 with the MMSE filter. This gain is further increased to about 3.8 dB with the ZF filter. When $N_{\mathrm{T}}=N_{\mathrm{R}}=4$, at the $\mathrm{TP_P}$ of 2.4, the SNR gains of the proposed strategy over the conventional strategy are about 2.8 dB with the MMSE filter and 4.2 dB with the

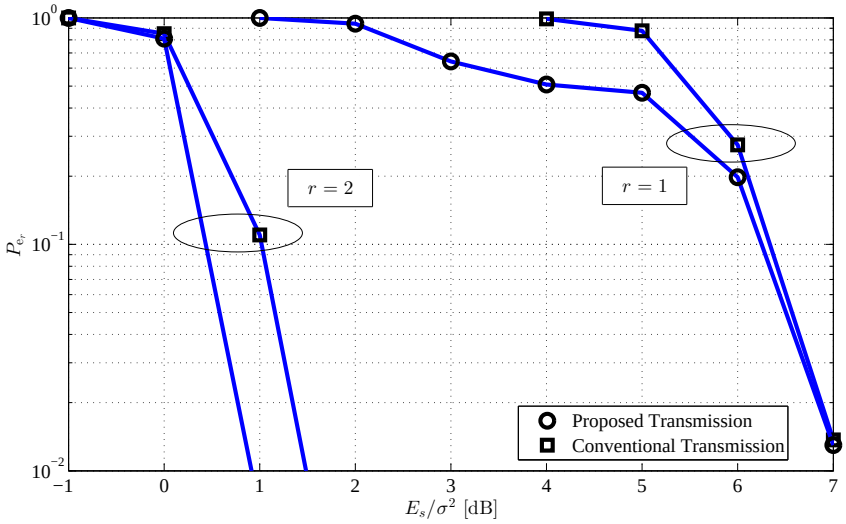

(a) MMSE filter.

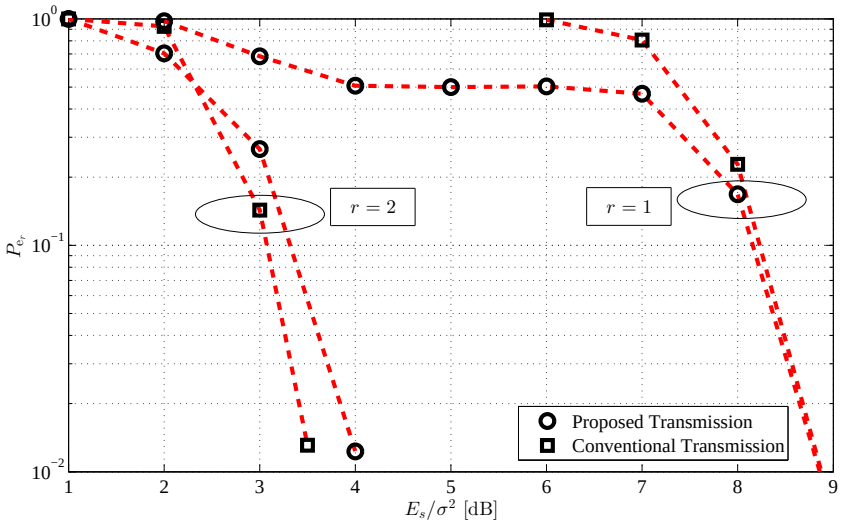

(b) ZF filter.

Figure 3.6: Average PERs with different transmission strategies when $N_{\mathrm{T}} = N_{\mathrm{R}} = 2$, $R = 2$, $B = N_{\mathrm{T}}$ and $2N_{\mathrm{T}}$ for the conventional and proposed transmission strategies, respectively.

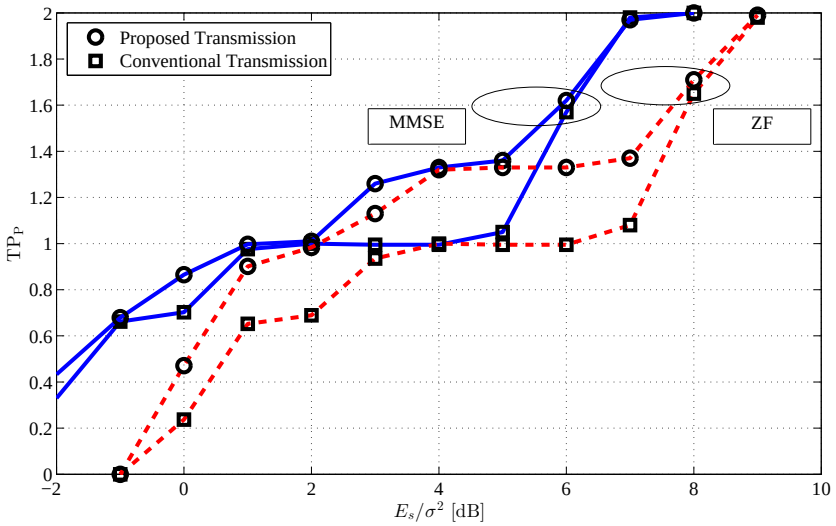

(a) $N_{\mathrm{T}} = N_{\mathrm{R}} = 2$ and $R = 3$.

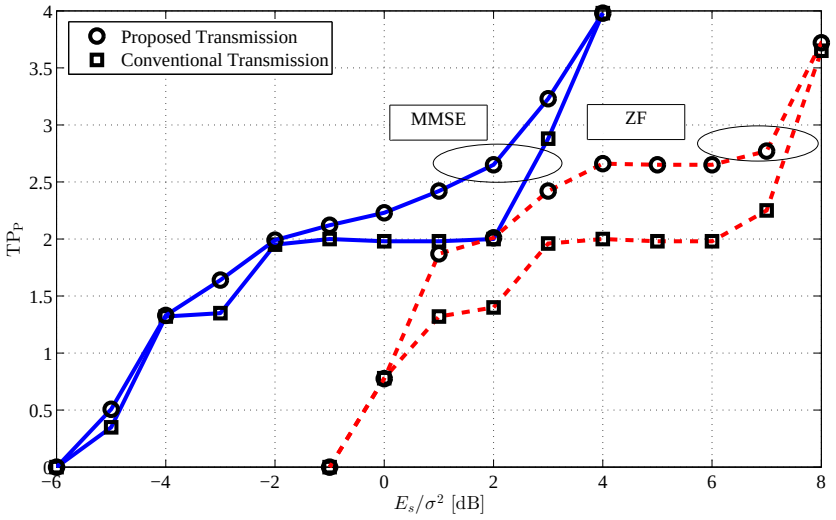

(b) $N_{\mathrm{T}} = N_{\mathrm{R}} = 4$ and $R = 3$.

Figure 3.7: Average throughputs of the transmission strategies by the number of successfully decoded packets per PTTIs when $B = N_{\mathrm{T}}$ and $2N_{\mathrm{T}}$ for the conventional and proposed transmission strategies, respectively.

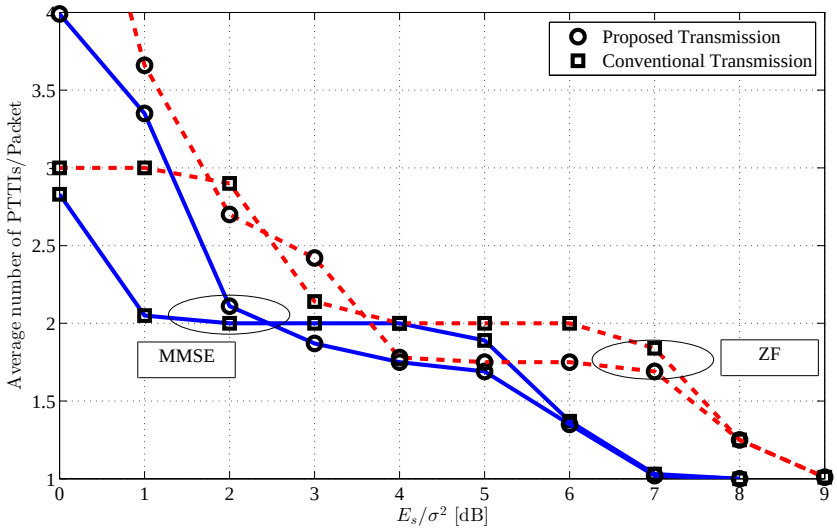

(a) $N_{\mathrm{T}} = N_{\mathrm{R}} = 2$ and $R = 3$.

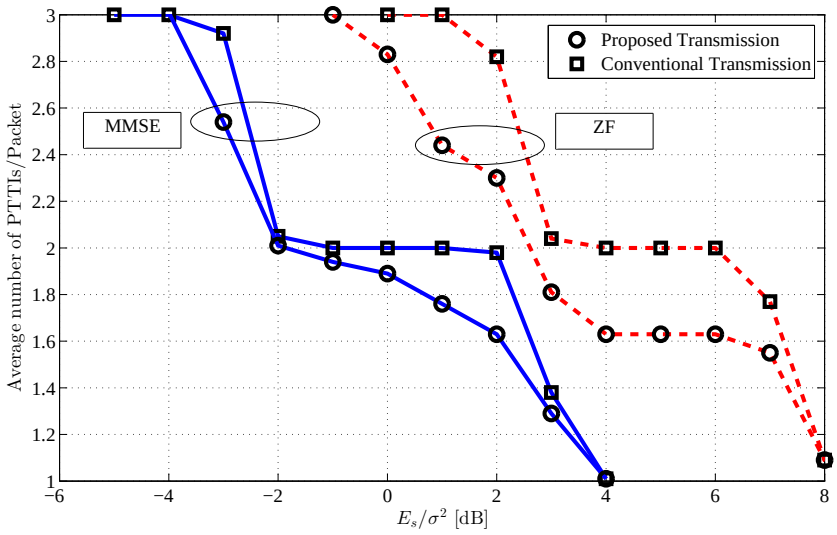

(b) $N_{\mathrm{T}} = N_{\mathrm{R}} = 4$ and $R = 3$.

Figure 3.8: Average number of required PTTIs per terminated packet with the transmission strategies when $B = N_{\mathrm{T}}$ and $2N_{\mathrm{T}}$ for the conventional and proposed transmission strategies, respectively.

ZF filter.

Since the packets to be transmitted in the next PTTI are determined by the EIL in the proposed strategy, the packets in the proposed transmission strategy can have a larger latency than the conventional strategy, which immediately retransmits the previously failed packets. In Figs. 3.8(a) and 3.8(b), we compare the average number of required PTTIs from the initial transmission up to the termination per packet, where $N_{\mathrm{T}} = N_{\mathrm{R}} = 2$ and $R = 3$ are assumed in Fig. 3.8(a) and $N_{\mathrm{T}} = N_{\mathrm{R}} = 4$ and $R = 3$ are assumed in Fig. 3.8(b). When $N_{\mathrm{T}} = N_{\mathrm{R}} = 2$, the proposed strategy has a longer latency than the conventional strategy as shown in Fig. 3.8(a), but this happens only when the number of HARQ rounds for the termination of a packet is large, i.e., in the low E_s/σ^2 region. As E_s/σ^2 increases, the proposed strategy requires a similar or even lower average latency than the conventional strategy because of the improved throughput. When $N_{\mathrm{T}} = N_{\mathrm{R}} = 4$, the proposed strategy requires a lower average latency than the conventional strategy in the entire E_s/σ^2 region. In contrast to the results in Fig. 3.8(a), the proposed strategy shows a lower average latency than the conventional strategy even in the low E_s/σ^2 region in Fig. 3.8(b). This is because a packet with a higher number of HARQ round can be transmitted sooner without a long delay as the number of packets simultaneously transmitted in one PTTI ($= N_{\mathrm{T}}$) increases.

3.5 Conclusion

A new HARQ packet transmission strategy based on the concept of the EIL is proposed for MIMO systems with HARQ and IC detection. The proposed scheme successively minimises the EIL of the packets from the lowest to the highest HARQ round in order to improve the system throughput. Simulation results demonstrate that the proposed

packet transmission strategy outperforms the conventional packet transmission strategy in terms of system throughput without sacrificing the latency and error performance. Since the number of HARQ rounds of each packet is the only required information to calculate an EIL, no additional feedback overheads are required to operate the proposed scheme.

Chapter 4: Low-Complexity SLC for CC-HARQ in MIMO Systems with Linear Detection

4.1 Introduction

Based on which part of a mother codeword is used for retransmissions, HARQ schemes can be mainly classified into the following three types: CC-HARQ [11], PIR-HARQ [28], and FIR-HARQ [29]. In CC-HARQ, all the coded bits for the initial transmission are reutilized for retransmissions. In PIR-HARQ, a part of the coded bits for the initial transmission, mainly the systematic part, is exploited for retransmissions, while some additional parity bits are newly sent for each retransmission. Finally, in FIR-HARQ, new parity bits which have not been sent up to the previous transmission are sent without the systematic part utilization for each retransmission. Therefore, in terms of coding gain provided by parity bits, FIR-HARQ shows the best performance and PIR-HARQ outperforms CC-HARQ [30].

Nevertheless, owing to sending the same transmit symbols over transmissions, CC-HARQ can be jointly used with other techniques in a much easier way than PIR-HARQ and FIR-HARQ [20, 28, 32–37], e.g., precoding scheme at the transmitter [32–34] and the SLC scheme at the receiver [20, 28, 35–37]. Specifically, in MIMO systems [2], these SLC schemes can provide additional space diversity as well as time diversity, and therefore a number of SLC schemes [35–37] have been developed for CC-HARQ in MIMO systems.

The goal of this thesis is to develop a low-complexity SLC scheme for CC-HARQ

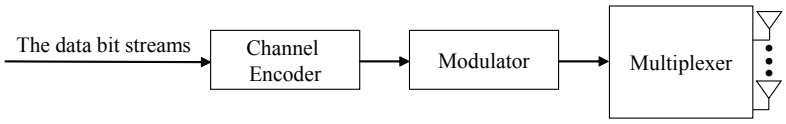

Figure 4.1: Transmitter block diagram.

in MIMO systems, when the linear detection is considered at the receiver [52]. In the proposed scheme, instead of using the entire channel matrix as in the existing SLC schemes, a subset of row vectors in the channel matrix is selected in the proposed scheme, and the selected row vectors are sequentially utilized during the estimation procedures of the retransmitted symbols, where the sequential utilization is enabled by using the SMW lemma [41,42]. Therefore, according to the number of the selected row vectors, this approach enables the proposed SLC scheme to have an advantage in complexity compared to the existing SLC schemes. In addition, we develop a row vector selection criterion for the proposed scheme to compute the amount of the SINR improvement by using a squared norm of each row vector with a significantly lower computational complexity. Simulation results show that compared to the existing SLC schemes, the proposed SLC scheme achieves similar or better error performance, while its computational complexity is lower or in the worst case similar.

4.2 System Model

We consider a vertical BLAST-type SM MIMO system [2], where CC-HARQ is assumed and N_{T} transmit and N_{R} ($\geq N_{\mathrm{T}}$) receive antennas are considered. The transmitter block diagram is illustrated in Fig. 4.1. K data bits for a packet are encoded as C coded bits, and the coded bits are modulated as L transmit symbols, where $Q = C/L$ is the number

of coded bits per symbol. Then, the transmit symbols are spatially multiplexed across the transmit antennas to generate J transmit signal vector, and thereby $J = L/N_{\mathrm{T}}$. Let $\mathbf{s}_{r,j} = [s_{r,j,1}, \cdots, s_{r,j,N_{\mathrm{T}}}]^T$ be the jth transmit signal vector for the rth HARQ round of a packet for $1 \leq j \leq J$, where $s_{r,j,n}$ for $1 \leq n \leq N_{\mathrm{T}}$ is the transmit symbol in $\mathbf{s}_{r,j}$ at the nth transmit antenna. It is assumed that any $\mathbf{s}_{r,j}$ satisfies $\mathbb{E}[\mathbf{s}_{r,j}\mathbf{s}_{r,j}^H] = E_s\mathbf{I}_{N_{\mathrm{T}}}$, where E_s denotes the average transmit symbol energy. Since CC-HARQ is considered, $\mathbf{s}_{1,j} = \mathbf{s}_{r,j}$ for $1 \leq r \leq R$, where R is the maximum number of transmissions allowed (the highest HARQ round) per packet. Then, the index r can be omitted from $\mathbf{s}_{r,j}$. Let $\mathbf{s}_j = [s_{j,1}, \cdots, s_{j,N_{\mathrm{T}}}]^T$ be the jth transmit signal vector for a packet. Then, the MIMO system model for $\mathbf{s}_j$ at the rth HARQ round can be written as

$$\mathbf{y}_{r,j} = \mathbf{H}_{r,j}\mathbf{s}_j + \mathbf{n}_{r,j}. \tag{4.1}$$

In Eq. (4.1), $\mathbf{y}_{r,j} = [y_{r,j,1}, \cdots, y_{r,j,N_{\mathrm{R}}}]^T$ is the $N_{\mathrm{R}} \times 1$ receive signal vector for $\mathbf{s}_{r,j}$ and $\mathbf{n}_{r,j}$ is the $N_{\mathrm{R}} \times 1$ additive white Gaussian noise vector whose elements follow complex Gaussian distributions with zero mean and variance σ^2. Therefore, the average SNR is defined as E_s/σ^2. $\mathbf{H}_{r,j}$ in Eq. (4.1) is the $N_{\mathrm{R}} \times N_{\mathrm{T}}$ channel matrix for $\mathbf{s}_{r,j}$ with $\mathrm{rank}(\mathbf{H}_{r,j}) = N_{\mathrm{T}}$ and can be written as

$$\mathbf{H}_{r,j} = \begin{bmatrix} \mathbf{h}_{r,j,1} \\ \vdots \\ \mathbf{h}_{r,j,N_{\mathrm{R}}} \end{bmatrix}, \tag{4.2}$$

where $\mathbf{h}_{r,j,n}$ for $1 \leq n \leq N_{\mathrm{R}}$ is the $1 \times N_{\mathrm{T}}$ row vector of $\mathbf{H}_{r,j}$.

4.3 Existing SLC Schemes

4.3.1 Brute-Force Combining Scheme

In the brute-force combining scheme, all MIMO system models up to the current HARQ round are interpreted as the single aggregated MIMO system model. At the rth HARQ round, this can be written as

$$\begin{bmatrix} \mathbf{y}_{1,j} \\ \vdots \\ \mathbf{y}_{r,j} \end{bmatrix} = \begin{bmatrix} \mathbf{H}_{1,j} \\ \vdots \\ \mathbf{H}_{r,j} \end{bmatrix} \mathbf{s}_j + \begin{bmatrix} \mathbf{n}_{1,j} \\ \vdots \\ \mathbf{n}_{r,j} \end{bmatrix}. \tag{4.3}$$

Therefore, at the rth HARQ round, the aggregated MIMO system model has the $(r+1)N_{\mathrm{R}} \times N_{\mathrm{T}}$ channel matrix and $(r+1)N_{\mathrm{R}} \times 1$ aggregated receive signal vector. Then, using Eq. (4.3), the detection criteria such as the ML, MMSE, and ZF are utilized to estimate $\mathbf{s}_j$.

By utilizing the entire information up to the current HARQ round, the brute-force combining scheme obtains a significantly better error performance than the detection and combining approaches such as the post-combining scheme [36]. However, the sizes of the aggregated channel matrix and receive signal vector increase with r as shown in Eq. (4.3), and the computational complexity for the brute-force combining scheme rapidly grows with r.

4.3.2 Post-Combining Scheme

In the post-combining scheme, the interference suppression by the linear detection is performed before the combining process [35]. Let $\mathbf{x}_{r,j} = \mathbf{H}_{r,j}^H \mathbf{y}_{r,j}$ and $\mathbf{C}_{r,j} = \mathbf{H}_{r,j}^H \mathbf{H}_{r,j}$. Then, after post-combining with the ZF detection, the filtered output vector for the jth transmit signal vector at the rth HARQ round is given by

$$\mathbf{z}_{\mathrm{PST},r,j}^{\mathrm{ZF}} = \frac{1}{N} \sum\nolimits_{i=1}^{r} (\mathbf{C}_{i,j})^{-1} \mathbf{x}_{i,j}, \tag{4.4}$$

where $\mathbf{z}_{\mathrm{PST},r,j}^{\mathrm{ZF}}$ is the $N_{\mathrm{T}} \times 1$ filtered output vector for $\mathbf{s}_j$ by the post-combining scheme with the ZF detection at the rth HARQ round. Similarly, after post-combining with the MMSE detection, the filtered output vector for $\mathbf{s}_j$ at the rth HARQ round is given by

$$\mathbf{z}_{\mathrm{PST},r,j}^{\mathrm{MMSE}} = \frac{1}{N} \sum\nolimits_{i=1}^{r} \left(\mathbf{C}_{i,j} + \frac{\sigma^2}{E_s} \mathbf{I}_{N_{\mathrm{T}}} \right)^{-1} \mathbf{x}_{i,j}, \tag{4.5}$$

where $\mathbf{z}_{\mathrm{PST},r,j}^{\mathrm{MMSE}}$ is the $N_{\mathrm{T}} \times 1$ filtered output vector for $\mathbf{s}_{r,j}$ by the post-combining scheme with the MMSE detection at the rth HARQ round.

As shown in Eqs. (4.4) and (4.5), the post-combining scheme performs the separate detection procedure for each HARQ round before the combining procedure. That is, if the combining procedures in Eqs. (4.4) and (4.5) are modified appropriately, then the post-combining scheme can be utilized even when the different transmit signal vectors are transmitted upon repeat requests. Therefore, the post-combining scheme can be applicable for PIR-HARQ and FIR-HARQ as well as CC-HARQ [35].

4.3.3 Pre-Combining Scheme

In the pre-combining scheme, opposite to the post-combining scheme, the interference suppression by the linear detection is performed after the combining process [35]. After pre-combining with the ZF detection, the filtered output vector for the jth transmit signal vector at the rth HARQ round is given by

$$\mathbf{z}_{\mathrm{PRE},r,j}^{\mathrm{ZF}} = \left(\sum_{i=1}^{r} \mathbf{C}_{i,j}\right)^{-1} \sum_{i=1}^{r} \mathbf{x}_{i,j}, \tag{4.6}$$

where $\mathbf{z}_{\mathrm{PRE},r,j}^{\mathrm{ZF}}$ is the $N_{\mathrm{T}} \times 1$ filtered output vector for $\mathbf{s}_j$ by the pre-combining scheme with the ZF detection at the rth HARQ round. Also, after pre-combining with the MMSE detection, the filtered output vector at the rth HARQ round is given by

$$\mathbf{z}_{\mathrm{PRE},r,j}^{\mathrm{MMSE}} = \left(\sum_{i=1}^{r} \mathbf{C}_{i,j} + \frac{\sigma^2}{E_s}\mathbf{I}_{N_{\mathrm{T}}}\right)^{-1} \sum_{i=1}^{r} \mathbf{x}_{i,j}, \tag{4.7}$$

where $\mathbf{z}_{\mathrm{PRE},r,j}^{\mathrm{MMSE}}$ is the $N_{\mathrm{T}} \times 1$ filtered output vector for $\mathbf{s}_j$ by the pre-combining scheme with the MMSE detection at the rth HARQ round.

It is shown in Eqs. (4.6) and (4.7) that the pre-combining scheme performs the combining procedure of all available HARQ rounds before the detection procedure. Therefore, for the pre-combining scheme, the same transmit signal vector should be repeatedly sent throughout retransmissions. Consequently, the pre-combining scheme is only applicable to CC-HARQ. However, as shown in [36], the pre-combining scheme is equivalent to the brute-force combining scheme with the same linear detection criterion. The entire information about $\mathbf{s}_j$ obtained up to the current HARQ round is utilized during the detection of $\mathbf{s}_j$ in the pre-combining scheme. Therefore, comparing with the post-combining scheme that utilizes only a part of the entire information during the detection

and combines such detection results, the pre-combining scheme obtains a significantly better error performance for CC-HARQ in MIMO systems with the same detection criterion [35].

4.3.4 QRD-SLC Scheme

In [37], two concatenation-assisted SLC (CASLC) schemes were proposed, which consist of the CASLC with the direct QRD (CASLC-DQ) and the CASLC with the incremental QRD (CASLC-IQ). Since the CASLC-IQ achieves a performance identical to that of the CASLC-DQ with a reduced computational complexity, only the CASLC-IQ is considered in this thesis.

At the first HARQ round, the CASLC-IQ performs the following linear transformation before the linear detection as

$$\begin{aligned} \overline{\mathbf{y}}_{1,j} &= \mathbf{Q}_{1,j}^{H}\mathbf{y}_{1,j} = \mathbf{Q}_{1,j}^{H}(\mathbf{H}_{1,j}\mathbf{s}_j + \mathbf{n}_{1,j}) \\ &= \mathbf{Q}_{1,j}^{H}(\mathbf{Q}_{1,j}\mathbf{R}_{1,j}\mathbf{s}_j + \mathbf{n}_{1,j}) = \mathbf{R}_{1,j}\mathbf{s}_j + \overline{\mathbf{n}}_{1,j}, \end{aligned} \tag{4.8}$$

where $\overline{\mathbf{y}}_{1,j}$ denotes the $N_{\mathrm{T}} \times 1$ receive signal vector for the equivalent system model, $\mathbf{Q}_{1,j}$ is the $N_{\mathrm{R}} \times N_{\mathrm{T}}$ matrix with orthogonal columns, $\mathbf{R}_{1,j}$ is the $N_{\mathrm{T}} \times N_{\mathrm{T}}$ upper-triangular matrix, and $\overline{\mathbf{n}}_{1,j}$ is the $N_{\mathrm{T}} \times 1$ noise vector obtained after the linear transformation using $\mathbf{Q}_{1,j}^{H}$.

Then, we derive the generalized equivalent system model and the filtered output vectors for the CASLC-IQ. At the r ($\geq$ 2)th HARQ round, the CASLC-IQ concatenates $\overline{\mathbf{y}}_{r-1,j}$ and $\overline{\mathbf{R}}_{r-1,j}$ respectively with $\mathbf{y}_{r,j}$ and $\mathbf{H}_{r,j}$, and then it performs the QRD on the

$(N_{\mathrm{T}} + N_{\mathrm{R}}) \times N_{\mathrm{T}}$ concatenated matrix of $\overline{\mathbf{R}}_{r-1,j}$ and $\mathbf{H}_{r,j}$ as

$$\begin{bmatrix} \overline{\mathbf{R}}_{r-1,j} \\ \overline{\mathbf{H}}_{r,j} \end{bmatrix} = \overline{\mathbf{Q}}_{r,j}\overline{\mathbf{R}}_{r,j}, \tag{4.9}$$

where $\overline{\mathbf{Q}}_{r,j}$ and $\overline{\mathbf{R}}_{r,j}$ are the $(N_{\mathrm{T}} + N_{\mathrm{R}}) \times N_{\mathrm{T}}$ matrix with orthogonal columns and the $N_{\mathrm{T}} \times N_{\mathrm{T}}$ upper-triangular matrix, respectively. Then, $\overline{\mathbf{Q}}_{r,j}^{H}$ is multiplied by the $(N_{\mathrm{T}} + N_{\mathrm{R}}) \times 1$ concatenated vector of $\overline{\mathbf{y}}_{r-1,j}$ and $\mathbf{y}_{r,j}$ to obtain the equivalent system model for the rth HARQ round as

$$\overline{\mathbf{y}}_{r,j} = \overline{\mathbf{Q}}_{r,j}^{H} \begin{bmatrix} \overline{\mathbf{y}}_{r-1,j} \\ \mathbf{y}_{r,j} \end{bmatrix} = \overline{\mathbf{R}}_{r,j}\mathbf{s}_j + \overline{\mathbf{n}}_{r,j}, \tag{4.10}$$

where $\overline{\mathbf{n}}_{r,j}$ is the $N_{\mathrm{T}} \times 1$ noise vector after the linear transformation using $\overline{\mathbf{Q}}_{r,j}^{H}$. Then, using Eq. (4.10), the filtered output vectors for $\mathbf{s}_j$ after the CASLC-IQ with the ZF and MMSE detections at the rth HARQ round are respectively written as

$$\mathbf{z}_{\mathrm{IQ},r,j}^{\mathrm{ZF}} = \left(\overline{\mathbf{R}}_{r,j}^{H}\overline{\mathbf{R}}_{r,j}\right)^{-1}\overline{\mathbf{R}}_{r,j}^{H}\overline{\mathbf{y}}_{r,j} \tag{4.11}$$

and

$$\mathbf{z}_{\mathrm{IQ},r,j}^{\mathrm{MMSE}} = \left(\overline{\mathbf{R}}_{r,j}^{H}\overline{\mathbf{R}}_{r,j} + \frac{\sigma^2}{E_s}\mathbf{I}_{N_{\mathrm{T}}}\right)^{-1}\overline{\mathbf{R}}_{r,j}^{H}\overline{\mathbf{y}}_{r,j}, \tag{4.12}$$

where $\mathbf{z}_{\mathrm{IQ},r,j}^{\mathrm{ZF}}$ and $\mathbf{z}_{\mathrm{IQ},r,j}^{\mathrm{MMSE}}$ are the $N_{\mathrm{T}} \times 1$ filtered output vector for $\mathbf{s}_j$ by the CASLC-IQ with the ZF and MMSE detections at the rth HARQ round, respectively.

As shown in [37], the performance of CASLC-IQ is identical to that of the brute-force combining scheme and the pre-combining scheme. In addition, in case of the ML

detection, the CASLC-IQ also has a lower computational complexity than the brute-force combining scheme by maintaining the $N_{\mathrm{T}} \times N_{\mathrm{T}}$ equivalent channel matrix for every HARQ round. However, by performing the QRD on the concatenated matrix in every HARQ round, it could have a higher computational complexity than the pre-combining when linear detection criteria such as the MMSE and ZF are used.

4.4 Proposed Low-Complexity SLC Scheme

4.4.1 SMW Lemma-based Combining and Detection Procedures

This section describes the proposed SLC scheme and its associated combining and detection procedures. First, let $\mathbf{F}_{r,j}$ denote the $N_{\mathrm{T}} \times N_{\mathrm{T}}$ matrix after the inverse operation in Eqs. (4.6) and (4.7) for the pre-combining scheme, which can be written as

$$\mathbf{F}_{r,j} = \left(\sum_{i=1}^{r} \mathbf{C}_{i,j}\right)^{-1} \tag{4.13}$$

for the ZF detection, and

$$\mathbf{F}_{r,j} = \left(\sum_{i=1}^{r} \mathbf{C}_{i,j} + \frac{\sigma^2}{E_s}\mathbf{I}_{N_{\mathrm{T}}}\right)^{-1} \tag{4.14}$$

for the MMSE detection. Since

$$\mathbf{C}_{r,j} = \mathbf{H}_{r,j}^{H}\mathbf{H}_{r,j} = \sum_{n=1}^{N_{\mathrm{R}}} \mathbf{h}_{r,j,n}^{H}\mathbf{h}_{r,j,n}, \tag{4.15}$$

where $\mathbf{h}_{r,j,n}$ is the nth row vector of $\mathbf{H}_{r,j}$, $\mathbf{F}_{r,j}$ can be rewritten as

$$\mathbf{F}_{r,j} = \left(\mathbf{F}_{r-1,j}^{-1} + \sum_{n=1}^{N_{\mathrm{R}}} \mathbf{h}_{r,j,n}^{H}\mathbf{h}_{r,j,n}\right)^{-1} \tag{4.16}$$

regardless of the detection criterion.

For a matrix inversion problem of $(\mathbf{A}+\mathbf{a}^{H}\mathbf{b})^{-1}$, if $1+\mathbf{b}\mathbf{A}^{-1}\mathbf{a}^{H} \neq 0$, then the SMW matrix inversion lemma [41,42] can be utilized to obtain the solution instead of the direct inversion of matrix as

$$(\mathbf{A}+\mathbf{a}^{H}\mathbf{b})^{-1} = \mathbf{A}^{-1} - \frac{\mathbf{A}^{-1}\mathbf{a}^{H}\mathbf{b}\mathbf{A}^{-1}}{1+\mathbf{b}\mathbf{A}^{-1}\mathbf{a}^{H}}, \tag{4.17}$$

where both $\mathbf{a}$ and $\mathbf{b}$ are $1 \times M$ vectors with $\mathrm{rank}(\mathbf{a}^{H}\mathbf{b}) = 1$ and $\mathbf{A}$ is the $M \times M$ matrix with $\mathrm{rank}(\mathbf{A}) = M$.

Let $\mathbf{F}_{r,j,0} = \mathbf{F}_{r-1,j}$. Then, $\mathbf{F}_{r,j,n}$ can be sequentially calculated from $n = 1$ to $n = N_{\mathrm{R}}$ as

$$\mathbf{F}_{r,j,n} = \left(\mathbf{F}_{r,j,n-1}^{-1} + \mathbf{h}_{r,j,n}^{H}\mathbf{h}_{r,j,n}\right)^{-1}. \tag{4.18}$$

Then, by applying Eq. (4.17), Eq. (4.18) can be rewritten as

$$\mathbf{F}_{r,j,n} = \mathbf{F}_{r,j,n-1} - \frac{\mathbf{F}_{r,j,n-1}\mathbf{h}_{r,j,n}^{H}\mathbf{h}_{r,j,n}\mathbf{F}_{r,j,n-1}}{1+\mathbf{h}_{r,j,n}\mathbf{F}_{r,j,n-1}\mathbf{h}_{r,j,n}^{H}}, \tag{4.19}$$

where $\mathbf{F}_{r,j,N_{\mathrm{R}}}$ is identical to $\mathbf{F}_{r,j}$ for the pre-combining scheme.

Using the above observations, the combining and detection procedures of the proposed low-complexity SLC scheme are derived as follows. The main idea of the proposed low-complexity SLC scheme is to perform the SMW matrix inversion lemma G ($\leq N_{\mathrm{R}}$)

times, instead of N_{R} times, when a retransmission occurs. At the first HARQ round, the proposed scheme performs the conventional linear detection based on the system model in Eq. (4.1). Then, the filtered output vectors for $\mathbf{s}_j$ after the proposed SLC with the ZF and MMSE detections at the first HARQ round are respectively written as

$$\mathbf{z}_{\mathrm{SLC},1,j}^{\mathrm{ZF}} = \mathbf{C}_{1,j}^{-1}\mathbf{x}_{1,j} \tag{4.20}$$

and

$$\mathbf{z}_{\mathrm{SLC},1,j}^{\mathrm{MMSE}} = \left(\mathbf{C}_{1,j} + \frac{\sigma^2}{E_s}\mathbf{I}_{N_{\mathrm{T}}}\right)^{-1}\mathbf{x}_{1,j}, \tag{4.21}$$

which are the same output vectors as existing SLC schemes in Sec. 4.3. Let

$$\mathbf{E}_{1,j}^{\mathrm{ZF}} = \mathbf{C}_{1,j}^{-1} \tag{4.22}$$

for the ZF detection, and let

$$\mathbf{E}_{1,j}^{\mathrm{MMSE}} = \left(\mathbf{C}_{1,j} + \frac{\sigma^2}{E_s}\mathbf{I}_{N_{\mathrm{T}}}\right)^{-1} \tag{4.23}$$

for the MMSE detection. Then, for the proposed scheme from the second HARQ round, $\mathbf{E}_{r,j}^{\mathrm{ZF}}$ and $\mathbf{E}_{r,j}^{\mathrm{MMSE}}$ with $r \geq 2$ are obtained by performing the the SMW matrix inversion lemma G times. Let $\mathbf{E}_{r,j,0}^{\mathrm{ZF}} = \mathbf{E}_{r-1,j}^{\mathrm{ZF}}$ and $\mathbf{E}_{r,j,0}^{\mathrm{MMSE}} = \mathbf{E}_{r-1,j}^{\mathrm{MMSE}}$. Then, $\mathbf{E}_{r,j,n}^{\mathrm{ZF}}$ and $\mathbf{E}_{r,j,n}^{\mathrm{MMSE}}$ can be sequentially calculated from $n = 1$ to $n = G$, which are respectively written as

$$\mathbf{E}_{r,j,n}^{\mathrm{ZF}} = \mathbf{E}_{r,j,n-1}^{\mathrm{ZF}} - \frac{\mathbf{E}_{r,j,n-1}^{\mathrm{ZF}}\mathbf{h}_{o(r,j,n)}^{H}\mathbf{h}_{o(r,j,n)}\mathbf{E}_{r,j,n-1}^{\mathrm{ZF}}}{1 + \mathbf{h}_{o(r,j,n)}\mathbf{E}_{r,j,n-1}^{\mathrm{ZF}}\mathbf{h}_{o(r,j,n)}^{H}} \tag{4.24}$$

and

$$\mathbf{E}_{r,j,n}^{\mathrm{MMSE}} = \mathbf{E}_{r,j,n-1}^{\mathrm{MMSE}} - \frac{\mathbf{E}_{r,j,n-1}^{\mathrm{MMSE}}\mathbf{h}_{o(r,j,n)}^{H}\mathbf{h}_{o(r,j,n)}\mathbf{E}_{r,j,n-1}^{\mathrm{MMSE}}}{1+\mathbf{h}_{o(r,j,n)}\mathbf{E}_{r,j,n-1}^{\mathrm{MMSE}}\mathbf{h}_{o(r,j,n)}^{H}}, \tag{4.25}$$

where $\mathbf{E}_{r,j,G}^{\mathrm{ZF}} = \mathbf{E}_{r,j}^{\mathrm{ZF}}$, $\mathbf{E}_{r,j,G}^{\mathrm{MMSE}} = \mathbf{E}_{r,j}^{\mathrm{MMSE}}$, and $o(r,j,n)$ is the index of the row vector in $\mathbf{H}_{r,j}$ selected for $\mathbf{E}_{r,j,n}^{\mathrm{ZF}}$ and $\mathbf{E}_{r,j,n}^{\mathrm{MMSE}}$.

As shown in Eqs. (4.24) and (4.25), only G row vectors in $\mathbf{H}_{r,j}$ are selected and utilized to calculate $\mathbf{E}_{r,j}^{\mathrm{ZF}}$ and $\mathbf{E}_{r,j}^{\mathrm{MMSE}}$. Consequently, $\mathbf{x}_{r,j} = \mathbf{H}_{r,j}^{H}\mathbf{y}_{r,j}$ utilized in the post-combining scheme and the pre-combining scheme also should be modified according to $\mathbf{E}_{r,j}^{\mathrm{ZF}}$ and $\mathbf{E}_{r,j}^{\mathrm{MMSE}}$. Let $\mathbf{P}_{r,j}$ be the $G \times N_{\mathrm{T}}$ matrix containing the selected G row vectors in $\mathbf{H}_{r,j}$, and let $\mathbf{v}_{r,j}$ be the $G \times 1$ vector containing the G elements in $\mathbf{y}_{r,j}$, which correspond to the row vectors in $\mathbf{P}_{r,j}$, i.e., $\mathbf{y}_{r,j} = [y_{r,j,o(r,j,1)}, \cdots, y_{r,j,o(r,j,G)}]^{T}$. Then, the vector utilized for the proposed scheme instead of $\mathbf{x}_{r,j}$ is written as

$$\mathbf{w}_{r,j} = \mathbf{P}_{r,j}^{H}\mathbf{v}_{r,j}. \tag{4.26}$$

Note that $\mathbf{w}_{1,j} = \mathbf{x}_{1,j}$, $\mathbf{P}_{1,j} = \mathbf{H}_{1,j}$, and $\mathbf{v}_{1,j} = \mathbf{y}_{1,j}$ since all N_{R} row vectors in $\mathbf{H}_{1,j}$ are utilized in the proposed scheme at the first HARQ round. Then, using $\mathbf{w}_{r,j}$, the filtered output vectors for $\mathbf{s}_j$ after the proposed SLC with the ZF and MMSE detections at the rth HARQ round are respectively written as

$$\mathbf{z}_{\mathrm{SLC},r,j}^{\mathrm{ZF}} = \mathbf{E}_{r,j}^{\mathrm{ZF}}\left(\sum\nolimits_{i=1}^{r}\mathbf{w}_{i,j}\right) \tag{4.27}$$

and

$$\mathbf{z}_{\mathrm{SLC},r,j}^{\mathrm{MMSE}} = \mathbf{E}_{r,j}^{\mathrm{MMSE}}\left(\sum\nolimits_{i=1}^{r}\mathbf{w}_{i,j}\right). \tag{4.28}$$

Note that the proposed scheme with $G = N_{\mathrm{R}}$ utilizes all the row vectors in each $\mathbf{H}_{r,j}$. That is, the channel matrix $\mathbf{H}_{r,j}$ is fully utilized for the proposed SLC scheme. In this case, $\mathbf{z}_{\mathrm{SLC},r,j}^{\mathrm{ZF}}$ and $\mathbf{z}_{\mathrm{SLC},r,j}^{\mathrm{MMSE}}$ become equivalent to $\mathbf{z}_{\mathrm{PRE},r,j}^{\mathrm{ZF}}$ and $\mathbf{z}_{\mathrm{PRE},r,j}^{\mathrm{MMSE}}$, respectively, and therefore the proposed SLC scheme achieves the identical performance to the pre-combining scheme as well as the brute-force combining and CASLC-IQ schemes but it has similar computational complexity compared to the existing SLC schemes, as shown in Sec. 4.4.3.

4.4.2 Squared Norm-based Row Vector Selection Criterion

As shown in Eqs. (4.24) and (4.25), G row vectors in each $\mathbf{H}_{r,j}$ are selected for the proposed scheme to obtain the filtered output vector. Therefore, unless $G = N_{\mathrm{R}}$, the selection of G row vectors in each $\mathbf{H}_{r,j}$ will greatly affect the performance of the proposed scheme. When $G = N_{\mathrm{R}}$, there is only one combination of the G row vectors in $\mathbf{H}_{r,j}$. Further, as explained in Sec. 4.4.1, the performance of the proposed SLC scheme is identical to the pre-combining scheme regardless of the row vector selection criterion. Therefore, the row vector selection criterion in this section does not need to be operated when G is set to N_{R} at the receiver. To enhance the error performances of the proposed scheme, it is possible to find a combination of the row vectors that achieves the highest SINR for the filtered outputs among all possible combinations. However, there are $\binom{N_{\mathrm{R}}}{G}$ possible combinations of the row vectors at each HARQ round. Furthermore, the exact values of SINR for each combination of the row vectors should be calculated in order to find such a combination, and each calculation for a given MMSE or ZF detection is composed of a number of matrix operations including the multiplication and inverse operations [41]. In other words, the optimal row vector selection criterion based on the

highest SINR with the exact SINR computation according to a given detection criterion requires a significantly higher computational complexity.

Therefore, we develop a low-complexity row vector selection criterion for the proposed SLC scheme, which is termed as the squared norm-based row vector selection criterion in the rest of this thesis. In the successive interference cancellation schemes for MIMO systems, the cancellation order among the transmitted symbols is usually decided by the summation of the squared norms of the row vectors in the channel matrix [2]. That is, the SINR of the symbols after linear detections can be predicted by the summation of the squared norms of the row vectors in the channel matrix. Motivated by this approach, the proposed selection criterion interprets the squared norm of a row vector in $\mathbf{H}_{r,j}$ as the amount of the SINR improvement by using the row vector in the proposed SLC scheme. For that, first, the proposed criterion calculates the squared norms of all row vectors in $\mathbf{H}_{r,j}$, which can be written as

$$u_{r,j,n} = \|\mathbf{h}_{r,j,n}\mathbf{h}_{r,j,n}^{H}\|^{2}, \tag{4.29}$$

where $u_{r,j,n}$ for $1 \leq n \leq N_{\mathrm{R}}$ is the squared norm of $\mathbf{h}_{r,j,n}$, which corresponds to the estimated amount of the SINR improvement when $\mathbf{h}_{r,j,n}$ is selected and utilized in the proposed scheme. Then, the calculated $u_{r,j,n}$ for $1 \leq n \leq N_{\mathrm{R}}$ are sorted in descending order and the G row vectors in $\mathbf{H}_{r,j}$ which have the higher $u_{r,j,n}$ than the other row vectors are selected for the proposed scheme, i.e.,

$$o(r,j,n) = \arg \max_{n^{*} \in \mathsf{N}_{r,j,n}} u_{r,j,n^{*}}, \tag{4.30}$$

where $\mathsf{N}_{r,j,n}$ is the set including the indices of the row vectors in $\mathbf{H}_{r,j}$ which have

Table 4.1: Computational complexity of the SLC schemes with linear detection for re-transmissions.

Brute-Force Combining [36]	$\mathcal{O}\left((r+1)N_{\mathrm{R}}N_{\mathrm{T}}^2 + N_{\mathrm{T}}^3\right)$
Post-Combining [35]	$\mathcal{O}\left(N_{\mathrm{R}}N_{\mathrm{T}}^2 + N_{\mathrm{T}}^3\right)$
Pre-Combining [35]	$\mathcal{O}\left(N_{\mathrm{R}}N_{\mathrm{T}}^2 + N_{\mathrm{T}}^3\right)$
CASLC-IQ [37]	$\mathcal{O}\left(N_{\mathrm{R}}N_{\mathrm{T}}^2 + 3N_{\mathrm{T}}^3\right)$
Proposed SLC [52]	$\mathcal{O}\left(2GN_{\mathrm{T}}^2\right)$
Proposed SLC w/ Optimal SINR Selection [52]	$\mathcal{O}\left((2G+N_{\mathrm{R}})N_{\mathrm{T}}^2 + N_{\mathrm{T}}^3\right)$
Proposed SLC w/ Squared Norm Selection [52]	$\mathcal{O}\left(2GN_{\mathrm{T}}^2 + N_{\mathrm{R}}N_{\mathrm{T}}\right)$

not been selected until $o(r, j, n-1)$ with $o(r, j, 0) = \emptyset$, i.e., $\mathsf{N}_{r,j,n} = \{1, \cdots, N_{\mathrm{R}}\} - \{o(r, j, 1), \cdots, o(r, j, n-1)\}$.

When the proposed low-complexity SLC scheme operates with the MMSE or ZF detection, proposed squared norm-based row vector selection criterion in Eqs. (4.29) and (4.30) cannot be the optimal criterion in the aspect of the performance. However, the proposed squared norm criterion requires the calculations of the squared norm of the $1 \times N_{\mathrm{T}}$ row vector for N_{R} times regardless of G values and therefore can operate at a significantly lower computational complexity, which is further investigated in the following section.

4.4.3 The Complexity of Existing and Proposed SLC Schemes

In this section, we analyze the computational complexity of the existing and proposed SLC schemes with the linear detection criterion for one transmit signal vector, and the results are summarized in Table 4.1, where the big O notation, $\mathcal{O}(n)$ donates the computational complexity that is linear in $n \in \mathbb{R}^+$ [41]. Since all schemes have the same computational complexity when $r = 1$, we only consider the computational complexity of

the SLC schemes for retransmissions, i.e., $r \geq 2$. Further, the results can be applied for both MMSE and ZF detections, since only one matrix addition is additionally required for the MMSE detection compared to the ZF detection [2], which has a negligible complexity.

In the brute-force combining scheme, the multiplication of the $N_{\mathrm{T}} \times (r+1)N_{\mathrm{R}}$ matrix and the $(r+1)N_{\mathrm{R}} \times N_{\mathrm{T}}$ matrix is performed, and the inverse of the $N_{\mathrm{T}} \times N_{\mathrm{T}}$ matrix is performed after the multiplication. Therefore, the computational complexity of the brute-force combining scheme is $\mathcal{O}\left((r+1)N_{\mathrm{R}}N_{\mathrm{T}}^2 + N_{\mathrm{T}}^3\right)$ as r increases.

In the post-combining scheme, as shown in Eqs. (4.4) and (4.5), the multiplication of the $N_{\mathrm{T}} \times N_{\mathrm{R}}$ matrix and the $N_{\mathrm{R}} \times N_{\mathrm{T}}$ matrix is performed, and the inverse of the $N_{\mathrm{T}} \times N_{\mathrm{T}}$ matrix is performed after the multiplication. Therefore, ignoring the summation operations, the complexity complexity of the post-combining scheme is $\mathcal{O}\left(N_{\mathrm{R}}N_{\mathrm{T}}^2 + N_{\mathrm{T}}^3\right)$.

Meanwhile, if the summation operations in Eqs. (4.6) and (4.7) are ignored, then the multiplication of the $N_{\mathrm{T}} \times N_{\mathrm{R}}$ matrix and the $N_{\mathrm{R}} \times N_{\mathrm{T}}$ matrix and the inverse of the $N_{\mathrm{T}} \times N_{\mathrm{T}}$ matrix are required for the pre-combining scheme. Therefore, the pre-combining scheme has the same computational complexity order to the post-combining scheme, which is $\mathcal{O}\left(N_{\mathrm{R}}N_{\mathrm{T}}^2 + N_{\mathrm{T}}^3\right)$.

In the CASLC-IQ, first the QRD on the $(N_{\mathrm{T}} + N_{\mathrm{R}}) \times N_{\mathrm{T}}$ concatenated matrix is performed. Then, after the linear transformation, the multiplication of the two $N_{\mathrm{T}} \times N_{\mathrm{T}}$ matrices and the inverse of the $N_{\mathrm{T}} \times N_{\mathrm{T}}$ matrix is performed as shown in Eqs. (4.11) and (4.12). Since the QRD on the $M \times N$ matrix has the complexity order of $\mathcal{O}\left(MN^2\right)$ [49], the computational complexity of the CASLC-IQ is $\mathcal{O}\left((N_{\mathrm{T}} + N_{\mathrm{R}})N_{\mathrm{T}}^2 + N_{\mathrm{T}}^3 + N_{\mathrm{T}}^3\right) = \mathcal{O}\left(N_{\mathrm{R}}N_{\mathrm{T}}^2 + 3N_{\mathrm{T}}^3\right)$. Therefore, although the CASLC-IQ can require a lower computational complexity than the brute-force combining scheme, it requires a significantly higher computational complexity than the post-combining and pre-combining schemes when the linear detection criterion is considered.

Finally, the computational complexity of the proposed SLC scheme is derived. As shown in Eqs. (4.24) and (4.25), the proposed scheme requires the multiplication of $N_{\mathrm{T}} \times N_{\mathrm{T}}$ matrix and the $N_{\mathrm{T}} \times 1$ vector, i.e., $\mathbf{E}^{\mathrm{ZF}}_{r,j,n-1}\mathbf{h}^{H}_{o(r,j,n)}$ in Eq. (4.24) and $\mathbf{E}^{\mathrm{MMSE}}_{r,j,n-1}\mathbf{h}^{H}_{o(r,j,n)}$ in Eq. (4.25), which has the complexity of $\mathcal{O}\left(N_{\mathrm{T}}^2\right)$. Since any $\mathbf{E}^{\mathrm{ZF}}_{r,j,n-1}$ or $\mathbf{E}^{\mathrm{MMSE}}_{r,j,n-1}$ is an inverse matrix of an Hermitian matrix, $\mathbf{E}^{\mathrm{ZF}}_{r,j,n-1}\mathbf{h}^{H}_{o(r,j,n)} = (\mathbf{h}_{o(r,j,n)}\mathbf{E}^{\mathrm{ZF}}_{r,j,n-1})^{H}$ or $\mathbf{E}^{\mathrm{MMSE}}_{r,j,n-1}\mathbf{h}^{H}_{o(r,j,n)} = (\mathbf{h}_{o(r,j,n)}\mathbf{E}^{\mathrm{MMSE}}_{r,j,n-1})^{H}$, respectively. Therefore, the most complexity burden on the remaining operations is the multiplication of the $N_{\mathrm{T}} \times 1$ vector and the $1 \times N_{\mathrm{T}}$ in the numerators of Eqs. (4.24) and (4.25), which has the complexity order of $\mathcal{O}\left(N_{\mathrm{T}}^2\right)$. Since these operations have to be performed G times for the proposed scheme, the overall computational complexity of the proposed scheme in Eqs. (4.24) and (4.25) is $\mathcal{O}\left(2GN_{\mathrm{T}}^2\right)$. Further, the proposed row vector selection criterion in Eqs. (4.29) and (4.30) requires the calculations of the squared norm of the $1 \times N_{\mathrm{T}}$ row vector for N_{R} times, which has the complexity of $\mathcal{O}\left(N_{\mathrm{T}}N_{\mathrm{R}}\right)$ regardless of G. Therefore, the computational complexity of the squared norm-based row vector selection criterion is negligible compared to those for the SLC schemes. Further, even considering the complexity of the squared norm criterion, the proposed scheme shows a significantly better computational complexity reduction than the brute-force combining scheme and the CASLC-IQ. When $G = N_{\mathrm{R}} = N_{\mathrm{T}}$, the proposed scheme without considering the complexity of the squared norm criterion has the same computational complexity order as the post-combining and pre-combining schemes, and considering the complexity of the squared norm criterion, the proposed scheme has a slightly higher computational complexity than the post-combining and pre-combining schemes. By the way, as G decreases when $N_{\mathrm{R}} = N_{\mathrm{T}}$, the proposed scheme can have an advantage in computational complexity over the post-combining and pre-combining schemes regardless of utilizing the squared norm-based row vector selection criterion.

4.5 Simulation Results

In this section, the error performances of the post-combining scheme, the pre-combining scheme, and the proposed SLC scheme are derived and compared via simulations. In order to verify the impact of the squared norm-based row vector selection criterion (denoted as the squared (SQ) criterion in the sequel) on the performance of the proposed SLC scheme, we also consider the ascending order-based row vector selection criterion (denoted as the ascending (ASC) criterion in the sequel), i.e., $o(r, j, n) = n$ regardless of r, j, as the proposed SLC scheme. In addition, the optimal row vector selection criterion (denoted as the optimal (OPT) criterion in the sequel) based on the highest SINR with the exact SINR computation according to a given detection criterion is considered for the proposed SLC scheme as well, where the OPT criterion finds a combination of the row vectors that achieves the highest SINR for a given MMSE or ZF detection among all possible combinations. Since the brute-force combining scheme and the CASLC-IQ have the identical error performances to the pre-combining scheme [37], the results for their error performances are omitted in this section. It is worthwhile to mention that the cases of $G = 3$ for the proposed scheme in Figs. 4.2–4.4 correspond to both the ASC, SQ, and OPT criteria, since the proposed scheme for $G = N_{\mathrm{R}}$ has the identical performance to the pre-combining scheme regardless of the row vector selection criterion, as explained in Sec. 4.4.

The MIMO system with $N_{\mathrm{T}} = N_{\mathrm{R}} = 3$ is considered, and QPSK modulation with $Q = 2$ is used to generate the transmit symbols. The numbers of data and coded bits, K and C are set to 360 and 720, respectively, and the numbers of transmit symbols and vectors, L and J are set to 360 and 120, respectively. The maximum allowable number of transmissions, R is set to 3. A rate 1/2 convolutional code with a constraint length

of 3 and code generator polynomials of 7 and 5 in octal numbers is considered at the transmitter and a hard decision based Viterbi decoder with a traceback depth of 9 is considered at the receiver [27]. Independent Rayleigh fading channel is considered, and thereby all elements of $\mathbf{H}_{r,j}$ are complex Gaussian random variables with zero mean and unit variance and $\mathbf{H}_{r,j}$ varies independently for every jth transmit signal vector at the rth HARQ round.

First, the average BER performances of the existing and proposed SLC schemes are compared in Figs. 4.2 and 4.3. To show the estimation quality of the SLC schemes, no decoding is performed and the results correspond to the average uncoded BER performances of the SLC schemes. Also, for the same reason, it is assumed in Figs. 4.2 and 4.3 that a retransmission always occurs up to the rth HARQ round.

In Fig. 4.2, the average uncoded BER performances of the SLC schemes with the ZF detection are compared, where $r = 2$ and 3 in Figs. 4.2(a) and 4.2(b), respectively. It is shown that the proposed scheme obtains a better BER as G increases by utilizing more information during the combining and detection procedures regardless of the row vector selection criterion. Further, as predicted in Sec. 4.4, the proposed scheme for $G = 3$ ($= N_{\mathrm{R}}$) and the pre-combining scheme show the near-identical BER performances regardless of r. Comparing with the post-combining scheme, the proposed scheme outperforms the post-combining scheme and, by utilizing more information for a larger G, the SNR gain of the proposed scheme over the post-combining scheme increases with G regardless of the rth HARQ round. Specifically, at a BER of 10^{-4}, the SNR gains of the proposed scheme with SQ criterion for $G = 2$ when $r = 2$ and 3 over the post-combining scheme are about 21.3 dB and 24.8 dB, respectively. Meanwhile, the proposed scheme with the SQ criterion show a better performance than the ASC criterion regardless of G and r. In detail, when $r = 2$, at a BER of 10^{-4}, the SNR gains of proposed scheme with the

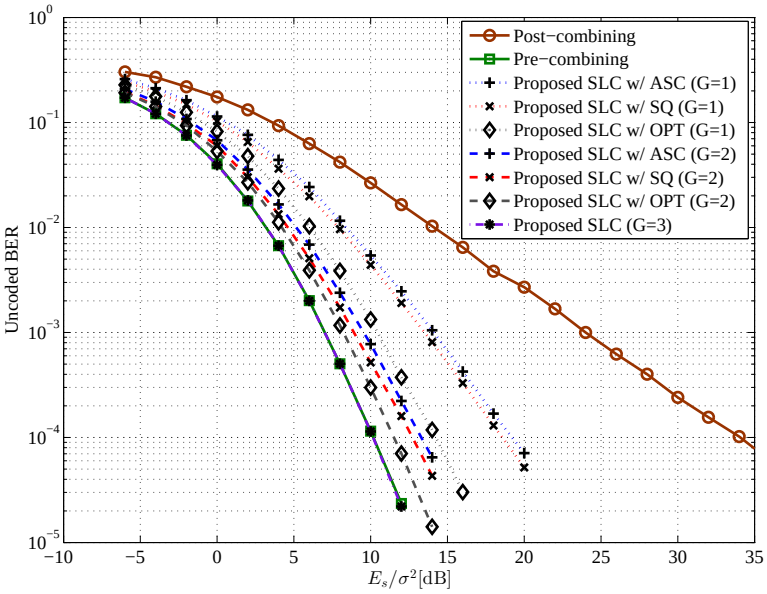

(a) $r = 2$.

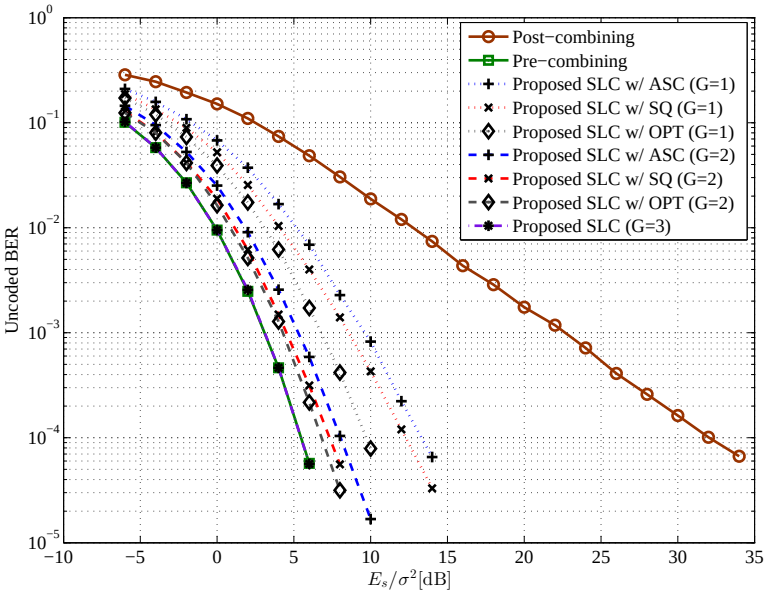

(b) $r = 3$.

Figure 4.2: Average uncoded BER performances of the SLC schemes based on the ZF detection when $N_{\mathrm{T}} = N_{\mathrm{R}} = 3$.

SQ criterion over the proposed scheme with the ASC criterion for $G = 1$ and 2 are both about 0.43 dB. These gains further increase when $r = 3$, which are about 0.87 dB and 0.56 dB, respectively.

In Fig. 4.3, the average uncoded BER performances of the SLC schemes with the MMSE detection are compared, where $r = 2$ and 3 in Figs. 4.3(a) and 4.3(b), respectively. Similar to the results in Fig. 4.2, the BER performances of the proposed scheme for $G = 3$ $(= N_{\mathrm{R}})$ and the pre-combining scheme are near-identical regardless of r. Meanwhile, unlike the results in Fig. 4.2, the post-combining scheme shows a better BER performance than the proposed scheme with the ASC criterion for $G = 1$. Nevertheless, the proposed scheme with the SQ criterion for $G = 1$ shows a similar BER performance to the post-combining scheme at the high SNR region, and the proposed scheme for $G = 2$ outperforms the post-combining scheme regardless of the row vector selection criterion. Specifically, at a BER of 10^{-4}, the SNR gains of the proposed scheme with the SQ criterion for $G = 2$ over the post-combining scheme when $r = 2$ and 3 are about 5.82 dB and 4.85 dB, respectively. Meanwhile, similar to the results in Figs. 4.2, the proposed scheme with the SQ criterion show a better performance than the proposed scheme with the ASC criterion regardless of G and r. In detail, when $r = 2$, at a BER of 10^{-4}, the SNR gains of the proposed scheme with the SQ criterion over the proposed scheme with the ASC criterion for $G = 2$ is about 0.59 dB. This gain further increases about 0.88 dB, when $r = 3$.

Finally, in Fig. 4.4, the average FER performances of the SLC schemes are illustrated, where the ZF and MMSE detections are considered in Figs. 4.4(a) and 4.4(b), respectively. The average FER is defined as the number of erroneous packets after the Rth HARQ round divided by the number of total packets transmitted. Unlike the simulation environments for Figs. 4.2 and 4.3, if a decoding is failed when $r = R$ or the

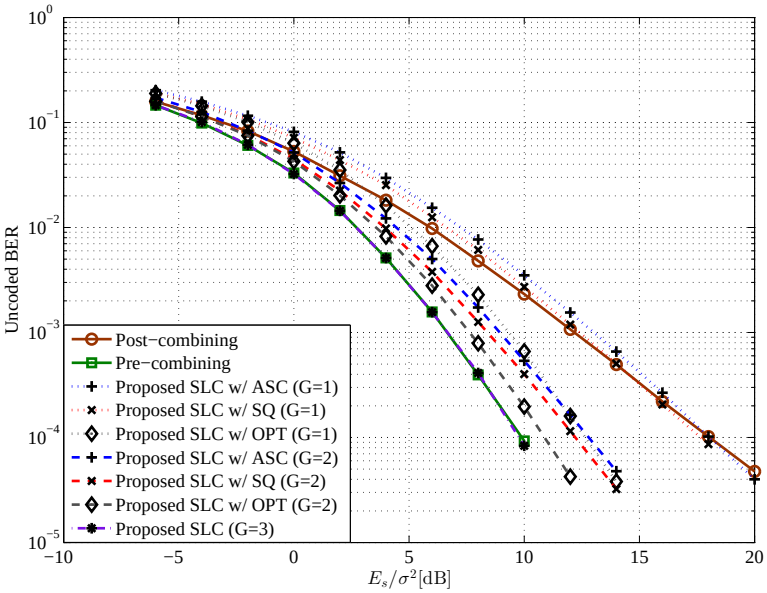

(a) $r = 2$.

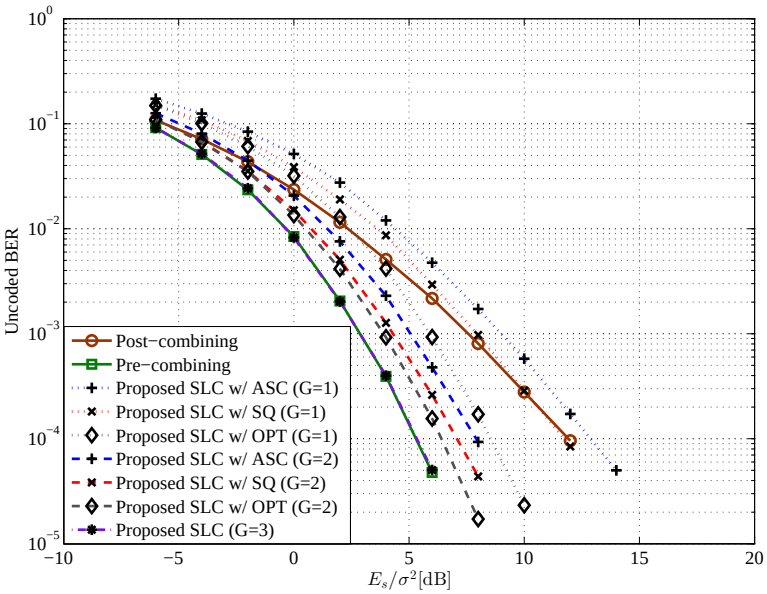

(b) $r = 3$.

Figure 4.3: Average uncoded BER performances of the SLC schemes based on the MMSE detection when $N_{\mathrm{T}} = N_{\mathrm{R}} = 3$.

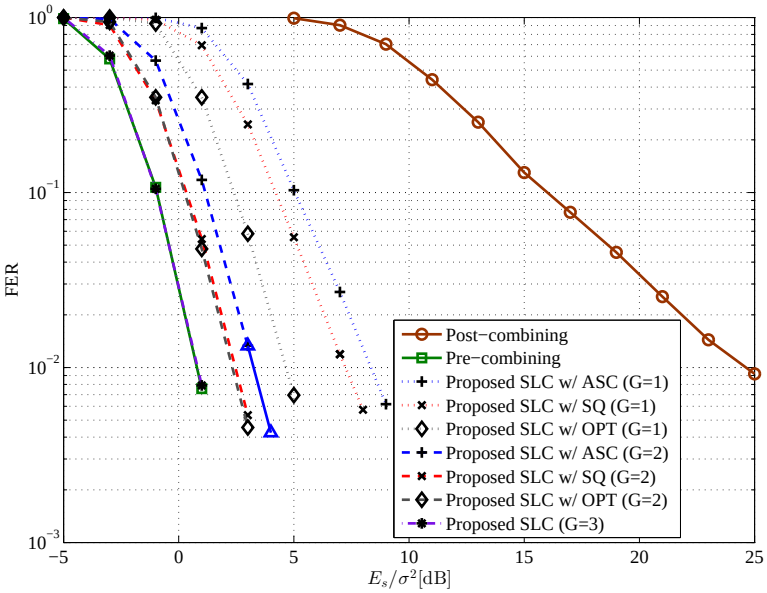

(a) ZF detection.

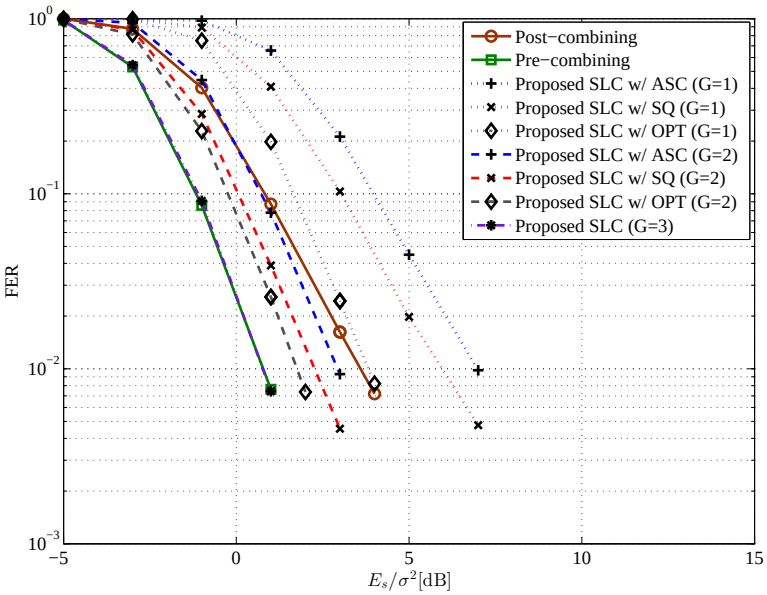

(b) MMSE detection.

Figure 4.4: Average FER performances of the SLC schemes when $N_{\mathrm{T}} = N_{\mathrm{R}} = 3$ and $R = 3$.

decoding is successfully performed, then the transmission for the current packet is terminated and the next packet is transmitted from the next transmission time slot. Similar to the results in Figs. 4.2 and 4.3, the proposed scheme for $G = 3$ $(= N_{\mathrm{R}})$ and the pre-combining scheme achieve the near-identical FER performances regardless of r and the detection criterion. Also, in cases of the ZF detection, the proposed scheme shows a better average FER than the post-combining scheme regardless of G and the row vector selection criterion. Meanwhile, in cases of the MMSE detection, the post-combining scheme outperforms the proposed scheme for $G = 1$ regardless of the row vector selection criterion. However, for $G = 2$, the proposed scheme with the ASC criterion shows a similar FER performance to the post-combining scheme, and the proposed scheme with the SQ criterion outperforms the post-combining scheme. In detail, at a FER of 10^{-2}, the SNR gains of the proposed scheme with the SQ criterion over post-combining scheme is about 0.96 dB.

As shown in Figs. 4.2–4.4, the proposed scheme with the OPT criterion outperforms the SQ and ASC criteria regardless of G, r, and the detection scheme. However, as already explained in Sec. 4.3, calculating exact values of SINR for each combination of the row vectors for a given MMSE or ZF detection is composed of a number of matrix operations including the multiplication and inverse operations, which requires a significantly high computational complexity. Specifically, $\mathbf{F}_{r,j,N_r}$ should to be calculated first to obtain the exact SINR values of the filtered outputs for a given MMSE of ZF detection [2], and the calculation of $\mathbf{F}_{r,j,N_r}$ requires the computational complexity equal to that of the pre-combining scheme. That is, regardless of G and r, the computational complexity of the OPT criterion itself is at least equal to that of the pre-combining scheme which achieves the near-identical performance to the proposed scheme for $G = N_r$. Therefore, the OPT criterion with the exact SINR computation is unpractical for

the proposed SLC scheme.

The results in Figs. 4.2–4.4 show that the proposed SLC scheme can achieve a better performance than the post-combining scheme regardless of the row vector selection criterion. Further, as derived in Sec. 4.4.3, the computational complexity of the proposed SLC scheme with the ASC or SQ criterion for retransmissions decreases with G, whereas the post-combining and pre-combining schemes require a fixed computational complexity equivalent to the one for the proposed SLC scheme with the ASC or SQ criterion when $G = N_{\mathrm{R}}$.

4.6 Conclusion

We have proposed a low-complexity SLC scheme for CC-HARQ in MIMO systems with a linear receiver. Instead of using the entire channel matrix as in the existing SLC schemes, a subset of row vectors in the channel matrix is selected in the proposed scheme, and the selected row vectors are sequentially used during combining and detection procedures of the retransmitted symbols by the SMW lemma. Therefore, according to the number of the selected row vectors, this approach enables the proposed SLC scheme to reduce complexity compared to the existing SLC schemes. Moreover, a squared norm based row vector selection criterion has been developed to calculate the SINR improvement. Simulation results demonstrated that compared to the existing SLC schemes, the proposed SLC scheme achieves similar or better error performance, while its computational complexity is lower or at the worst similar.

Chapter 5: Conclusions and Future Work

5.1 Conclusions

In this thesis, efficient HARQ transmission and combining schemes have been proposed for MIMO systems with IC and linear detections in the aspect of performance and complexity, respectively. Our contributions and future works can be summarized as follows:

Firstly, we have developed a simple HARQ transmission state control algorithm for MIMO systems with IC detection. By increasing the opportunity of simultaneous transmissions of initial packets and retransmission packets, the proposed algorithm improves the average PER of the initial packets, and thus enhances the system throughput. However, it is assumed that only one HARQ retransmission for any packets is allowed.

Secondly, to extend the analysis for a more general maximum allowable number of retransmission for a packet, a HARQ packet transmission strategy based on the concept of the EIL has been proposed. The proposed scheme successively minimizes the EIL of the packets from the lowest to the highest HARQ round in order to improve the system throughput. Simulation results demonstrate that the proposed strategy outperforms the conventional strategy in terms of system throughput without sacrificing the latency and error performance. Since the number of HARQ rounds of each packet is the only required information to calculate the EIL, the proposed algorithm is very simple to implement as well.

Thirdly, we have proposed a low-complexity SLC scheme for CC-HARQ in MIMO

systems with a linear receiver. Instead of using the entire channel matrix as in the existing SLC schemes, a subset of row vectors in the channel matrix is selected in the proposed scheme, and the selected row vectors are sequentially used during combining and detection procedures of the retransmitted symbols by the SMW lemma. Therefore, according to the number of the selected row vectors, the proposed SLC scheme is able to have an advantage in complexity compared to the existing SLC schemes. Moreover, we developed a row vector selection criterion to calculate the SINR improvement based on the squared norm of each row vector with a significantly lower computational complexity. Simulation results verified that compared with existing SLC schemes, the proposed SLC scheme achieves similar or better error performance while its computational complexity is lower or at the worst similar.

5.2 Future Work

For proposed EIL-based transmission strategy, the EIL defined in this thesis could be used to represent the reliability of the packet, such as the average SNR, the channel variations, the interference level, and so on. However, EIL is not an optimal selection criterion for packet transmission in the aspect of performance. Hence, it is necessary to propose another suboptimal packet set selection criterion for better performance than EIL as one of future works.

Moreover, since the proposed a low-complexity SLC scheme selects a subset of all row vectors for retransmissions, it is possible to utilize the previously unselected row vectors at the subsequent HARQ round. In addition, although the number of the selected row vectors is fixed in this thesis, it is possible to have a different number of the selected row vectors for each retransmission. These approaches can be jointly used to optimize

the error performance and complexity of several HARQ rounds. The development and mathematical analysis of such SLC schemes for CC-HARQ in MIMO systems remain future works. Furthermore, another selection criterion can be used to improve the performance with similar complexity compared to squared norm. Moreover, BLC schemes can be proposed to achieve good trade-offs between performance and complexity, no matter what type of HARQ process is used for MIMO systems.

Finally, this thesis considered only single-user MIMO systems for transmission and combining schemes. If extended to the multiple-user MIMO systems, cooperative relays, cognitive radio and heterogeneous networks, various transmission and combining strategies need to be mathematically analyzed and developed according to system topology.

Bibliography

[1] S. Sesia, I. Toufik, and M. Baker, *LTE: The UMTS long term evolution*, Wiley, 2009.

[2] A. Paulraj, R. Nabar, and D. Gore, *An introduction to space-time wireless communication*, Cambridge University Press, 2003.

[3] G. J. Foschini, "Layered space-time architecture for wireless communication in a fading environment when using multiple antennas," *Bell Labs. Tech. J.*, vol. 1, no. 2, pp. 41–59, Autumn 1996.

[4] M. Sellathurai and S. Haykin, "Turbo-BLAST for wireless communications: theory and experiments," *IEEE Trans. Signal Process.*, vol. 50, no. 10, pp. 2538–2546, Oct. 2002.

[5] Y. Li, J. Z. Winters, and N. R. Sollenberger, "MIMO-OFDM for wireless communications: signal detection with enhanced channel estimation," *IEEE Trans. Commun.*, vol. 50, no. 9, pp. 1471–1477, Sep. 2002.

[6] X. Wang and H. V. Poor, "Iterative (turbo) soft interference cancellation and decoding for coded CDMA," *IEEE Trans. Commun.*, vol. 47, no. 7, pp. 1046–1061, Jul. 1999.

[7] G. J. Foschini, *et al.* "Analysis and performance of some basic space-time architectures," *IEEE J. Sel. Areas Comm.*, vol. 47, no. 7, pp. 303–320, Apr. 2003.

[8] J.-H. Park, Y. Whang, and K. S. Kim, "Low complexity MMSE-SIC equalizer employing time-domain recursion for OFDM systems," *IEEE Signal Process. Lett.*, vol. 15, pp. 633–636, Oct. 2008.

[9] Y. Whang, J.-H. Park, and R. Whang, "Low complexity successive interference cancellation for OFDM systems over time-varying multipath channels," in *Proc. IEEE Veh. Technol. Conf. (VTC)*, Barcelona, Spain, Apr. 2009, pp. 1–5.

[10] IEEE P802.16e, "IEEE standard for local and metropolitan area networks part 16: Air interface for fixed and mobile broadband wireless access systems," Feb. 2006.

[11] D. Chase, "Code combining–a maximum-likelihood decoding approach for combining an arbitrary number of noisy packets," *IEEE Trans. Commun.*, vol. 33, no. 5, pp. 385–393, May 1985.

[12] J. Hagenauer, "Rate-compatible punctured convolutional codes (RCPC codes) and their applications," *IEEE Trans. Commun.*, vol. 36, no. 4, pp. 389-400, Apr. 1988.

[13] A. Nakajima, D. Garg, and F. Adachi, "Throughput of turbo coded hybrid ARQ using single-carrier MIMO multiplexing," in *Proc. IEEE Veh. Technol. Conf. (VTC)*, Stockholm, Sweden, May 2005, pp. 610–614.

[14] Y. Zhou and J. Wang, "Optimum subpacket transmission for hybrid ARQ systems," *IEEE Trans. Commun.*, vol. 54, no. 5, pp. 934–942, May 2006.

[15] J. Lee, H. Lou, D. Toumpakaris, E.W. Jang, and J.M. Cioffi, "Transceiver design for MIMO wireless systems incorporating hybrid ARQ," *IEEE Commun. Mag.*, vol. 47, no. 1, pp. 32–40, Jan. 2009.

[16] S. Park, Y. Whang, and S. Choi, "Extended detection for MIMO systems with partial incremental redundancy based hybrid ARQ," *IEEE Trans. Wireless Commun.*, vol. 11, no. 10, pp. 3714–3722, Oct. 2012.

[17] S. Park, "Multiple retransmission strategy-based HARQ for MIMO systems with acknowledgment bundling," *Electron. Lett.*, vol. 50, no. 8, pp. 637–639, Apr. 2014.

[18] H. Zheng, A. Lozano, and M. Haleem, "Multiple ARQ processes for MIMO systems," *EURASIP J. Appl. Signal Process. Special Issue on MIMO Commun. Signal Process.*, vol. 2004, no. 5, pp. 772–784, 2004.

[19] H. Wang, G. Lu, X. Qin, K. Wu, Y. Chang, X. Zhang, and D. Yang, "Research on hybrid-ARQ Chase combining algorithms in ZF-SIC V-BLAST," in *Proc. IEEE Wireless Commun. and Netw. Conf. (WCNC)*, Las Vegas, NV, USA, Apr. 2008, pp. 699-704.

[20] C. Bai, W. A. Krzymien, and I. J. Fair, "Hybrid-ARQ for layered space time MIMO systems with channel state information only at the receiver," *IET Commun.*, vol. 4, no. 14, pp. 1765–1773, Sep. 2010.

[21] M. Agrawal, Z. Chance, D. J. Love, and V. Balakrishnan, "Using channel output feedback to increase throughput in hybrid-ARQ," *IEEE Trans. Signal Process.*, vol. 60, no. 12, pp. 6465–6480, Aug. 2012.

[22] J. W. Lee, "Spectrally efficient multiple-ARQ scheme for MIMO channel," *Electronics Lett.*, vol. 49, no. 4, pp. 261–263, Feb. 2013.

[23] S. H. Kim, D. K. Sung, and T. Le-Ngoc, "Performance analysis of incremental redundancy type hybrid ARQ for finite-length packets in AWGN channel," in *Proc. IEEE Global Commun. Conf. (GLOBECOM)*, Atlanta, GA, USA, Dec. 2013, pp. 2063–2068.

[24] I. Menache and A. Ozdaglar, *Network games: Theory, models, and dynamics*, Synthesis Lectures on Communication Networks, Morgan & Claypool, 2010.

[25] T. J. Richardson and R. L. Urbanke, "The capacity of low-density parity-check codes under message-passing decoding," *IEEE Trans. Inf. Theory*, vol. 47, no. 2, pp. 599–618, Feb. 2001.

[26] M. Zwingelstein-Colin and M. Debbah, "Random matrix theory based resource allocation in correlated MIMO systems with ARQ feedback," *IEEE Commun. Lett.*, vol. 18 , no. 5, pp. 793–796, May 2014.

[27] T. K. Moon, *Error correction coding: Mathematical methods and algorithms*, John Wiley and Sons, 2005.

[28] C. R. Jeong, H. Y. Park, K. S. Kim, and K. C. Whang, "A partial IR hybrid ARQ scheme using rate-compatible punctured LDPC codes in an HSDPA system," *IEICE Trans. Commun.*, vol. E92-B, no. 2, pp. 604–607, Feb. 2009.

[29] D. N. Rowitch and L. B. Milstein, "On the performance of hybrid FEC/ARQ systems using rate compatible punctured turbo (RCPT) codes," *IEEE Trans. Commun.*, vol. 48, no. 6, pp. 948–959, Jun. 2000.

[30] J. Cheng, "Coding performance of hybrid ARQ schemes," *IEEE Trans. Commun.*, vol. 54, no. 6, pp. 1017–1029, Jun. 2006.

[31] H. Kwon, J. Lee, and I. Kang, "Symbol-level combining for hybrid ARQ on interference-aware successive decoding," in *Proc. IEEE Global Commun. Conf. (GLOBECOM)*, Atlanta, GA, USA, Dec. 2013, pp. 3650–3654.

[32] H. Sun and Z. Ding, "Iterative transceiver design for MIMO ARQ retransmissions with decision feedback detection," *IEEE Trans. Signal Process.*, vol. 55, no. 7, pp. 3405–3416, Jun. 2007.

[33] Z. Zhang and L. Qiu, "Optimal progressive precoder design for ARQ packet retransmissions in nonregenerative MIMO relay systems," in *Proc. IEEE Veh. Technol. Conf. (VTC)*, Yokohama, Japan, May 2012, pp. 1–5.

[34] X. Liang, C. Zhao, and Z. Ding, "Piggyback retransmissions over wireless MIMO channels: Shared hybrid-ARQ (SHARQ) for bandwidth efficiency," *IEEE Trans. Wireless Commun.*, vol. 12, no. 8, pp. 3770–3782, Aug. 2013.

[35] E. N. Onggosanusi, A. G. Dabak, Y. Hui, and G. Jeong, "Hybrid ARQ transmission and combining for MIMO systems," in *Proc. IEEE Int. Commun. Conf. (ICC)*, Anchorage, AK, USA, May 2003, pp. 3205–3209.

[36] E. W. Jang, J. Lee, H. L. Lou, and J. M. Cioffi, "On the combining schemes for MIMO systems with hybrid ARQ," *IEEE Trans. Wireless Commun.*, vol. 8, no. 2, pp. 836–842, Feb. 2009.

[37] E. W. Jang, J. Lee, L. Song, and J. M. Cioffi, "An efficient symbol-level combining scheme for MIMO systems with hybrid ARQ," *IEEE Trans. Wireless Commun.*, vol. 8, no. 5, pp. 2443–2451, May 2009.

[38] J. Xia, T. Lv, Y Li, and J. M. Cioffi, "A novel bit-level DS combining scheme for MIMO systems with HARQ," in *IEEE Int. Symp. on Inf. Theory (ISIT)*, Seoul, Korea, Jun. 2009, pp. 244–248.

[39] J. Xia and T. Lv, "Uncertainty processing applied to packet combining in MIMO-HARQ systems," in *Proc. IEEE Global Commun. Conf. (GLOBECOM)*, Honolulu, HI, USA, Dec. 2009, pp. 1–5.

[40] N. Prasad and X. Wang, "Efficient combining techniques for multi-input multi-output multi-user systems employing hybrid automatic repeat request," *IET Commun.*, vol. 5, no. 13, pp. 1785–1796, Sep. 2011.

[41] D. Bernstein, *Matrix mathematics*, Princeton University Press, 2005.

[42] R. A. Horn and C. R. Johnson, *Matrix analysis*, Cambridge University Press, 1985.

[43] L. N. Trefethen and D. Bau, III, *Numerical linear algebra*, SIAM, 1997.

[44] J. W. Demmel, *Applied numerical linear algebra*, SIAM, 1997.

[45] Yousef Saad, *Iterative methods for sparse linear systems*, Second edition, SIAM, 2003.

[46] A. Bjorck, *Numerical methods for least squares problems*, SIAM, 1996.

[47] N. J. Higham, *Accuracy and stability of numerical algorithms*, Second edition, SIAM, 2002.

[48] J. Dennis and R. Schnabel, *Numerical methods for unconstrained optimization and nonlinear equations*, Prentice Hall, 1983.

[49] T. Kim, "Low-complexity sorted QR decomposition for MIMO systems based on pairwise column symmetrization," *IEEE Trans. Wireless Commun.*, vol. 13, no. 3, pp. 1388–1396, Mar. 2014.

[50] Y. Whang, H. Liu, and S. Park, "HARQ transmission state control algorithm in MIMO systems with IC detection," in *Proc. IEEE Veh. Technol. Conf. (VTC)*, Glasgow, Scotland, UK, May 2015, pp. 1–5.

[51] Y. Whang, S. Park, and H. Liu, "Effective interference level-based packet transmission for multiple-input multiple-output systems with hybrid auto repeat request," *IET Commun.*, vol. 9, no. 18, p. 2208–2215, Dec. 2015.

[52] Y. Whang, S. Park, and H. Liu, "Low-complexity symbol-level combining for hybrid auto repeat request in multiple-input multiple-output systems with linear detection," accepted for publication in *IET Commun.*, Feb. 2016.

[53] S. Ge, Y. Xi, S. Huang, and J. Wei, "Packet error rate analysis and power allocation for CC-HARQ over Rayleigh fading channels," *IEEE Commun. Lett.*, vol. 8, no. 18, pp. 1467–1470, Aug. 2014.

[54] S. Ge, Y. Xi, S. Huang, Y. Ma, and J. Wei, "Approximate closed-form power allocation scheme for multiple-input multiple-output hybrid automatic repeat request protocols over Rayleigh block fading channels," *IET Commun.*, vol. 9, no. 16, pp. 2023–2032, Nov. 2015.

[55] S. Ge, Y. Xi, H. Zhao, S. Huang, and J. Wei, "Energy efficient optimization for CC-HARQ over block Rayleigh fading channels," *IEEE Commun. Lett.*, vol. 19, no. 10, pp. 1467–1470, Oct. 2015.

[56] T. Ait-Idir and S. Saoudi, "Turbo packet combining strategies for the MIMO-ISI ARQ channel," *IEEE Trans. Commun.*, vol. 57, no. 12, pp. 3782–3793, Dec. 2009.

[57] T. Ait-Idir, H. Chafnaji, and S. Saoudi, "Turbo packet combining for broadband space-time BICM hybrid-ARQ systems with co-channel interference," *IEEE Trans. Wireless Commun.*, vol. 9, no. 5, pp. 1686–1697, May 2010.

[58] B. Makki and T. Eriksson, "On the performance of MIMO-ARQ systems with channel state information at the receiver," *IEEE Trans. Commun.*, vol. 62, no. 5, pp. 1588–1603, Apr. 2014.

[59] P. Larsson, L. K. Rassmusen, and M. Skoglund, "Analysis of rate-optimized throughput for large-scale MIMO-ARQ schemes," in *Proc. IEEE Global Commun. Conf. (GLOBECOM)*, pp. 3760–3765, Austin, TX, USA, Dec. 2015.

[60] P. Wu and N. Jindal, "Performance of hybrid-ARQ in block-fading channels: A fixed outage probability analysis," *IEEE Trans. Commun.*, vol. 58, no. 4, pp. 1129–1141, Apr. 2010.

[61] P. Larsson, L. K. Rassmusen, and M. Skoglund, "Throughput analysis of ARQ schemes in Gaussian block fading channels," *IEEE Trans. on Commun.*, vol. 62, no. 7, pp. 2569–2588, Jul. 2014.

[62] P. Larsson, L. K. Rassmusen, and M. Skoglund, "Analysis of rate optimized throughput for ARQ in fading interference channels," in *Proc. IEEE Int. Conf. Commun. (ICC)*, Sydney, Australia, Jun. 2014, pp. 5926–5931.

[63] P. Larsson, B. Smida, T. Koike-Akino, and V. Tarokh, "Analysis of network Coded HARQ for multiple unicast flows," *IEEE Trans. on Commun.*, vol. 61, no. 2, pp. 722–732, Feb. 2013.

[64] R. Narasimhan, "Throughput-delay performance of half-duplex hybrid-ARQ relay channels," in *Proc. IEEE Int. Conf. Commun. (ICC)*, Beijing, China, May 2008, pp. 986–990.

[65] T. V. K. Chaitanya and E. G. Larsson, "Outage-optimal power allocation for hybrid ARQ with incremental redundancy," *IEEE Trans. Wireless Commun.*, vol. 10, no. 7, pp. 2069–2074, Jul. 2011.

[66] R. Cam and C. Leung, "Throughput analysis of some ARQ protocols in the presence of feedback errors," *IEEE Trans. Commun.*, vol. 45, no. 1, pp. 35–44, Jan. 1997.

[67] S. M. Kim, W. Choi, T. W. Ban, and D. K. Sung, "Optimal rate adaptation for hybrid ARQ in time-correlated Rayleigh fading channels," *IEEE Trans. Wireless Commun.*, vol. 10, no. 3, pp. 968–979, Mar. 2011.

[68] I. Stanojev, O. Simeone, Y. Bar-Ness, and C. You, "Performance of multi-relay collaborative hybrid-ARQ protocols over fading channels," *IEEE Commun. Lett.*, vol. 10, no. 7, pp. 522–524, Jul. 2006.

[69] J. Perret and D. Tuninetti, "Repetition protocols for block fading channels that combine transmission requests and state information," in *Proc. IEEE Int. Conf. Commun. (ICC)*, Beijing, China, May 2008, pp. 1297–1301.

[70] E. Malkamaki and H. Leib, "Performance of truncated type-II hybrid ARQ schemes with noisy feedback over block fading channels," *IEEE Trans. Commun.*, vol. 48, no. 9, pp. 1477–1487, Sep. 2000.

[71] V. K. Oduol and S. D. Morgera, "Performance evaluation of the generalized type-II hybrid ARQ scheme with noisy feedback on Markov channels," *IEEE Trans. Commun.*, vol. 41, no. 1, pp. 32–40, Jan. 1993.

[72] A. Chuang, A. Guillen i Fabregas, L. K. Rasmussen, and I. B. Collings, "Optimal throughput-diversity-delay tradeoff in MIMO ARQ block-fading channels," *IEEE Trans. Inf. Theory*, vol. 54, no. 9, pp. 3968–3986, Sep. 2008.

[73] S. Sesia, G. Caire, and G. Vivier, "Incremental redundancy hybrid ARQ schemes based on low-density parity-check codes," *IEEE Trans. Commun.*, vol. 52, no. 8, pp. 1311–1321, Aug. 2004.

[74] B. Makki, A. Graell I Amat, and T. Eriksson, "Power allocation in repetition time diversity hybrid automatic repeat request feedback," in *IEEE Wireless Commun. and Netw. Conf. (WCNC)*, Apr. 2012, pp. 2329–2334.

[75] B. Makki, A. Graell I Amat, and T. Eriksson, "HARQ feedback in spectrum sharing networks," *IEEE Commun. Lett.*, vol. 16, no. 9, pp. 1337–1340, Sep. 2012.

[76] A. Chelli and M.-S. Alouini, "On the performance of hybrid-ARQ with incremental redundancy and with code combining over relay channels," *IEEE Trans. Wireless Commun.*, vol. 12, no. 8, pp. 3860–3871, Aug. 2013.

[77] K. D. Nguyen, L. K. Rasmussen, A. Guillen i Fabregas, and N. Letzepis, "MIMO ARQ with multibit feedback: Outage analysis," *IEEE Trans. Inf. Theory*, vol. 58, no. 2, pp. 765–779, Feb. 2012.

[78] M. Zorzi and R. R. Rao, "On the use of renewal theory in the analysis of ARQ protocols," *IEEE Trans. Commun.*, vol. 44, no. 9, pp. 1077–1081, Sep. 1996.

[79] J.-F. Cheng, "Coding performance of hybrid ARQ schemes," *IEEE Trans. Commun.*, vol. 54, no. 6, pp. 1017–1029, Jun. 2006.

[80] A. Annamalai and V. K. Bhargava, "Analysis and optimization of adaptive multi-copy transmission ARQ protocols for time-varying channels," *IEEE Trans. Commun.*, vol. 46, no. 10, pp. 1356–1368, Oct. 1998.

[81] H. Shirani-Mehr, H. Papadopoulos, S. A. Ramprashad, and G. Caire, "Joint scheduling and ARQ for MU-MIMO downlink in the presence of inter-cell interference," *IEEE Trans. Commun.*, vol. 59, no. 2, pp. 578–589, Feb. 2011.

[82] R. Huang, C. Feng, and T. Zhang, "Energy efficiency analysis of cooperative ARQ in amplify-and-forward relay networks," in *Proc. IEEE Asia Pacific Conf. on Commun. (APCC)*, Sabah, Malaysia, Oct. 2011, pp. 197–202.

[83] W. C. Ao and K. C. Chen, "End-to-end HARQ in cognitive radio networks," in *Proc. IEEE Wireless Commun. and Netw. Conf. (WCNC)*, Sydney, Australia, Apr. 2010, pp. 1–6.

[84] C. Cheung and R. S. K. Cheng, "Performance analysis for superposition modulated cooperative relay HARQ networks," *IEEE Trans. Veh. Technol.*, vol. 61, no. 7, pp. 2978–2990, Sep. 2012.

[85] B. Maham, A. Behnad, and M. Debbah, "Analysis of outage probability and throughput for half-duplex hybrid-ARQ relay channels," *IEEE Trans. Veh. Technol.*, vol. 61, no. 7, pp. 3061–3070, Sep. 2012.

[86] K. D. Nguyen, "Adaptive transmission for block-fading channels," Ph.D. dissertation, University of South Australia, 2009.

[87] T. T. Kim, "Limited feedback information in wireless communications: Transmission schemes and performance bounds," Ph.D. dissertation, KTH School of Electrical Engineering, 2008.

[88] S. Ekbatani, "Communication over multiple antenna fading channels using quantized and erroneous feedback information," Ph.D. dissertation, University of California, Irvine, 2008.

[89] E. Dahlman, S. Parkvall, and J. Skold, *4G LTE/LTE-advanced for mobile broadband*, Academic Press, 2011.

[90] S. Nanda, R. Walton, J. Ketchum, M.Wallace, and S. Howard, "A high-performance MIMO OFDM wireless LAN," *IEEE Commun. Mag.*, vol. 43, no. 2, pp. 101–109, Feb. 2005.

[91] H. Seo and B. G. Lee, "Optimal transmission power for single- and multi-hop links in wireless packet networks with ARQ capability," *IEEE Trans. Commun.*, vol. 55, no. 5, pp. 996–1006, May 2007.

[92] D. V. Djonin, A. K. Karmokar, and V. K. Bhargava, "Joint rate and power adaptation for type-I hybrid ARQ systems over correlated fading channels under different buffer-cost constraints," *IEEE Trans. Veh. Technol.*, vol. 57, no. 1, pp. 421–435, Jan. 2008.

[93] D. Gesbert, S. Hanly, H. Huang, S. Shamai, O. Simeone, and W. Yu, "Multi-cell MIMO cooperative networks: A new look at interference," *IEEE J. Sel. Areas Commun.*, vol. 28, no. 9, pp. 1380–1408, Dec. 2010.

[94] A. Wiesel, Y. C. Eldar, and S. Shamai, "Zero-forcing precoding and generalized inverses," *IEEE Trans. Signal Process.*, vol. 56, no. 9, pp. 4409–4418, Sep. 2008.

[95] L. Yang and M.-S. Alouini, "Performance analysis of multiuser selection diversity," *IEEE Trans. Veh. Technol.*, vol. 55, no. 6, pp. 1848–1861, Nov. 2006.

[96] L. Yang, M. Kang, and M.-S. Alouini, "On the capacity-fairness tradeoff in multiuser diversity systems," *IEEE Trans. Veh. Technol.*, vol. 56, no. 4, pp. 1901–1907, Jul. 2007.

[97] V. Hassel, M.-S. Alouini, D. Gesbert, and G. E. Oien, "Exploiting multiuser diversity using multiple feedback thresholds," in *Proc. IEEE Veh. Technol. Conf. (VTC)*, Stockholm, Sweden, May 2005, vol. 2, pp. 1302–1306.

[98] J. Zhang, "Networked MIMO with clustered linear precoding," *IEEE Trans. Wireless Commun.*, vol. 8, no. 4, pp. 1910–1921, Apr. 2009.

[99] R. U. Nabar, H. Bolcskei, and F. W. Kneubuhler, "Fading relay channels: Performance limits and space-time signal design," *IEEE J. Sel. Areas Commun.*, vol. 22, no. 6, pp. 1099–1109, Aug. 2004.

[100] T. Holliday, A. J. Goldsmith, and H. V. Poor, "Joint source and channel coding for MIMO systems: Is it better to be robust or quick?" *IEEE Trans. Inf. Theory*, vol. 54, no. 4, pp. 1393–1405, Apr. 2008.

[101] J. Choi and D. To, "Energy efficiency of HARQ-IR for two-way relay systems with network coding," in *Proc. European Wireless Conf. (EW)*, Poznan, Poland, Apr. 2012, pp. 1–5.

[102] Y. Whang and S.-W. Hwang, "Multilevel control signaling for hybrid ARQ," in *Proc. IEEE Int. Conf. on Wireless Commun., Netw. and Mobile Comput. (WICOM)*, Dalian, China, Oct. 2008, pp. 1–3.

[103] Y. Whang and H. Y. Park, "An adaptive space-time receiver for time-varying channel with imperfect channel estimation," in *Proc. IEEE Int. Conf. on Wireless Commun., Netw. and Mobile Comput. (WICOM)*, Dalian, China, Oct. 2008, pp. 1–5.

[104] G. Kramer, I. Maric, and R. D. Yates, *Cooperative communications*, Now, 2007.

[105] J. G. Proakis, *Digital communication*, Fourth edition, McGraw Hill, 2000.

[106] D. Tse and P. Viswanath, *Fundamentals of wireless communication*, Cambridge University Press, 2005.

[107] M. K. Simon and M.-S. Alouini, *Digital communication over fading channels*, John Wiley and Sons, 2000.

[108] H. Jafarkhani, *Space-time coding: Theory and practice*, Cambridge University Press, 2005.

[109] C. Oestges and B. Clerckx, *MIMO wireless communications: From real-world propagation to space-time code design*, Academic Press, 2007.

[110] E. G. Larsson and P. Stoica, *Space-time block coding for wireless communications*, Cambridge University Press, 2005.

[111] A. B. Gershman and N. D. Sidiropoulos, *Space-time block coding for MIMO communications*, John Wiley and Sons, 2005.

[112] U. Madhow, *Fundamentals of digital communication*, Cambridge University Press, 2008.

[113] K. J. R. Liu, *et al.*, *Cooperative communications and networking*, Cambridge University Press, 2009.

[114] E. Biglieri, *et al.*, *MIMO wireless communications*, Cambridge University Press, 2007.

[115] P. Marsch and G. P. Fettweis, *Coordinated multi-point in mobile communications: From theory to practice*, Cambridge University Press, 2011.

[116] J. R. Barry, E. A. Lee, and D. G. Messerschmitt, *Digital communication*, Third edition, Kluwer Academic Publishers, 2004.

[117] Y. S. Cho, J. Kim, W. Y. Yang, and C. G. Kang, *MIMO-OFDM wireless communications with MATLAB*, John Wiley and Sons, 2010.

[118] S. Lin and D. J. Costello, *Error control coding*, Second edition, Prentice Hall, 2004.

[119] A. Goldsmith, *Wireless communications*, Cambridge University Press, 2005.

[120] H. Blcskei, D. Gesbert, and C. B. Papadias, *Space-time wireless systems: From array processing to MIMO communications*, Cambridge University Press, 2006.